

STUDY OF STRUCTURE-PROPERTY RELATIONSHIP IN HIGH TENSION CERAMIC INSULATOR

Rashed Adnan Islam



A thesis submitted to the Department of Materials and Metallurgical Engineering (MME) of Bangladesh University of Engineering and Technology (BUET), Dhaka, in partial fulfillment of the requirements for the degree of Master of Science in Engineering (Materials and Metallurgy).

DECEMBER, 2002

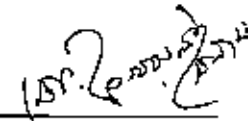
BANGLADESH UNIVERSITY OF ENGINEERING AND TECHNOLOGY
DHAKA, BANGLADESH.




DECLARATION

This is to certify that this research work has been carried out by the author under the supervision of Dr. Md. Fakhru Islam, Associate Professor, Department of Materials and Metallurgical Engineering, BUET, Dhaka, and it has not been submitted elsewhere for the award or degree of any kind.

Countersigned by

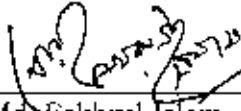

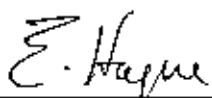
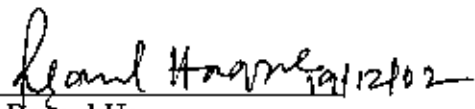
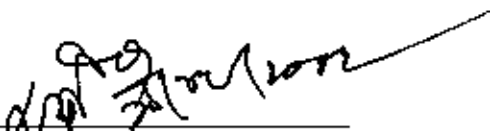


Supervisor



Signature of the Author

The undersigned examiners appointed by the Committee of Advanced Studies and Research (CASR) hereby recommended to the Department of Materials and Metallurgical Engineering of Bangladesh University of Engineering and Technology, Dhaka, the acceptance of the thesis entitled "Study of Structure-Property Relationship in High Tension Ceramic Insulator" submitted by Rashed Adnan Islam, Lecturer, Department of Materials and Metallurgical Engineering, BUET, Dhaka, in partial fulfillment of the requirements for the degree of Master of Science in Engineering (Materials and Metallurgy).

1. 
19/12/02
Dr. Md. Fakhrul Islam
Associate Professor
Department of Materials and Metallurgical Engineering
BUET, Dhaka. Chairman
(Supervisor)
2. 
19/12/02
Dr. A.K.M. Bazlur Rashid
Head of the Department
Department of Materials and Metallurgical Engineering
BUET, Dhaka. Member
3. 
Professor Dr. Ehsanul Haque
Department of Materials and Metallurgical Engineering
BUET, Dhaka. Member
4. 
19/12/02
Professor Md. Rezaul Haque
Department of Materials and Metallurgical Engineering
BUET, Dhaka. Member
5. 
Engg. Zahed Kabir
Managing Director
BISF LTD. Member
(External)

ACKNOWLEDGEMENTS

The author expresses his profound indebtedness and heartfelt gratitude to his thesis supervisor Dr. Md Fakhru Islam, Associate Professor, Department of Materials and Metallurgical Engineering, Bangladesh University of Engineering and Technology (BUET), Dhaka for his valuable suggestions, constant guidance, encouragement and kind help in carrying out the project work as well as in writing this thesis.

The author is very much thankful to Dr. A.S.M.A. Haseeb, Head of the Department, Department of Materials and Metallurgical Engineering, Bangladesh University of Engineering and Technology (BUET), Dhaka for his kind inspiration in every step of work.

The author is grateful to Engg. Zahed Kabir, Managing Director of Bangladesh Insulator and Sanitary ware Factory Limited (BISF), Mirpur, Dhaka for giving him permission to use the industrial facility in every area of the industry. The author is also thankful to Md. Gias Uddin Ahmed, Deputy Chief Manager of BISF for their kind help and dynamic support in this regard.

Thanks are due to Mr. Jahl for his co-operation and thanks are also due to the officers and staff specially Mr. Yousuf Khan, Mr. Wasim Miah and Mr Shamsul Alam of the Department of Materials and Metallurgical Engineering of BUET and of BISF for their help in various stages of the study.

Finally the author wishes to record his gratitude to Allah, the most merciful and the most gracious, for giving him the ability to complete the project.

The Author

Department of Materials and Metallurgical Engineering (MME)

BUET, Dhaka.

ABSTRACT

Insulators are used in the power line to prevent the voltage or current regulation. Ceramic is one of the important insulating materials because of its very good thermal stability and inertness in severe environment. Among all the ceramic materials porcelain is the one which is cheaper and has good insulating properties like low loss, high dielectric strength and good mechanical strength. Dielectric strength of an insulator may be defined as the ability to withstand the voltage per unit thickness.

In this project the physical, mechanical and electrical properties of ceramic insulators fired at different temperature have been investigated along with microstructural characterization using optical and scanning electron microscopy in order to understand the structure-property relationship of ceramic insulator. The Mechanical and the electrical properties were measured on samples fired at different temperature from 1250 to 1400^oC at 25^o C interval. The dependency of bending and dielectric strength on microstructure developed due to firing at different temperatures was thoroughly examined. EDAX analysis and XRD techniques were also done to support the results.

The bending and the dielectric strength were found maximum at 1350^oC and decreases on both sides of the maxima. The microstructural features developed clearly describe that type of behavior and it is observed that the crystalline phase mullite contributes together with quartz particle to the dielectric and mechanical strength.

CONTENT

Acknowledgement

Abstract

Chapter 1: Introduction 1

Chapter 2: Literature Review

2.1 Ceramic Insulator	4
2.1.1 Properties of ceramic insulator	4
2.1.2 Application	5
2.2 Composition	5
2.3 Triaxial Porcelain	7
2.3.1 Mechanism of formation of porcelain	8
2.4 Ceramic Phase Equilibrium Diagram	11
2.4.1 Two Component system – Al_2O_3 - SiO_2 system	13
2.4.2 Three component system	15
2.5 Changes during firing	15
2.5.1 Phase changes that occur on heating kaolin clays	17
2.5.2 Changes in the range 600-800 ^o C	18
2.5.3 Changes in the range 800-1400 ^o C	19
2.5.4 The exothermic reaction at 900-1050 ^o C	19
2.6 Dielectric Properties	20
2.6.1 Different types of dielectric breakdown	22
2.6.1.1 Intrinsic Breakdown	22
2.6.1.2 Thermal Breakdown	23
2.6.1.3 Ionization Breakdown	24
2.6.1.4 Electromechanical Breakdown	24
2.7 Factors Affecting Dielectric Strength	25
2.8 Factors affecting mechanical strength	29

Chapter 3: Experimental

3.1. Introduction 33

3.2. Ceramic insulator body Preparation	33
3.2.1. Raw material selection	33
3.2.2 Chemical analysis	34
3.2.3 Crushing	34
3.2.4 Ball milling or pot milling	35
3.2.5 Magnetic particle separation	35
3.2.6 Reservoir	35
3.2.7 Filter press or casting in plaster of paris mould	36
3.2.8 Pug milling	36
3.2.9 Drying	36
3.2.10 Firing	37
3.3 Physical Properties Measurements	37
3.3.1 Density Measurements	37
3.3.2 Hardness measurement	37
3.3.3 Bending Strength Measurement	38
3.4 Microstructural Characterization	39
3.4.1 Optical Ceramography	39
3.4.1.1 Sample Preparation for ceramography	39
3.4.1.2 Etching	40
3.4.2 Scanning Electron Microscopy	41
3.4.2.1 Specimen Preparation	41
3.4.2.2 Coating	42
3.4.2.3 Sputtering	42
3.5 Phase Analysis by X-ray Diffraction	43
3.6 Chemical Properties Measurement	44
3.6.1 Glassy Phase Determination	44
3.6.2 EDAX analysis	45
3.6.3 X-ray Fluorescence	45
3.7 Electrical Properties Measurement	46
3.7.1 Dielectric Strength Measurement	46

Chapter 4: Results and Discussions		
4.1	Introduction	48
4.2	Density data	48
4.3	Hardness	49
4.4	Bending strength data	50
4.5	Determination of glassy phase content	50
4.6	X-ray Fluorescence	51
4.7	Optical metallography	51
4.8	SEM Image analysis	53
4.9	Dielectric Strength Data	56
4.10	Phase analysis by X-ray diffraction	59
4.11	EDAX Analysis	60
Chapter 5: Conclusion		62
Chapter 6: Suggested future works		63
Chapter 7: Bibliography		64



INTRODUCTION

Insulators are materials, which prevent or regulate current flow in electrical circuits by being inserted as a barrier between conductors. The properties required being an insulator is high resistivity, high dielectric strength and a low loss factor. In addition to preventing current flow between the conductors in electrical circuits the insulators also serves other important functions as giving mechanical properties, dissipation of heat and protection of conductors from severe environment, like humidity and corrosiveness. There are various materials used as insulating materials like acetate, acrylic, beryllium oxide, ceramic, epoxy/fiberglass, glass, melamine, mica, nylon P.E.T.: (polyethylene terephthalate), phenolics etc. Most other insulating materials are cheaper and can be fabricated with better dimensional accuracy. The advantage of ceramics insulator which frequently indicate their use, are superior electrical properties, absence of creep or deformation under stress at room temperature, greater resistance to environmental changes particularly at high temperatures at which other insulator (such as melamine, epoxy fiber, P E.T. etc.) frequently oxidize and the ability to form gas tight seals with metals and become integral part of an electronic devices. It should be noted that the selection of a particular dielectric material depends on the ability to be formed as a gas tight parts to operate under unusual environmental conditions, thermal expansion characteristics, thermal stress resistance and impact resistance, the ability to be formed into complex shapes with good dimensional accuracy and on other characteristics which are completely independent of electrical behavior but are essential for the building of practical devices.

Ceramics are widely used as insulating materials. For this application the properties most concerned are the dielectric and mechanical strength. Dielectric strength (represented by kilovolt per millimeter) measures the ability to withstand large field strength without electrical breakdown. For high-tension electrical insulation the dielectric strength has to be above 30kV/mm ¹¹ and the bending strength has to be such to prevent the load in application. One of the great advantages of ceramics as insulator is the fact that they are

nonsensitive to the minor changes in composition, fabrication, techniques, and firing temperature. This adaptability results from the interaction of phases present to increases continuously the viscosity of the fluid phases as more of it is formed at higher temperature. Other advantages are mainly their greater resistance to environmental changes and their capability for high-temperature operation without hazardous degradation in chemical, mechanical or dielectric property [2].

The processing of raw materials for ceramic insulator starts with the mixing of clay, feldspar and quartz. The processing follows the wet processing route. Forming of insulating body has specific importance as the body has to be pore free. Natural drying followed by drying in a drier is required to have the moisture free insulating body. At last the firing is done in a very long firing cycle. Temperature, time and atmosphere in the furnace affect chemical reactions and microstructural changes in the body [3].

The microstructure of porcelain electrical insulator body shows mullite needle in both glassy phase with some undissolved quartz particle and unresolved clay matrix. The thermal behavior of silica and alumina shows that the mullite ($3\text{Al}_2\text{O}_3 \cdot 2\text{SiO}_2$) phase starts to form at 1100°C and above this temperature mullite becomes larger and prominent [4]. Mullite is a crystalline phase in the Al_2O_3 - SiO_2 binary system. It has some specific properties like high creep resistance, low thermal expansion and good thermal and chemical stability which makes it desirable for high tension structural insulating material [5]. Slow firing and slow cooling favour the formation of mullite crystal and the size of the mullite crystal is increased with firing [6]. The glassy phase and the undissolved quartz particle enhance the properties of high voltage insulator in a way that they fill the pores, disconnect the conductivity and strengthen the rigid skeleton. But where high dielectric performance is required glassy phase and mobile ion content must be minimized [7].

Bangladesh Insulator and Sanitary ware Factory (BISF) Ltd. has been producing high-tension electrical insulators for quite a long time but the rejection rate in the factory is very high. The rejection is due to the presence of impurities in the raw materials, inaccurate firing temperature, improper control of firing temperature throughout the kiln

length etc. These result in ceramic insulator with low dielectric strength. The phases present in the ceramic insulator have a good impact over the properties like dielectric strength and mechanical strength. Through this project it is intended to identify the phase, which contributes the dielectric strength, and the phase, which is detrimental for producing high-tension dielectric insulators.

The objective of this thesis project is to find out the structure-property relationship in high-tension ceramic insulators. The various phases formed in ceramic insulator at different firing temperatures are identified using optical and scanning electron microscope. It is also tried to find out the phases, which are detrimental to high dielectric and mechanical strength. The specific aim of this thesis project is to select suitable firing temperature and to develop suitable microstructure for high-tension ceramic insulator.

LITERATURE REVIEW

2.1 Ceramic Insulator

The primary function of insulation in electrical circuits is the physical separation of conductors and the regulation or prevention of current flow between them. Ancillary but important other functions are to provide mechanical support, heat dissipation, and environmental protection for the conductors. Ceramic materials, which in use provide primarily these functions, are classified as ceramic insulators.

2.1.1 Properties of ceramic insulator

Ceramics are used where high strength, elevated temperature, heat dissipation, or long-term hermeticity (sealed from pressure to the atmosphere) is required. The most demanding application for high resistivity ceramics is insulators for high-voltage power lines. Most people are aware that ceramics are used for these insulators, but do not realize how demanding the application really is. First, the insulators must be very strong because they support the weight of the power lines and should endure during a heavy wind or any other catastrophic calamities. Then the material should be considered how long these insulators are designed to last. They must be highly reliable. Second, the insulator must be resistant to weather damage and to absorption of water. Internal adsorption can result in arcing at the high voltages involved. Ceramic materials that are good electrical insulators are referred to as dielectric materials^[2]. Although these materials do not conduct electric current when an electric field is applied, they are not inert to the electric field. The field causes a slight shift in the balance of charge within the material to form an electric dipole, thus the term "dielectric" applies. Electrons can move when a material has electron energy levels that overlap or are not filled. Ions can move when point defects are present in the crystal ions in large structural channels. Most ceramics do not have mobile electrons or ions and do not permit passage of an electrical current when placed in an electric field. These nonconductive ceramics are called electrical insulators. The high value of electrical resistivity for these materials results from the way that the electrons are

tioned up during atomic bonding. In each case, valence electrons are either shared (covalently) or transferred (ionically) such that each atom achieves a full outer shell of electrons. This leaves no overlap of electron energy bands and no low-energy mechanisms for electron conduction (fig. 2. 1).

2.1.2 Application

A distinction must be made between the categories of ceramic insulators described as low tension and high tension insulator [6]. The low-tension ceramic insulator generally have looser raw materials tolerances and are used unglazed for less exacting low-voltage and low-frequency applications, such as light sockets, fuse blocks, bushings, and hot plate and toaster insulation. They are usually sintered in the range 1260-1320^o C and are characterized by moderately low dielectric strengths (~ 9-11 kV/mm) and loss factors (0.05-0.1 at 1 kHz). In contrast, the high-tension ceramic insulators are sintered in the range 1350 to 1450^oC. Lower impurity content is achieved by reduction or elimination of ball clay, which is replaced by bentonite clay (~ 3 wt.%) or alkaline earth additives [11]. These insulators can be considered as low-loss, high dielectric-strength (~13-18 kV/mm) materials and are therefore suitable for such high-voltage applications as transmission line insulators, high-voltage circuit breakers, and cutouts. Because of these environmentally sensitive applications, the porcelain must be dense, moisture impervious, and have minimal mechanical flaws. This is aided by the use of a glaze coating, which may be a self-glaze, feldspathic glaze, or semiconducting brown glaze.

2.2 Composition

Among different types of ceramic insulator the distinction largely reflects the amount of glassy phase in the ceramics, which tends to control the dielectric properties. Where high dielectric performance is required, therefore, glassy phase content must be minimized in the insulator and mobile ion content should, as far as practicable, be minimized. Clay materials do not have strong bonding capacity when fired. Some clay does not have proper vitrification characteristics, that is, they are not plastic. Some clay shows

extensive plasticity. Plastic clays show excellent bonding characteristic but their linear coefficient of thermal expansion is very poor for the electrical porcelain ware. Since a steady dimensional property of the ceramic insulator material is must for every engineering application, a variety of clays with plastic and non-plastic property are mixed to get the highest possible stable form. In electrical power transmission system, the insulator materials not only withstand the electrical energy but also the line tension. A variety of fluxing materials can be added to the clay material to get not only the higher mechanical bonding strength but also lower the temperature at which mullite can form. Mullite, the only crystalline phase responsible for high strength, appears from clay materials at higher temperature, i.e., 1500 - 1600°C. This high temperature is not economical for the production of the insulators. Commercially added fluxing materials are usually potash feldspar. This feldspar not only produces the dense product but also lower down the firing temperature of the material. If adequate SiO₂ is not present in the clays, some quartz can be added. Actually silica and alumina are the basic constituents of the conventional ceramic insulator materials. Other oxides, which are present in the raw materials act as impurities, i.e., lower down the firing temperature of the material. Fig 2 2 shows how mechanical and electrical strength and thermal shock resistance depends on the composition of the body. It is evident that the best possible values of these three technically important properties cannot be attained in one and the same body. Fineness of grinding of the raw materials has a marked influence on the properties of porcelain, as has been confirmed by numerous detailed studies. The densification is due to the use of feldspar as a flux. The clay substance incorporated is nearly always in the form of kaolin, and quartz, is never absent. Raw material compositions for the triaxial porcelains can be given as 40- 60 wt % clays, 20- 35-wt %, feldspar, and 20- 30 %wt. flint. The raw materials each contribute different characteristics to the fired porcelain. The kaolinite clay provides the main body for the ceramics and controls the firing range and distortion during sintering. It also provides the first liquid phase in the system (at 900°C), from which a main crystalline phase, mullite, is subsequently developed.

2.3 Triaxial Porcelain

Porcelain is the term used to describe white vitrified ceramic ware, translucent in thin layers, impermeable to fluids, and manufactured from a fine mixture of kaolin, quartz, feldspar, and plastic white firing clay. Porcelain is the most noble of ceramic products: the fired ware is usually white, always translucent and of very low porosity (0.01- 6 per cent closed pores). Porcelains can also be described as polycrystalline ceramic bodies containing, typically, more than about 10% vol. of a vitreous second phase^[3]. This vitreous phase essentially controls densification, porosity, and phase distribution within the porcelain and to a large extent its mechanical and dielectric properties. Porcelain bodies can be classified as triaxial, steatite, or non-feldspathic types, depending on the composition and amount of the vitreous phase present within the ceramic.

Triaxial porcelains form a large base of the commonly used porcelain insulators. They exhibit fairly low mechanical strength, fair thermal shock resistance, and relatively poor high-frequency characteristics (due to alkali ion migration) but are generally satisfactory for low-frequency ($< 10^4$ Hz) use at ordinary temperatures. They are compounded from mixtures of feldspars $[(K, Na)_2O \cdot 3Al_2O_3 \cdot 6SiO_2]$, kaolinite clays $(Al_2O_3 \cdot 2SiO_2 \cdot 2H_2O)$, and flint or quartz (SiO_2), which places the triaxial porcelains in the phase system $[(K, Na)_2O \cdot 3Al_2O_3 \cdot 6SiO_2]$ in terms of oxide constituents^[3,4,5].

In most formulations, however, up to one-half the kaolinite content may be replaced by ball clay, which increases plasticity and green strength in the formed ware but may also be the source of impurities. The feldspar provides the main flux phase, which lowers the maturing temperature and accounts for the dense nonporous structure from which some mullite phase also develops. However, the increased glassy phase and alkali content tend to degrade both the dielectric properties and mechanical strength of the porcelain. Partial dissolution of the quartz phase above $1200^\circ C$ increases the liquid phase viscosity and helps to maintain shape during firing. An increase in the quartz content usually gives improved mechanical strength, provided that the grain size is below $10\mu m$, in order to minimize thermal expansion stresses. Minor ingredients (2~5 wt %) such as talc, zircon,

and the alkaline earth carbonates aid in the formation and control of low-temperature eutectic phase, resulting in generally improved dielectric and mechanical properties of the porcelain^[3].

2.3.1 Structure of Porcelain

Porcelain ware shows an almost complete lack of open pores (water absorption not greater than 0.5%) and has high strength, good spalling resistance, and chemical inertness. Various types of porcelain are obtained through the physical and chemical interaction of the clay, quartz, and feldspar at high temperatures. In fig.2.3 showing the ternary system kaolin-quartz-feldspar, the areas of formation of different types of porcelain are indicated by the sintering isotherms for different mixtures at 1160^o, 1200^o and 1280^oC. The degree of sintering changes sharply as a function of the firing period and the degree of pulverization of the materials. Individual structural elements in the porcelain have varying effects on its strength, whiteness, translucence, and certain other qualities. Study of the formation of porcelain has revealed the effect of technological factors on the development of special structural characteristics associated with the basic properties of a given type of porcelain product (the high mechanical and electric strength of insulators, the high chemical and spalling resistance of laboratory porcelain vessels etc.)^[10]. The phase composition and properties due to it depend on the kaolin and plastic clay, quartz, and feldspar content in the porcelain mixture, on the chemical composition of these materials and degree of pulverization, and also on the temperature and period of firing. Improvement of a particular property is often brought about at the expense of another; for example, an improvement in translucence is accompanied by reduction in mechanical strength and by an increase in the number of deformed items produced during firing. In such cases the problem arises of selecting a composition and firing conditions that will make it possible to obtain products with the right combination of properties for the given purpose. The texture of porcelain and its most important properties are determined by the quantitative relationship between the crystalline and vitreous phases. The amount and quality of the vitreous phase in the porcelain depend on the composition of the mixture, the fineness of grinding of the initial materials, and the firing conditions

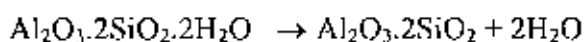
Extensive microscopic research has shown the following principal structural elements in porcelain

1. A vitreous isotropic mixture consisting of feldspar glass
2. Quartz particles which have not dissolved in the glass,
3. Mullite crystals ($3\text{Al}_2\text{O}_3 \cdot 2\text{SiO}_2$), distributed mainly in the silica-feldspar glass melt,
4. Pores;

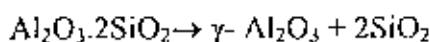
2.3.2 Mechanism of formation of porcelain

The formation of porcelain is shown schematically in fig. 2.4 the drawings represent the phenomena occurring at different stages of the process (I-V) between the grains of kaolinite, quartz, and feldspar, the basic components of the porcelain mixture. Small additions of other oxides finding their way into the mixture with the basic raw material are not taken into account in the diagram because of their negligible effect on the process. As shown in the diagram, the feldspar grains 3 are located between the aggregates of clay particles 1 and the quartz grains 2^[16-25].

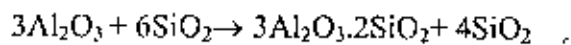
During the first stage of firing, principally within the temperature range as can be seen from the thermogram fig. 2.5 dehydration of the kaolin occurs in accordance with the following reaction:



with a corresponding endothermal effect. Between 800 and 900⁰ C the metakaolinite decomposes into oxides, the initial shape of the kaolinite platelets being preserved:



Within the range 950-1000⁰ C, crystallization of $\gamma\text{Al}_2\text{O}_3$ occurs, accompanied by a considerable exothermal effect. When the oxides are further heated, the Al_2O_3 and 2SiO_2 interact between 1150 and 1250⁰ C, accompanied by the formation of mullite and free silica in the form of cristobalite or tridymite (when the temperature is further raised) as follows:



The dissolving of the quartz and decomposition products of the kaolinite in the feldspar glass occur to a more or less complete extent, depending on the temperature and firing period, thus, the amount and composition of the feldspar glass in the porcelain vary within wide limits. On the basis of theoretical calculations as well as the study of different samples, it can be stated that porcelain contains about 50-volume percent feldspar glass. As the content of feldspar is increased, the translucence of the porcelain is improved. Increasing the temperature and prolonging the firing period, keeping all other things being equal, help to increase the amount of glass in the porcelain and also further enriches the SiO_2 and Al_2O_3 content. The properties of porcelain are determined to a considerable extent by the mullite content, the amount and properties of the feldspar glass, and also the volume of sealed pores. The technical properties of feldspar glass are improved as the amount of Al_2O_3 is increased. As the quartz and the residue left from other impurity dissolve in the glass, the porcelain skeleton becomes weaker and there is more deformation. Depending on the fineness of the grinding of the quartz, the composition of the mixture, the temperature and the period of the firing, 15 to 40% of the total amount of quartz added to the mixture enters the vitreous phase. The mullite crystals forming in the porcelain improve the structural toughness of the product during firing. An equally important structural component of porcelain is the quartz particles that have not dissolved in the feldspar glass, these particles, together with the mullite crystals, form the porcelain skeleton. Mullite possesses a number of valuable properties, such as a high melting point, high mechanical and electrical strength, chemical resistance, a low coefficient of thermal expansion, and, consequently, high spalling resistance. The nucleation of mullite crystals even occurs at temperatures, of about 1200⁰C. But at

comparatively low temperature, the crystals grow extremely slowly. At the firing temperature an intensive growth of the crystals, and the feldspar glass becomes abundantly inter grown with mullite needles. An increase in the amount of fusible in the porcelain and a higher firing temperature help to increase the amount of vitreous phase and help it to fill up the pores. However, firing porcelain at temperatures about the norm for the given mixture results in the liberation of gas from the feldspar glass, bloating of the porcelain, and a decline in quality. The pores reduce the mechanical and electrical strength of porcelain, its chemical resistance, translucence, and certain other valuable properties. Thus for critical parts the porosity should not exceed 0.1-0.3% (in terms of water absorption).

Raising the firing temperature and increasing the amount of vitreous phase above 45% slightly reduces the mechanical strength of the porcelain. The electrical strength increases with an increase in the firing temperature or in the length of the period for which the ware is held at the final temperature (fig. 2.6 and 2.7 curve 2). The curve showing the variation in mechanical strength as a function of the final holding period (fig. 2.8 curve 1) reveals that holding for 3-6 hours at the final temperature during the "maturation" period produces porcelain with maximum strength. If the holding period at the final firing stage is prolonged, the mullite crystals partly dissolve in the feldspar glass, as a result of which the dielectric characteristics of the vitreous phase and the porcelain are improved. A great effect on the mechanical, and particularly on the electric resistance of the porcelain, is exerted by the porosity of the products. In high-grade high-voltage insulators, there are usually no open pores at all. If the porcelain is held for a long enough period at the final firing temperatures, the pores become spherical in shape due to the increased viscosity of the vitreous phase. Thus loses its electrical breakdown strength.

2.4 Ceramic Phase Equilibrium Diagram

Fig. 2.9 shows the pressure - temperature equilibrium diagram of most common one component system, i.e., silica. There are five condensed phases which occur at equilibrium α -quartz, β -quartz, β_2 -tridymite, β -cristobalite, and liquid silica. The



transition temperatures at 1-atmosphere pressure are also shown in the diagram. The α to β quartz transition at 573°C is rapid and reversible. The volume change is almost 2%. The other transformations shown are sluggish and requires long periods of times to reach equilibrium. The vapor pressure shown in the diagram is a measure of the chemical potential of silica in different phases. The same kind of diagram can be extended to include the metastable forms of silica, which may occur (fig. 2.10). The phase with lowest vapor pressure (the darker lines on the diagram) is the most stable at any temperature, hence called the equilibrium phase. However, once formed the transition between cristobalite and quartz is so sluggish that β -cristobalite commonly transforms on cooling into α cristobalite. Similarly, β_2 tridymite commonly transforms into α and β -tridymite rather than into the equilibrium quartz forms. Similarly, when the liquid form silica glasses which can remain indefinitely in that state at room temperature. Those transformations produce lower volume change. At any constant temperature there is always a tendency to transform a phase into another phase of lower free energy (lower vapor pressure), and the reverse transition is thermodynamically impossible. It is not necessary, however, to transform into the lowest energy form. For example, at 1100°C silica glass could transform into β cristobalite, β_2 tridymite or β quartz. Which one of these transformations actually takes place is determined by the kinetics of these changes. In practice, when silica glass is heated for a long time at this temperature, it crystallizes, or devitrifies, to form cristobalite which is not the lowest energy form but is structurally the most similar to silica glass. On cooling, β cristobalite transforms into α cristobalite. The form with the lowest vapour pressure at a given temperature is the most stable. The diagram contains curves for quartz, tridymite, cristobalite and silica-glass. Part of each curve is in full line, part in broken; the former represents the stable, the latter the unstable region. The line for quartz is full up to 870°C , where it is cut by the curve for tridymite. This means that quartz is the stable form up to 870°C ; within this range it undergoes an enantiomorphic transformation from β to α quartz at 573°C . The quartz curve is continued in the form of a broken line up to 1600°C , the melting point of α quartz. Tridymite, like cristobalite and silica glass, is thus unstable up to 870°C , even though its conversion to quartz below this temperature may not take place in finite time. At 117°C (100 - 118°C) γ tridymite inverts to β tridymite, at 163°C (140° - 165°C) to α tridymite. This

is stable only up to 1470°C , at which point it inverts to cristobalite. Tridymite melts at higher temperature than quartz, namely at 1670°C [9].

Cristobalite has an inversion point at 230°C (180° - 260°C), is stable above 1470°C and has the highest melting point of all crystalline forms of silica (1728°C). Above this temperature only the melt is stable. If cooled rapidly below the melting point of cristobalite it remains in its amorphous condition and forms silica glass. Silica glass has the highest vapour pressure of all forms of silica and the largest internal energy content. On devitrifying (crystallizing) it liberates some of its internal energy in the form of heat of crystallization.

2.4.1 Two component system - The Al_2O_3 - SiO_2 system

The Al_2O_3 - SiO_2 diagram is of fundamental importance in ceramics. The diagram which is shown in fig 2.11 has been repeatedly studied, in view of its exceptional importance in the interpretation of the physicochemical processes which are involved in the firing, melting and crystallization of different aluminosilicate ceramics, and in the understanding of the effects resulting from the interaction of these ceramics with corrosive substances. In this system, there is one compound present, mullite, which is shown as melting congruently. The eutectic between mullite and cristobalite occurs at 1595°C and contains about 94% SiO_2 . The solidus temperature between mullite and alumina is at 1840°C . Factors affecting the fabrication and use of several ceramic products can be related to this diagram. They include refractory silica brick (0.2-1.0% Al_2O_3), clay products (35-50% Al_2O_3), high-alumina brick (60-90% Al_2O_3), pure fused mullite (72% Al_2O_3), and pure fused or sintered alumina (>99% Al_2O_3).

No less than three naturally occurring silicates of alumina are known. They all have the formula $\text{Al}_2\text{O}_3 \cdot \text{SiO}_2$ but differ in crystalline habit and physical properties. They are called sillimanite, andalusite and kyanite. Owing to their importance in mineralogy and ceramics these three minerals have been intensively studied. Of prime importance in ceramics are the conditions under which they are stable, under which they are mutually convertible and under which they may occur in industrial products. At normal

temperatures and pressures only one of them can be stable, and within its range of stability the other two must convert into the stable form unless the conversion rate is too low. This question was tested by Eitel and Neumanns by comparing their energy contents: as is well known, among various forms having the same chemical composition, that which has the lowest energy content is the most stable. Strictly speaking, all other forms must change into this stable form with evolution of heat (energy), though the rate of conversion may be extremely slow. The energy contents of different polymorphous but chemically identical compounds in a system can be determined by comparing their heats of chemical reaction: the unstable form has the highest, the most stable form the lowest value. Since, generally, the glass obtained by rapid cooling of the melt represents the most unstable form, a glass corresponding to the formula $Al_2O_3 \cdot SiO_2$ should be the least stable form of this compound. Unfortunately, this glass cannot be made because of its strong devitrification (crystallization) tendency. As sillimanite has lowest energy content, it is a stable mineral. All of the other minerals become unstable, however, on heating to a white heat. They are then transformed into a new silicate, $3Al_2O_3 \cdot 2SiO_2$, called mullite and a glassy melt. Mullite is the most stable aluminium silicate at high temperatures. It is of industrial importance because it occurs in ceramic bodies and is formed on solidification of melts of a suitable composition containing alumina and silica. Actually mullite forms in a variable temperatures scale, i.e. 1300-1600°C. The formation takes place over a large temperature interval, and in all cases a silica-rich glass is formed together with mullite. Free silica in the form of cristobalite has often been demonstrated in the glass. Silicates of alumina have aroused the interest of ceramists not merely as raw materials for incorporation in ceramic bodies but also as new materials often found in the fired wares, where they occur in the form of acicular crystals. They are usually felted together in a state of disorder and occur preferentially as local agglomerations.

There is most knowledge about those substances that are formed by solidification from melts. According to Bowen and Greig, apart from the pure components only a single compound can crystallize out from a melt of alumina and silica on solidification, namely mullite, $3Al_2O_3 \cdot 2SiO_2$, but neither sillimanite nor its polymorphic modifications, andalusite and kyanite. The two-component system ($Al_2O_3 + SiO_2$) is characterized by a

minimum melting point mixture with 5.5 per cent Al_2O_3 , a so called eutectic at 1545°C and a slight inflexion in the liquidus curve at about 100°C , a so called masked maximum indicating the presence of a compound which melts with decomposition (incongruently). This compound is mullite. From the melt the following minerals may crystallize out, depending on the contents of the two oxides: cristobalite, mullite, corundum. On further cooling and solidification from the melt there remains finally only mullite, intermingled with varying amounts of silica or corundum.

2.4.2 Three component systems

Many ternary systems are of interest in ceramic science and technology. The $\text{K}_2\text{O}-\text{Al}_2\text{O}_3-\text{SiO}_2$ system is illustrated in fig2.12. This system is important as the basis for many porcelain compositions. The eutectic in the subsystem potash feldspar-silica-mullite determines the firing behavior in many compositions. Porcelain compositions are adjusted mainly on the basis of (a) ease in forming and (b) firing behavior. Although real systems are usually somewhat more complex, this ternary diagram provides a good description of the compositions used. Very often constant temperature diagrams are useful. These are illustrated for subsolidus temperatures in figure by lines between the forms that exist at equilibrium. These lines form composition triangles in which three phases are present at equilibrium sometimes called compatibility triangles. Constant-temperature diagrams at higher temperatures are useful, as illustrated in fig2.12, where the 1200° isothermal plane is shown for the $\text{K}_2\text{O}.\text{Al}_2\text{O}_3-\text{SiO}_2$ diagram. The liquids formed in this system are viscous; in order to obtain vitrification, a substantial amount of liquid must be present at the firing temperature. From isothermal diagrams the composition of liquid and amount of liquid for different compositions can be determined easily at the selected temperature. Frequently it is sufficient to determine an isothermal plane rather than an entire diagram, and obviously it is much easier^[10-15].

2.5 Changes during Firing

The changes that occur in the structure of triaxial porcelain during firing depend to a great extent on the particular composition and conditions of firing. The ternary eutectic (fig 2.13) temperature in the system feldspar-clay-flint is at 990°C , whereas the temperature at which feldspar grains themselves form a liquid phase is 1140°C . At higher temperatures an increasing amount of liquid is formed which at equilibrium would be associated with mullite as a solid phase. In actual practice equilibrium is not reached during normal firing because diffusion rates are low and the free-energy differences are small between the various phases present. The general equilibrium conditions do not change at temperatures above about 1200°C so that long firing times at this temperature give results that are very similar to shorter times at higher temperatures. Also fine grinding to reduce diffusion paths gives equivalent results in shorter firing times or at lower temperatures. The initial mix is composed of relatively large quartz and feldspar grains in a fine-grained clay matrix. During firing the feldspar grains melt at about 1140°C , but because of their high viscosity there is no change in shape until above 1200°C . Around 1250°C feldspar grains smaller than about 10 microns have disappeared by reaction with the surrounding clay, and the larger grains have interacted with the clay (alkali diffuses out of the feldspar, and mullite crystals form in a glass). The clay phase initially shrinks and frequently fissures appear. As illustrated in fig 2.14, fine mullite needles appear at about 1000°C but cannot be resolved with an optical microscope until temperatures of at least 1250° are reached. With further increases of temperature mullite crystals continue to grow. After firing at temperatures above 1400°C , mullite is present as prismatic crystals up to about 0.01 mm in length. No change is observed in the quartz phase until temperatures of about 1250°C are reached; then rounding of the edges can be noticed in small particles. The solution rim of high-silica glass around each quartz grain increases in amount at higher temperatures. By 1350°C grains smaller than 20 microns are completely dissolved; above 1400°C little quartz remains, and the porcelain consists almost entirely of mullite and glass^[26]. The heterogeneous nature of the product is illustrated in fig 2.15, in which quartz grains surrounded by a solution rim of high-silica glass, the outlines of glass-mullite areas corresponding to the original feldspar grains, and the unresolved matrix corresponding to the original clay can be clearly distinguished. Pores are also seen to be present. Although mullite is the crystalline phase in both the

original feldspar grains and in the clay matrix, the crystal size and development are quite different. Large mullite needles grow into the feldspar relicts from the surface as the composition changes by alkali diffusion. A quartz grain and the surrounding solution rim of silica-rich glass are shown in fig 2.16. Mullite needles extend into the outer edge of the solution rim, and a typical microstress crack is seen; the crack is caused by the greater contraction of the quartz grain compared with that of the surrounding matrix. Usually the quartz forms only glass, but for some compositions fired at high temperatures there is a transformation into cristobalite, which starts at the outer surface of the quartz grain. The overall structure of quartz grains, microfissures, solution rims, feldspar relicts of glass and mullite, and fine mullite-glass matrices is shown with great clarity in fig. 2.17. The changes taking place during firing occur at a rate depending on time, temperature, and particle size. The slowest process is the quartz solution [27-34]. Under normal firing conditions equilibrium at the firing temperature is only achieved at temperatures above 1400°C, and the structure consists of a mixture of siliceous liquid and mullite. In all cases the liquid at the firing temperature cools to form a glass so that the resulting phases present at room temperature are normally glass, mullite, and quartz in amounts depending on the initial composition and conditions of firing treatment. Compositions with larger feldspar content form larger amounts of siliceous liquid at lower temperatures and correspondingly vitrify at lower temperatures than the compositions with larger clay contents.

2.5.1 Phase changes that occur on heating kaolin clays

As clays are the most important part of the raw materials of the ceramic products, their behavior during firing in different ranges must be discussed. This will provide a valuable key rule in determining the firing schedule when the products are fired. The method of differential thermal analysis, when applied to kaolin minerals and to clay deposits containing principally kaolin minerals, shows a prominent endothermic effect in the region of 550-700° C, due to the dehydration of the mineral (the precise temperature depends on the particular kaolin mineral), followed by two exothermic reactions, the first

at roughly 950- 1000°C and the second between 1150°C and 1250°C, which correspond to the formation of new ~~phases~~ ^{phases}. ~~Those nature are clearly~~ shown in fig 2.5

2.5.2 Changes in the range 600-800°C

It is generally misleading to regard the structural breakdown purely as a function of the temperature. The time of heating is also important and (when the temperature is variable) the rate of heat-treating. This applies equally to the exothermic processes at higher temperatures, and for this reason it is difficult to make precise comparisons between results obtained under very different thermal conditions. Extreme cases are those in which the mineral is soaked for a long period, e.g. 24 hours, at a fixed temperature, and in which it is brought quickly to give temperature and then immediately cooled. The water of constitution remaining in the clay after drying is not completely expelled below some temperature between 450° and 600°C. Water is slowly given up, however, below this temperature, and its loss is initially accompanied by a slight contraction. The contraction following the removal of moisture on drying in the air or heating at 110°C must be regarded as due to shrinkage of the gel films on the clay particles accompanying loss of gel water. This finding may be regarded as furnishing experimental support for the view that the plasticity of clays depends in part on the existence of swollen gel layers surrounding the clay particles. Slowly heated clays show that kaolin and most clay undergo expansion up to about 500-600°C, followed by contraction. Water of constitution is not expelled from the clay substance uniformly and gradually, but within a narrow temperature interval between 450° and 600°C. This has been clearly demonstrated for kaolin by Le Chatelier ^[35] who embedded a thermocouple junction in a sample, which was then heated in an electric oven, the temperature being raised steadily. As shown in the Fig, there was retardation in the temperature rise registered by the thermocouple at about 550°C and a marked acceleration at about 1000°C. This indicates absorption of heat, i.e. an endothermic reaction, at about 550°C and a strong development of heat, i.e. an exothermic reaction, at about 1000°C. LeChatelier and many investigators ^[36-43] after him confirmed this observation with all kinds of clays. The similarity in the changes in

the curves indicates that they are due to material changes common to all clays. Where the composition differs from $\text{Al}_2\text{O}_3 \cdot 2\text{SiO}_2 \cdot 2\text{H}_2\text{O}$, the clays will have other characteristic temperature. The rate of heating has a pronounced effect on this endothermic reaction and different research workers have given subsequently different decomposition temperatures for clays. At a rate of heating of $1000^\circ\text{C}/\text{h}$, decomposition starts at about 550°C but with the slower rate of $200^\circ\text{C}/\text{hr}$ it starts at about 460°C . By heating in vacuum the temperature of expulsion of water can be strongly depressed, as Mellor and Holderofts demonstrated.

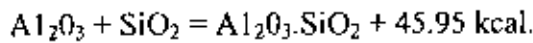
2.5.3 Changes in the range $800\text{-}1400^\circ\text{C}$

From a survey of published data it is difficult to arrive at any final conclusion. The conflicting conclusions of different workers, all of whom identified the phases present by X-ray methods, may perhaps be partly attributed to a number of causes, such as (i) the effect of impurities associated with the clay mineral, (ii) the variety of heat treatments employed. As an illustration of (ii), the following may be quoted: Insley and Ewell heated specimens of kaolinite and dickite at 6°C per minute and then air-quenched from 925°C and 985°C , temperatures corresponding to the beginning and the maximum of the first exothermic reaction, and also from 1000°C and 1200°C . They also examined the effect of preheating at constant temperature for various temperatures between 840° and 910°C . Hyslop¹² examined one Scottish clay, which was heated for 15 hours at 800°C followed by 20 hours at 1050°C hours at 1150°C .

2.5.4 The exothermic reaction at $900\text{-}1050^\circ\text{C}$:

The heating curves of clays depicted in figure exhibit sharp rises at 900 to 1000°C . This points to an exothermic reaction, taking place in the material. Two reactions may be considered as possible causes of the evolution of heat: conversion of alumina from the γ to the α form and a combination of γ alumina and silica to form sillimanite or mullite. The first has often been studied on heating curves of pure specimens. It takes place with strong evolution of heat but does not invariably occur with all forms of alumina. Exceptions are, for instance, diaspore, $\text{Al}_2\text{O}_3 \cdot \text{H}_2\text{O}$, and hydrargillite, $\text{Al}_2\text{O}_3 \cdot 3\text{H}_2\text{O}$, but it is

found with precipitated alumina, bauxite and γ alumina. It also observed the lines of alumina in X-ray spectra taken at 1000°C . On the basis of these observations, the formation of silicates from clay must be limited to higher temperature regions. The second reaction is theoretically possible, since the exothermic character of sillimanite formation from the oxides has been proved:



He originally gave the temperature of formation as $1100\text{-}1200^{\circ}\text{C}$. but it may be assumed to start several hundred degrees lower with the intimate mixture of extremely fine, molecularly dispersed reactants present in mildly calcined kaolin. In this connection the statement of Hyslop and Rooksby¹⁰ that sillimanite or mullite formation starts at 870°C deserves to be mentioned. Accordingly, we may attribute the exothermic reaction in this temperature range to the conversion of γ Al_2O_3 to α Al_2O_3 and to aluminium silicate formation. The specific surface, S, as determined by absorption of N_2 or O_2 , remains almost unchanged after heating to 800°C . It is practically uninfluenced by loss of water of constitution, although the 'holes' left in the lattice by the water lost are large enough to accommodate H^+ ions. Nevertheless, the dehydrated kaolin shrinks and its lattice is in disarray. Above 900°C the apparent density increases markedly, and S decrease.

2.6 Dielectric Properties

All dielectrics placed in an electric field will loose their insulating properties if the field exceeds a certain critical value. This phenomenon is called dielectric breakdown, and the corresponding electric field is referred to as the dielectric breakdown strength ^[44-46]. Dielectric strength, therefore, may be defined as the maximum potential gradient, to which a material can be subjected without insulation breakdown. that is,

$$\text{DS} = \left(\frac{dV}{dx} \right)_{\text{max}} = \frac{V_B}{d}$$

Where DS is the dielectric strength in kV/mm, V, the breakdown voltage, and d the thickness of the sample.

Dielectric Constant is the property of a ceramic material that determines the relative speed that an electrical signal will travel in the material. Signal speed is roughly inversely proportional to the square root of the dielectric constant. A low dielectric constant will result in a high signal propagation speed and a high dielectric constant will result in a much slower signal propagation speed.

Dielectric constant is not an easy property to measure or to specify, because it depends not only on the intrinsic properties of the material itself, but also on the test method, the test frequency and the conditioning of samples before and during the test. Dielectric constant tends to shift with temperature. Related to dielectric constant (or "permittivity") is dissipation factor. This is a measure of the percentage of the total transmitted power that will be lost as power dissipates into the laminate material. Dielectric constant and dissipation factor are not normally considered except in high-tension ceramic insulator. Often dielectric properties are hard to correlate and care must be taken in working with them. Many commercial laminators and most board producers do not have this equipment in house and depend on outside test facilities to do they're testing for them. The dielectric constant is the ratio of the permittivity of a substance to the permittivity of free space. It is an expression of the extent to which a material concentrates electric flux, and is the electrical equivalent of relative magnetic permeability.

As the dielectric constant increases, the electric flux density increases, if all other factors remain unchanged. This enables objects of a given size, such as sets of metal plates, to hold their electric charge for long periods of time, and/or to hold large quantities of charge. Materials with high dielectric constants are useful in the manufacture of high-value capacitors. A high dielectric constant, in and of it, is not necessarily desirable. Generally, substances with high dielectric constants break down more easily when subjected to intense electric fields, than do materials with low dielectric constants. For

example, dry air has a low dielectric constant, but it makes an excellent dielectric material for capacitors used in high-power radio frequency (RF) transmitters. Even if air does undergo dielectric breakdown (a condition in which the dielectric suddenly begins to conduct current), the breakdown is not permanent. When the excessive electric field is removed, air returns to its normal dielectric state. Solid dielectric substances such as polyethylene or glass, however, can sustain permanent damage.

2.6.1 Different types of dielectric breakdown

Dielectric breakdown occurs in gases due to corona discharge in non-uniform fields or to photo ionization and collision of electrons with gaseous atoms, leading to further ionization, increased conduction and dielectric breakdown. In liquids, breakdown is due primarily to dielectric heating and increased ionization processes. This process is greatly accelerated by the presence of impurities or high concentrations of mobile ions (Na^+ , Li^+) in the liquid. For solids, the main breakdown mechanisms can be described as intrinsic, thermal, and ionization breakdown. A possible fourth mechanism, electrochemical degradation or breakdown is associated with ion migration under a (dc) field gradient at elevated temperatures.

2.6.1.1 Intrinsic Breakdown

At high-applied fields electrons may be ejected from electrode materials or may even be generated from the valence band. These electrons are then accelerated through the crystal and some undergo electron-phonon interactions, generating heat and being absorbed in the process. Electrons collide with ions or atoms in the solid, knocking out the electrons and elevating them to the conduction band. These newly generated electrons are in turn accelerated by the field generating electrons, resulting finally in an "avalanche" of conducting electrons over a narrow area and breakdown generally through a channel. Electronic or intrinsic breakdown of this type can occur in all solids but is rarely observed, since the very high fields required (10^6 - 10^7 V/cm) usually trigger other breakdown mechanisms. Temperature has a very pronounced effect on the electron-

phonon interactions and hence on intrinsic breakdown. At very low temperatures ($\ll 25^\circ\text{C}$), phonon interactions are weak, so that electrons gain more energy from the field and are able to generate many free electrons. Hence breakdown voltages are relatively low. Intrinsic breakdown voltage peaks at room temperature, where phonon interactions become important, but decreases again above room temperature, since thermal vibrations can now generate free electrons as well. In glasses and amorphous materials the irregular structure makes the mean free path for electrons fairly uniform with temperature. Hence the decrease in strength with temperature is more gradual and such factors as composition pulse duration and field strength become more important. Intrinsic breakdown is characterized by short breakdown times, $\sim 10^{-8} - 10^{-6}$ sec, as well as by increased conductivity with increase in field strength.

2.6.1.2 Thermal Breakdown

This is the most common dielectric failure mode in ceramic insulators, the dielectric strengths typically two orders of magnitude lower than intrinsic breakdown strengths. Causes for failure are generally attributed to local heating or conduction losses, which generate heat at a faster rate than it can be removed. This increases the local temperature, even to the point of melting or evaporation. Depending on the material and the thermal gradients formed, cracks may develop around the local hot spot. The combination of ionized gases and increased conduction cause dielectric breakdown. The energy generated by an (ac) field can be given as:

$$W = \omega \epsilon_0 k' V^2 \tan \delta \sim \omega V^2 C \tan \delta$$

Where W (watts/cycle) is the energy generated, V the voltage, and C the capacitance of the sample (farads). The heat dissipated from the sample can be approximated by

$$H_D = Ah (T_s - T_A)$$

Where H_d represents the heat dissipated (watts, cal/sec), A the surface area of the sample (cm^2), h the surface heat transfer coefficient ($\text{cal/sec}^\circ\text{C-cm}^2$), and T_s and T_A the surface and ambient temperatures, respectively. To avoid heat accumulation and breakdown, the heat dissipated must equal the heat generated. As is evident from the expressions above, heat generation is dependent on both frequency and voltage and on the material parameters k' and $\tan\delta$. These different factors can, therefore, be manipulated to avoid thermal breakdown, as can the size, shape, and heat-transfer environment of the ceramic part. The latter equation, for example, can be used in the design of discrete capacitors, where the heat dissipated is dependent on the size (surface area), temperature gradient, and surface heat transfer coefficient (0.0002 - 0.002 cal/sec-C-cm^2 for low to moderate airflow conditions).

2.6.1.3 Ionization Breakdown

Ionization breakdown occurs in inhomogeneous dielectric solids mainly through the mechanism of partial discharges resulting from pores or cracks being present in the ceramic. Ionization of gases inside the pores in the ceramic when subjected to a high electric field results in the local generation of heat, which is transmitted to the surrounding ceramic, resulting in a temperature gradient, the generation of thermal stresses, increased dielectric losses, and increased conduction locally. The stresses can generate cracks, leading to further ionization, and breakdown occurs via a thermoionization process similar to that described for thermal breakdown. The presence of porosity in an insulator is, therefore, deleterious to high dielectric strengths.

2.6.1.4 Electromechanical Breakdown

This is caused usually by ion migration (Na^+ , Ag^+ , OH^-) under a continuously applied dc field at moderately elevated temperatures (50 - 200°C). This may lead to interelectrode shorting of closely spaced electrodes or to ion buildup or depletion at one or the other electrode, leading to high local fields and electrode corrosion. These conditions are all time dependent but can lead to thermal breakdown, after prolonged exposure. To evaluate

electrochemical breakdown, dc fields $>3000\text{V/cm}$ at $100\text{-}200^{\circ}\text{C}$ in dry ambient (N_2) for periods of 1000hr may be applied to the dielectric, with resulting current, voltage-time curves of the type shown in Figure. For most ceramic insulators, especially glasses, an initial absorption current is followed by a more gradual approach to equilibrium, reflecting rapid initial ion migration and subsequent slowing down by the uneven potential barriers in the structure. A steady-state condition is then maintained for several hours, culminating, if breakdown occurs, in a gradual to sudden increase in current flow. The point of departure from steady state can be taken as the electrochemical breakdown for the given conditions. Such information is frequently important for microelectronic circuit applications such as Ag conducting lines on an Al_2O_3 substrate, where a potential difference may exist between the lines. This situation is aggravated by the presence of high humidity; hence encapsulation of such circuits is often necessary.

2.7 Factors Affecting Dielectric Strength

Factors that may affect dielectric strength include composition, micro-structural features (porosity, cracks, flaws and second phases), and measurement parameters such as electrode configuration, specimen thickness, temperature, time, frequency, humidity, and heat transfer conditions. Compositional effects relate to the amorphous or crystalline nature of the material and to the presence of mobile ions in the structure. Increased alkali concentration, for example, not only leads to higher bulk conduction, but also renders the surface more hygroscopic. The combined effects of surface porosity, surface alkali, and moisture may lead to high surface currents and breakdown; hence porcelain bodies intended for high-voltage applications are typically glazed to minimize these effects. Microstructural features such as cracks and porosity can lead to ionization of entrapped gases at high fields, particularly under high-humidity conditions. This in turn can lead to high current flow, local heating, cracking, and thermal breakdown as described. The effect of grain size and second phases depends on the details of the structure, but smaller grains will, in general, result in higher dielectric strengths, reflecting the reduced conduction in the solid.

Dielectric strength is perhaps most sensitive to changes in measurement conditions. Electrode geometry is especially important since the breakdown voltage tends to decrease with electrode area. Because of the high fields involved, point contacts can precipitate breakdown through field injection of electrons into the dielectric. To minimize this effect and provide environmental control, measurements are usually carried out with the sample immersed in high-dielectric grade (silicone) oil. This essentially fixes the surface heat transfer and humidity conditions. Dielectric strength values are very sensitive to specimen thickness, which must be specified if results are to be meaningful. This is because flaw density and microstructural defects increase with the thickness (volume) of the specimen under test, leading to lower measured dielectric strengths as sample thickness is increased. Dielectric strength evaluations are typically carried out at room temperature and 60Hz. The measured dielectric strengths are higher for shorter pulse or time duration of the applied voltage, due to the decrease in conduction and polarization losses in the dielectric at higher frequencies. For particular applications, therefore, dielectric strength evaluations should be carried out within the temperature and frequency range of interest. The effect of higher temperatures is to decrease the dielectric strength due to higher conduction in the solid.

It is well recognized that during service, the properties of an insulating material become degraded and eventually dielectric breakdown occurs at a field below that predicted by experiments on fresh forms of the insulation. Aging is a term used to in-a general sense, the deterioration in the properties of the insulation. Aging therefore determines the useful life of the insulation. There are many factors that either directly or indirectly affect the property and performance of an insulator in service. Even in the absence of an electric field, the insulation will experience physical aging whereby its physical and chemical properties change considerably. An insulation that is subjected to temperature and mechanical stress variations can develop structural defects as microcracks, which are quite damaging to the dielectric strength, as mentioned above. Irradiation by ionizing radiation such as X-rays, exposure to severe ambient conditions such as excessive humidity, ozone and many other external conditions, through various chemical processes, deteriorate the chemical structure and properties of an insulator. This is generally much

more severe for polymers than ceramics, but it is not practical to use a solid ceramic insulation in a coaxial power cable.

The chemical aging processes are generally accelerated with temperature. In service, the insulation also experiences electrical aging as a result of the effects of the field on the properties of the insulation. For example, dc fields can dissociate and transport various ions in the structure and thereby slowly change the structure and properties of the insulation. Electrical trees develop as a result of electrical aging because, in service, the ac field gives rise to continual partial discharges in an internal or surface microcavity, which then erodes the region around it and slowly grows like a branching tree. In well-manufactured insulation systems, electrical treeing has been substantially reduced or eliminated from microvoids. A form of electrical aging that is currently in vogue is water treeing, which eventually leads to electrical treeing.

The surface of the insulation may become contaminated by ambient conditions such as excessive moisture, deposition of pollutants, dirt, dust, salt spraying etc. Eventually the contaminated surface develops sufficient conductance to allow discharge between the electrodes at a field below the normal breakdown strength of the insulator. This type of dielectric breakdown over the surface of the insulation is termed as surface tracking.

It is apparent that there are a number of dielectric mechanisms and the one that causes eventual breakdown depends not only on the properties and quality of the material but also on the operating conditions, environmental factors being no less important. It is apparent that it is not possible to clearly identify a specific dielectric breakdown mechanism for a given material. Polycrystalline dielectrics contain the crystalline as well as amorphous phase. The inhomogeneity of the ceramic body depends on its composition and on the forming and firing process. Behind the low dielectric strength porosity is one of the cause

The formation of closed pores depends on the firing process. Form and size of the pores depend chiefly on the properties of the vitreous phase. Thus, for instance, high voltage porcelain insulators contain, if properly fired, spherical pores of about 15 μm .

The inhomogeneity of the dielectric causes the ion of the electric field. From the point of view of their influence of the electric field the gas-filled voids are of particular interest. At first approximation there are two cases: non-ionized voids and, ionized voids. The breakdown field of a thin air gap increases considerably with decreasing thickness. The ionized spherical void induces in its vicinity a strong inhomogeneous field with a higher field stress in the direction of the external field. This may account for the lower breakdown voltage of inhomogeneous dielectrics with higher dielectric constants.

The thickness used in computing the dielectric strength shall be the average thickness of the specimen measured as specified in the test method for the material involved. For a description of test specimens of materials and their preparation, reference shall be made to the ASTM methods (D3755) applicable to the materials to be tested. Sheets and plates less than 3 mm thick are used as standard thickness. The thickness is kept below 3mm to reduce the probability of remaining cracks, porosities and other microstructural flaws, which will lead to the low dielectric strength. This is because some conductive medium like air and water may present and this will conduct current in a higher rate than solid porcelain.

In the preparation of test specimen from solid material care should be taken that the surface in contact with the electrodes are parallel and as plane and smooth as the material permits. The dielectric strength of solid commercial electrical insulating material is greatly dependent upon the specimen thickness. Experience has shown that for solid and semi solid materials, the dielectric strength varies inversely as a fractional power of the specimen thickness and there is a substantial amount of evidence that for relatively homogenous solids, the dielectric strength varies approximately as the reciprocal of the square root of the thickness.

Sometimes the oxide particles, non-metallic inclusion or other form of impurities are present on the surface of the specimen. So the applied voltage find a conductive path on the surface and passed through the surface instead of through the entire insulator. This is known as flash over. Because of flash over the dielectric strength becomes lower. The breakdown of thick solid materials is generally so high that the specimen must be immersed in insulating fluid to prevent flash over and to minimize partial discharge. Transformer oil was used in the experiment to prevent flash over.

The relative humidity influences the dielectric strength to the extent that moisture absorbed by, or on the surface of, the material under test affects the dielectric and surface conductivity. Hence its importance will depend to a large extent upon the nature of the material being tested. However even materials that absorbed little or no moisture may be affected because of greatly increased chemical effects of discharge in the presence of moisture. The combined effect of surface porosity and moisture may lead to high surface current and breakdown.

Test result is influenced by the rate of voltage application. In general, the background voltage will tend to increase with increasing rate of voltage application. This is to be expected because the thermal breakdown mechanism is time dependent, although in some cases the later mechanism may rapid failure by producing critically high local field intensifies.

The surrounding medium can effect the results of dielectric strength. Because it affects the heat transfer rate, external discharges, the field uniformity, thereby greatly influencing the test results. Results in one medium cannot be compared with those in a different medium.

2.8 Factors affecting mechanical strength

The mechanical strength measures the ability of the ceramic material to withstand the thermal and mechanical stresses to which it might be subjected during use. It is also

related to the composition and structure of the material, but micro structural features such as pores, cracks, flaws, second phases, grain size, and grain boundary stresses are usually dominant. These factors are rarely quantifiable, and therefore scatter in measured data tends to be large. As with thermal conduction, dense single-phase tend to have high rupture moduli, possibly for the same reasons, whereas complex mixed oxides and glasses have moderate to low values. The practical range of values for ceramic insulators is 40-800 MPa, but higher values can be achieved with special processing. The properties discussed above often interact, especially where use condition result in development of thermal stresses, due to the existence of thermal or expansion gradients in the ceramic. Such conditions may occur where localized hot spots develop on a substrate due to direct heating or to dissipation of heat from a resistor or active device. A combination of high specific heat and high thermal conductivity would thus serve to minimize the rise in temperature and the accompanying thermal stresses. If not relieved, such stresses can result in mechanical and dielectric degradation of the system. Similar considerations arise where there is thermal expansion mismatch across interfaces, as in the use of enamel or glaze coatings and passivation layers on metal or ceramic substrates. For ceramic insulators, possible destructive effects on heating are controlled by the thermal diffusivity, expansion coefficient, elastic modulus, and tensile strength of the material. These properties may be conveniently grouped as components of the thermal shock resistance, defined as the maximum quenching or heating rate to which the material can be subjected without undergoing physical damage or rupture. A practical measure of this quantity is the maximum temperature to which the ceramic can be heated and then quenched in water at 250° C without causing physical damage.

The mechanical strength depends strongly on size and shape (S) of the test specimens as well as on transient factors such as thermal diffusivity, which may be difficult to define precisely under test conditions. Thermal shock resistance is, nonetheless, an important design parameter in choosing ceramic insulators for applications, where temperature changes may be severe, such as for heater and resistor core and thick-film substrate applications. Of the properties contributing to the thermal shock resistance, the modulus ration and the thermal diffusivity tend to vary only over narrow ranges. The thermal

diffusivity range for most ceramic insulators is $0.1-0.3\text{cm}^2/\text{sec}$. This is generally true also for the tensile strength and elastic modulus, which are closely related to chemical bonding and structure in the different solids. The elastic moduli for ceramic insulators fall in the narrow range of 34-414 GPa, reflecting the very strong ionic or covalent bonding. Tensile strengths for ceramic insulators are considerably lower and more variable, since they are dependent on processing, test conditions, and flaws in the ceramic. Even so, high elastic moduli can usually be correlated with high tensile strengths, so that variability in the ratio of the two is small.

Ceramic insulator does absorb a certain amount of water. Insulator with low water absorption is far more resistant to frost. Also with lower water absorption bending strength of insulator will increase. Water absorption is measured in percentage of liquid absorbed by insulator compared to a dry insulator.

Ceramics insulator shows brittle failure. In ceramic insulator, due to the combined ionic and covalent bonding mechanism, the particles cannot shift easily. The ceramic insulator breaks when too much force is applied, and the work done in breaking the bonds creates new surfaces upon cracking. Brittle fracture occurs by the formation and rapid propagation of cracks. In crystalline solids, cracks grow through the grain transgranular and along cleavage planes in the crystal. The resulting broken surface may have a grainy or rough texture. Amorphous materials do not contain grains and regular crystalline planes, so the broken surface is more likely to be smooth in appearance.

Any flaw, such as a pore, crack, or inclusion, results in stress concentration, which amplifies the applied stress. Pores also reduce the cross-sectional area over which a load is applied. Thus, denser, less porous materials are generally stronger. Similarly, the smaller the grain size the better the mechanical properties. In fact, ceramic-insulating materials are the strongest known monolithic materials, and they typically maintain a significant fraction of their strength at elevated temperatures.

Bending strength is important in ceramic insulator used in power transmission. The bending strength of a ceramic is usually much greater than their tensile strength. To make up for this, ceramic insulators are sometimes prestressed in a compressed state. Thus, when a ceramic insulator is subjected to a tensile force, the applied load has to overcome the compressive stresses (within the object) before additional tensile stresses can increase and break the object. Ceramic insulators are generally quite inelastic and do not bend like metals. Rigidity varies with the composition and structure. The ability to deform reversibly is measured by the elastic modulus. Materials with strong bonding require large forces to increase space between particles and have high values for the modulus of elasticity. In amorphous materials, however, there is more free space for the atoms to shift to under an applied load. As a result, amorphous materials such as glass are more easily flexed than crystalline materials such as alumina or alumina-silica porcelain.

EXPERIMENTAL

3.1. Introduction

The study was undertaken to identify different phases in the microstructure and to determine properties of the ceramic insulators. To perform the study a variety of samples were prepared. The samples were prepared conforming to the same chemical composition used in Bangladesh Insulator and Sanitary ware Factory Ltd. (BISF) and varying the proportion of the raw materials used in BISF body and their properties were studied. Although the BISF technology (fig. 3. 1) for the commercial manufacture of ceramic insulator product was followed to prepare the samples, certain steps in the process was altered. After processing, the structural characterization was carried out by x-ray diffraction technique, the electric property like dielectric strength was measured by high voltage dielectric tester. to develop microstructural development the specimens were prepared by ceramographic technique followed by optical and Scanning Electron microscopy. Chemical analysis was done by traditional gravimetric analysis, EDAX analysis and X-ray fluorescence (XRF). Some physical and mechanical property i.e., density, hardness, bending strength, were also measured to establish the adaptability of the products at high tension.

3.2. Ceramic insulator body Preparation

3.2.1. Raw material selection

The raw materials used to prepare BISF body samples are listed below:

1. China Clay
2. China Clay (Rajmahal)
3. Ball Clay (White)
4. Bejoypur Clay (Grade 1)

5. Washed Bejoypur Clay
6. Ball Clay (Black)
7. Feldspar
8. Quartz

Table 3.1 and 3.2 show the grain size distribution and the chemical analysis of each raw material respectively. The detailed description about these raw materials is available in the Technological Report on 'Evaluation of Raw Materials from Bangladesh 98'. The percentage of raw materials added to prepare the BISF body is shown in the Table 3.3, and the resultant final BISF body composition is shown in the Table 3.4. Number of samples were prepared using different firing temperatures and the chemical composition is shown in table 3.5

3.2.2 Chemical analysis

The basic requirement of the quality product is to use high-grade raw materials and for this reason chemical analysis of the raw materials is mandatory in every batch. The analysis of the raw material was done by conventional volumetric method and XRF. Again the chemical analysis was also done to find out the constituents of the final products. Here mainly the weight percentage of SiO_2 , Al_2O_3 , Fe_2O_3 , K_2O , Na_2O , MgO , CaO and TiO_2 in the raw materials and the final product were measured.

3.2.3 Crushing

Many raw materials need to have the size of their lumps, aggregates, particles, etc., reduced before they can be used in ceramic manufacture. In general, crushing refers to reduction of large lumps to a convenient size for secondary reduction. Actually in the processing of ceramic insulator materials the raw materials used were clays, feldspar and quartz. The components to be crushed are feldspar and quartz. The jaw crushers were used to perform this operation. After that secondary crusher and grinder like ball mill or attrition mill were used to reduce the size.

3.2.4 Ball milling or pot milling

Clays, feldspar and quartz with different percentages were mixed in the pot mill and the mills were rotated at a speed at which the pebbles (or grinding balls), etc., are carried up the side and then roll over each other to the bottom. The grinding is therefore effected by impact and rubbing. Water was added to the clays with the ratio of 1:1 so that a proper consistency of the mixing was happened. The duration of milling, one of the determining factors of the particle size of the raw materials was 16 to 18 hours. The final particle size after milling was about 50 to 60 μm .

3.2.5 Magnetic particle separation

Certain minerals can be purified by magnetic methods although they are not ferromagnetic. The susceptibility to intense magnetic fields of such feebly magnetic materials is insufficient to attract them against the force of gravity, as is done in the removal of strongly magnetic material. But by applying very high magnetic field intensity horizontally to a falling stream the more susceptible particles can be deflected sufficiently to effect a separation. The raw materials were crushed and ground to a size where the minerals to be separated were no longer mechanically bound together. The particle size was less than 60 μm . The magnetic separation was carried out by applying strong magnetic field when the material is in the wet condition. The raw materials were passed through the field and the separation was carried out.

3.2.6 Reservoir

After grinding and milling, many materials are stored for short or long periods. Clay slips, mixed body slips may be stored in tanks which are kept agitated just enough to prevent separation. They operate much like blungers, but less vigorously. In the present research, the need of reservoir was limited. Actually the slip was produced and the

material was cast directly, as the amount of the material was small. But for the large scale production the reservoir is must.

3.2.7 Filter press or casting in plaster of paris mould

In the large scale production the clay slurries and slips used for purifying and mixing can be dewatered by a number of ways. The commonest method is filter pressing. Actually filter clothes are used with applying pressure mechanically in the dewatering. This process is rapid and economical. In the present research work, no filter press was used. As the amount of material required to produce samples was small, the slip was cast directly into the plaster of paris mould. The slurry was processed to lower down the moisture content to 18-20% in the plaster of paris mould. The dry plaster mould will suck the water down to 18-20%. The slurry was kept in the mould for sufficient time to lower the moisture content.

3.2.8 Pug milling

The function of pugmill is to improve the uniformity of a plaster clay body giving it greater workability because of the proper coating of clay particles with water. The vacuum machine that is fixed with the pug mill does this more thoroughly as they also remove any air bubbles. The materials under study were pugged with the pug mill and rod type samples of 10 mm in diameter and 135 mm in length was prepared.

3.2.9 Drying

The humidity was first increased to 60 to 70% so that the initial drying rate was low while at the same time the temperature was raised. The humidity was kept high to control drying during the critical period of drying shrinkage. Subsequently the later stages were rapid. This allowed the process to be carried out rapidly without causing defects in the ware. Drying temperatures in the tunnel dryers was kept at 120-130⁰C and the duration of drying was 24 hours.

3.2.10 Firing

Firing was fired in tunnel kilns. In tunnel kilns, ware passed through the kiln the temperature distribution along the kiln was kept constant. Air for combustion was heated by the cooling ware, and the combustion gases passed over the kiln and heated all the ware entering. In this way the heat content of the combustion process was utilized with great efficiency. The firing curves for the production of the samples is shown in fig 3.2(a). The deviation of this curve can be compared with the standard firing cycle curve in fig 3.2(b). An irregularity in the firing insulators at the BISF is clearly noticeable. The cooling too fast to introduce serious residual stresses in the fired product. Also, the heating cycle was not uniform and may cause warpage or crack in the product.

3.3 Physical Properties Measurements

3.3.1 Density Measurements

Average thickness and diameter of each sample was measured to calculate the average volume (V) of each sample. The weight (W) of the sample was taken and the density of the sample was calculated using the formula

$$D = \frac{W}{V}$$

3.3.2 Hardness Measurements

Vickers microhardness test was applied to the specimen fired at different temperatures. The place was chosen so that the point of indentation doesn't fall on the pores. The Vickers hardness test uses a pyramidal diamond with an angle of 136° between faces. The Vickers hardness number of a material is defined as the load applied divided by the contact area of the indenter. For the standard Vickers indenter this reduces to

$$\text{Hardness} = \frac{1.8544P}{d^2}$$

The Vickers microhardness test applied the load of 200gm. The standard of the Vickers microhardness, which was followed, can be found on ASTM E384.

3.3.3 Bending Strength Measurement:

High demands are made on commercial ceramic insulator in respect of mechanical strength. For this reason it is tested for bending strength. On bending a rod the lower layers are stressed in compression, the upper in tensions. For ceramic product cross breaking strength is usually more important than crushing or tensile strength, but bodies with the highest crushing strength usually also have the highest strength. Bending strength measurements were carried out for the samples prepared. The machine that was employed for bending test measurements is called Bending strength tester. Here a static load was employed at the center of the specimen. The specimen was held by supports at the both ends. A scale recorded the load employed, which was not the direct reading. This reading then converted into actual reading (Kg/cm²). A formula was employed to convert the machine reading, which is presented below:

$$\sigma_{bh} = \frac{F_b L_s}{4M}$$

where

F_b = Breaking load in N (Scale value)

L_s = Width between supports in mm

M = Moment of resistance in mm³ (Dependent on the cross section shape of the specimen)

$$= \frac{\pi d^3}{32}$$

where d is the diameter of the sample

σ_{bh} = Ultimate breaking end bending stress (N/mm²)

3.4 Microstructural Characterization

Ceramic materials are finding increased application in many areas of technology and the microstructural analysis of ceramic materials is therefore more becoming common in materials testing laboratory. Among others light and electron microscopy play an important. Like metallic material the prepared specimens are preferably examined with reflected light or scanning electron microscope. The methods for metallographic sample preparation can, with some modifications, also be used for ceramic materials. The microstructural examination of ceramic materials is known as "ceramography."

3.4.1 Optical Ceramography

Ceramic materials are extremely hard materials requiring different procedures than those used for metals. Although some samples were sectioned with special abrasive wheels, however, diamond wheels are preferred in other cases. Grinding with emery or silicon carbide paper was not used because very little material would be removed before the paper wears out. Diamond pastes were used, almost exclusively, for all stages of preparation.

3.4.1.1 Sample Preparation for ceramography

Sampling is done almost exclusively by sectioning with motorized cutoff machines using water emulsions as lubricants and coolants. Low speed (1000 rpm) was applied which is suitable for ceramic insulator. As in metallography, mechanical grinding and polishing methods are also most common in ceramography, where materials are successively removed from the surface by the grinding and polishing media. Hand grinding is a very tiring chore; automatic devices are definitely preferred. Several procedures were used to hold the diamond abrasives during rough and fine grinding, such as diamond on cast-iron or cerad wheels, rosewood rods, and resin or metal bonded diamond laps. The samples were prepared by the diamond cerad wheels in the laboratory. Depending on the smoothness of the cut, preparation commenced with 60-, 45- or 30- μm diamond discs.

With automatic devices, relatively high pressures and short times (1 to 2 min) were used with a wheel speed of about 300rpm and copious water-cooling. Coarser grits were required to grind an as-sintered surface. Rough polishing was conducted using 6- or 1- μm diamond paste on nylon, Texmet, or Pellon cloths. Polishing times of 1 to 2 min were used with very high pressure and low (150 rpm) wheel speeds. Final polishing was performed using 1/4 μm diamond paste on a low nap or napless cloth with high pressure for about 1 min. These procedures are necessary to minimize stress relief in ceramic materials.

3.4.1.2 Etching

It is good practice to examine a ceramic specimen in its as-polished condition under the microscope before etching. This permits the evaluation of the amount of pores and their distribution and possibly the evidence of breakouts, inclusions, contaminations and cracks should be analyzed first on the unetched specimen. They will have to be etched, though, to reveal the grain boundaries, phases and the other microstructural features. The etching were performed by immersing the samples in 1 % hydrofluoric acid for 10 to 15 minutes. Another etching techniques were followed where etching was performed by immersing the sample in 4% hydrofluoric acid maintained at 0^o C for 10-15 seconds. After etching the samples were observed under optical microscope at high magnification (x100 and x400) and micrographs were taken as necessary. Optical contrasting techniques such as darkfield, polarized light, and phase contrast play only a minor role in the examination of microstructures in advanced ceramics prior to etching. They are more successfully applied in combination with etching. This is related to the fact that chemically etched ceramic specimens, examined under the microscope with reflective brightfield illumination, produce a low contrast and whitish image. Ceramics permit the light ray to penetrate the surface, resulting in scattering and internal reflections of the light, rendering it difficult to obtain a true image of the surface. To eliminate light scattering and to improve the reflectivity, it is recommended that the specimen surface be coated with a reflective layer. Such a layer should be between 5 and 10 nm thick and can

be sputter coated with either Au or Al. This way the details of the structure's topography are truly revealed.

3.4.2 Scanning Electron Microscopy

The Scanning Electron Microscope (SEM) is one of the most versatile and widely used tools of modern science as it allows the study of both morphology and composition of biological and physical materials. By scanning an electron probe across a specimen, high-resolution images of the morphology or topography of a specimen, with great depth of field, at very low or very high magnifications can be obtained. Compositional analysis of a material may also be obtained by monitoring secondary X-rays produced by the electron-specimen interaction. Thus detailed maps of elemental distribution can be produced from multi-phase materials like our ceramic materials. Characterization of fine particulate matter in terms of size, shape, and distribution as well as statistical analyses of these parameters, may be performed. For ceramic insulator the scanning electron microscopy is a must because it will reveal very fine micron size cracks within the phases and will also show the characteristics of different phases, their orientation and other topographical effect over the surface. The size of the porosity and the microcracks can be greatly analyzed by SEM and as porosity and cracks influence the mechanical strength and dielectric strength, we can make comments on dielectric and mechanical behavior by observing the SEM images.

3.4.2.2 Specimen Preparation

Three requirements for preparing ceramic samples for a regular SEM are

- 1) Remove all water, solvents, or other materials that could vaporize while in the vacuum.
- 2) Firmly mount all the samples.
- 3) Ceramics should be coated so they are electrically conductive.

The preparation of sample usually follows the same as cinematography. After etching if the sample produces good images under microscope then it will be prepared for SEM. First it is cleaned ultrasonically to remove all the loose particles, water, etching reagents or other materials that are harmful in vacuum. Then the specimen is mounted in SEM stand and ready for coating.

3.4.2.3 Coating

Coating used in SEM analysis is aimed mainly at the following:

1. Preventing the charge-up on the specimen surface by covering it with a conductive material.
2. Increasing secondary electron emission by covering a specimen of low secondary electron emission with a metal of high secondary electron yield.

For coating, the sputtering method is generally used. With the improved resolution of the SEM, coating techniques for high magnification are still under study. However, various substances are being used i.e., C, AU, AU-Pd, and Pt, which must be selected depending on the purpose and magnification. For our convenience we have coated with carbon. It is necessary to select a coating suitable for the observation magnification. If the coating is too thick, its particles become visible while at the same time the structures of interest are may be obscured.

3.4.2.4 Sputtering

This device is most widely used for observing specimen surface morphology. When coating polymer materials that are easily damaged by ion irradiation and electron irradiation, the triode-type magnetron-sputtering device is recommended over the diode sputtering. As metals, AU and AU-pd are generally used because they are easily obtained and generate secondary electrons well. Recently, however, high-melting metals such as Pt

and W have been used for high magnification observation, because of their high granularity

In our laboratory we have used the Agar SEM Carbon coater

3.5 Phase Analysis by X-ray Diffraction

A given substance always produces a characteristic diffraction pattern, whether that substance is present in the pure state or as one constituent of a mixture of substances. This fact is the basis for the diffraction method of chemical analysis, i.e., phase analysis. Qualitative analysis for a particular substance is accompanied by identification of the pattern of that substance. The particular advantage of diffraction analysis is that it discloses the presence of a substance as that substance actually exists in the sample, and not in terms of its constituent chemical elements. For example, if a sample contains the compound A_xB_y , the diffraction method will disclose the presence of A_xB_y as such, whereas ordinary chemical analysis would show only the presence of elements A and B. Furthermore, if the sample contained both A_xB_y and A_xB_{2y} , both of these compounds would be disclosed by the diffraction method, but chemical analysis would again indicate only the presence of A and B. Another rather obvious application of diffraction analysis is in distinguishing between different allotropic modifications of the same substance. Solid silica, for example, exists in one amorphous and six crystalline modifications, and the diffraction patterns of these seven forms are all different

The powder pattern of a substance is characteristic of that substance and forms a sort of fingerprint by which the substance may be identified. If we had on hand a collection of diffraction patterns for a great many substances, it could be identified an unknown by preparing its diffraction pattern and then locating in the field of interest of known patterns one which matched the pattern of the unknown exactly. The collection of known patterns has to be fairly large, if it is to be at all useful, and then pattern by pattern comparison in order to find a matching one becomes out of the question. What is needed is a system of classifying the known patterns so that the one, which matches the unknown, can be

located quickly. Hanawalt devised such a system in 1936. A set of line positions 2θ and a set of relative line intensities I . But the angular positions of the lines depend on the wavelength used, and a more fundamental quality is the spacing d of the lattice planes forming each line. Hanawalt therefore decided to describe each pattern by listing the d and I value of its diffraction lines, and to arrange the known patterns in decreasing value of d for the strongest line in the pattern. This arrangement made possible a search procedure, which would quickly locate the desired pattern.

Phase analysis by X-ray diffraction was carried out according to Hanawalt method. 2 to 3 gm of the powdered samples of fired body (fired at 1250°C, 1275°C, 1300°C, 1325°C, 1350°C, 1375°C and 1400°C) were put in a slide and pressed so that these were attached with the surface of the slot of the slide. Then x-ray patterns were recorded. The powder was characterized by a set of line positions 2θ and a set of relative line intensities I . The angular positions of the lines depended on the wavelength used, and a more fundamental quality was the spacing d of the lattice planes forming each line. Thus by listing the d and I values of its diffraction lines, and to arrange the known patterns in decreasing values of d for the strongest line in the pattern. This process identified the phases present in the samples. All the samples were examined according to the following specifications.

3.6 Chemical Properties Measurement:

3.6.1 Glassy Phase Determination

For determining the glassy phase a special technique has been taken. Here first the fired specimen has been grounded very fine and screened those powders into 300-mesh screen. The particles that pass the screen are taken for experiments. Then those particles are dried to become moisture free condition and then a sample weight of 0.125 gm is taken. In the mean time 1% hydrofluoric acid solution is prepared and 100 cc solution is taken for the operation to proceed. In a plastic pot we allowed the particles to react with the solution for two hours. Then the solution was filtered through pulp. Continuous water wash would give us the better result and then the residue plus the pulp is dried and fired at 800°C.

The weight of residue is the weight of crystalline body and the part of the powder lost in solution is the weight of glassy phase which has been corroded by the hydrofluoric acid. So the weight loss will give us the percentage of glassy phase in the structure

The operation was run on a number of sample like fired body at 1250^o, 1275^o, 1300^o, 1325^o, 1350^o, 1375^o and 1400^o.

3.6.2 EDAX Analysis:

Scanning Electron Microscopy (SEM) in conjunction with Energy Dispersive X-Ray Analysis (EDAX) allows detailed characterization of Porcelain ceramic insulator. Electron Microscopy allows detailed magnification of up to x50000 while EDAX allows qualitative and semi-quantitative elemental analysis SEM combined with EDAX is a very powerful tool and finds wide and varied use from all type of industries. Spot analyzed has been taken in SEM images. 4 spot analysis was taken by EDAX analyzer and where the qualitative and semi quantitative results were gathered

3.6.2 X-ray Fluorescence

When a primary x-ray excitation source from a x-ray tube or a radioactive source strikes a sample, the x-ray can either be absorbed by the atom or scattered through the material. The process in which a x-ray is absorbed by the atom by transferring all of its energy to an innermost electron is called the "photoelectric effect." During this process, if the primary x-ray had sufficient energy, electrons are ejected from the inner shells, creating vacancies. These vacancies present an unstable condition for the atom. As the atom returns to its stable condition, electrons from the outer shells are transferred to the inner shells and in the process give off a characteristic x-ray whose energy is the difference between the two binding energies of the corresponding shells. Because each element has a unique set of energy levels, each element produces x-rays at a unique set of energies,

allowing one to non-destructively measure the elemental composition of a sample. The process of emissions of characteristic x-rays is called "X-ray Fluorescence," or XRF. Analysis using x-ray fluorescence is called "X-ray Fluorescence Spectroscopy."

In this project chemical analysis is also done by X-ray spectroscopy to check the exact chemical analysis for all raw materials and also the fired body of the final product. The raw materials include ball clay, feldspar (local and imported), china clay (body and plastic), bijoypur clay (washed and unwashed), Sylhet clay and the fired body of the final product.

XRF is a very important tool in case of ceramic materials because in traditional chemical analysis it takes so much time and also the result is not always accurate. That's why XRF technique is applied for higher accuracy of the analysis result. The XRF method is widely used to measure the elemental composition of ceramic materials. Since this method is fast and non-destructive to the sample, it is the method of choice for field applications and industrial production for control of materials.

3.7 Electrical Properties Measurement

3.7.1 Dielectric Strength Measurement

Dielectric strength of an insulating body is measured by passing high voltage through a certain thickness of the body. The specimen thickness must be limited to 3 mm to minimize the probability of having cracks and other defects which may lower the result, thus we made the specimen with thickness varying from 0.5 mm to about 2.8 mm. A standard specimen is shown in fig .3.4a. The standard test procedure follows as ASTM methods (D3755). Thus the dielectric strength is measured as:

$$DS = \left(\frac{dV}{dx} \right)_{max}$$

But very thin specimen preparation is troublesome as it turns into wavy shape during firing. That's why the whole body is made of several mm thicknesses and depression of around 7mm was made. Through this depressed point high voltage is passed until fracture spark occurs. The samples prepared and fired in MME department ceramic laboratory are also tested. The applied breakdown voltage was measured as follows

The breakdown voltage of a spark gap between two metal spheres may be used as a measure of voltages up to the highest encountered in high voltage testing. The normal arrangement consists of two equal sized, polished aluminium spheres separated by an air gap. The spheres are usually mounted vertically one above the other, with the lower sphere earthed. The voltage between the spheres is raised till a spark passes between the two spheres the value of voltage required to spark over (breakdown) depends upon the dielectric strength of air, the size of spheres, the distance between the spheres and many the factors. A typical dielectric strength tester is shown in fig.3.4.

RESULTS AND DISCUSSIONS

4.1 Introduction

In order to find out the relation between the structure and properties of ceramic insulator the physical, mechanical and electrical properties of ceramic insulator were measured and the properties measured in each test were compared with the optical micrograph or SEM micrography. The mechanical strength includes bending strength and hardness of samples fired in different firing condition and chemical composition measurement also describes the chemical proportion of each raw material and the fired body to show the impurity content. The dielectric strength was also measured in high voltage tester.

4.2 Density Data

Table 4.1 shows the density variation with temperature. Here the density of sample fired at different temperatures was measured. This indicates the increase in the percentage of mullite phase increases the density. Density data can be related with the microstructure in such a way that where the glassy phase increases the density decreases and again the mullite increase the density increases. Now with increasing temperature the amount of glassy phase as well as the mullite percentage also increases. Now in these circumstances a temperature has to be set where the optimum density can be found for samples fired at different temperature. Looking at the data for density measurement it is found that the density is maximum at 1350^o C. Actually the density data shows quite a similar result for samples fired from 1325 to 1350^o C. This is because in these temperatures the amount of glassy phase developed from the quartz particles and the amount of mullite formed during firing balance each other.

4.3 Hardness

The hardness of samples fired at different firing condition was also measured. The hardness was found to be varied with different temperatures. The Vickers microhardness result shows lower hardness in 1250⁰C, 1275⁰C and 1300⁰C but increases when temperatures increases and found to be maximum at 1350⁰C. The hardness profiles also show slight decrease in hardness when the temperature drops from 1350⁰C to 1375⁰C and the decreases more with further drop in temperature. Table 4.2 shows the hardness profile data and figure 4.2 shows the variation graphically.

This is because the amount of phases present and the amount of glassy phase present in the structure. In general it is known that the temperature has a marked effect on structure. The quartz content decreases and the mullite content and the glassy phase content increase with temperature increases. Quartz and mullite contribute to the mechanical strength of the insulator and glassy phase content only increases the volume but do not have any strength increasing effect. The effect of these is quite clear on the results of the hardness profile.

At 1250⁰ C and 1275⁰ C, the hardness is almost 6429 and 6773 kg/mm² and when the temperature increases to 1325⁰C there is a rise in hardness (6960 kg/mm²). Although the quartz content decreases, the mullite content increases with temperature and that's why the hardness increases. Again the adverse effect is the increase of the amount of glassy phase content. But the increase of mullite phase offset those disadvantages.

Again when the temperature increases from 1325⁰ C to 1350⁰C the hardness increase continues from 6960 to 7153 kg/mm² mainly due to the increase in mullite content. The maxima were found at 1350⁰C and again the hardness decrease with temperature. The highest bending strength was also found at this temperature. The reason behind this is the maximum offset power of mullite to the increasing glassy phase and decreasing quartz content. At temperatures above 1350⁰C, although the mullite content increases the

increased amount of glassy phase along with lower undissolved quartz content, decreases the hardness.

4.4 Bending strength

The table 4.3 shows the bending strength for different types of samples fired in different firing conditions. The data shows that at the higher temperatures, with the increase in temperature the bending strength decreases slightly but at lower temperatures (from 1250 to 1350°C) the strength increases with temperatures. Although there is some slight variations but the result almost characterizes the above principle. The reason behind this is the amount of glassy phase contents. With the increase in glassy phase increase the liquid viscosity and helps to maintain the shape during firing. On the other hand mullite, which is a crystalline phase, has a vital role on mechanical strength. As the matrix of the ceramic sample is either undissolved clay matrix or the glassy phase the needle shape mullite maintains the stress level in a higher order as just in a composite matrix. Although the mullite forms above 1100°C the mullite needles become prominent above 1300°C. But with increasing the temperature the partial dissolution of quartz phase occurs which starts at 1200°C. Increased glassy phase content tends to decrease the bending strength of the porcelain ceramic insulator. The bending strength data shows that the highest bending strength was found in the samples fired at 1350°C.

4.5 Determination of glassy phase content

The amount of glassy phase was measured by gravimetric analysis. The data in table 4.4 shows that the amount of glassy phase increases with the temperature. The graphical representation was also shown in fig 4.4. As the temperature increases the glassy phase increases with the dissolution of quartz. The partial dissolution of quartz starts at 1200°C, which can also be seen as a rim around the quartz particle. With increasing temperature the area of glass rim increases and the particles become smaller. These effects can also be seen on the microstructure of the samples. It was found that at lower temperature like 1250°C the quartz particle was larger (microstructure of X100 magnifications) and with

increasing temperature the particles become smaller and the glass rim area becomes larger. The maximum content of glassy phase was found in the samples fired at higher temperatures like 1375⁰C and 1400⁰ C. The glassy phase content is 7.34% at 1250⁰C and increases with temperature increases to 28.89% at 1400⁰C.

4.6 X-ray Fluorescence

X-ray fluorescence result shown in fig 4.21 shows higher amount of silica content in the local clay such as 63.90% in Sylhet clay, 83.84 % in unwashed bejoypur clay, 73.92% in washed bijoypur clay. As the insulator body contains considerable amount of bijoypur clay the body produce sufficient amount of glassy phases in the higher temperature. That's why the dielectric strength drops after 1350⁰C. So it can be stated that after 1350⁰C the glassy phase no longer fill up the pores and cracks and starts decreasing the strength both mechanical and dielectric. China clay shows lower silica content (55.80% and 53.17%) and higher alumina contents (39.74%). That's why if the body prepared with china clay will shows higher mechanical and dielectric strength. The fired body also shows 70% silica and 22.64% alumina in sample fired at BISP at 1325⁰C. Stoichiometric formula of mullite shows that there has to be 2.55 times alumina than silica. So the results shows very low mullite has formed in the fired body. From this it can be concluded that alumina content if high, will be desirable for mullite nucleation. Higher amount of silica in fired body will result for larger amount of glassy phase, which in turn reduce the properties of ceramic insulator.

4.7 Optical Metallography:

The heterogeneous nature of the ceramic insulator product was observed in the fig 4.5 to fig 4.11 where the microstructure of the fired body was shown in X100 magnifications. The microstructure shows the quartz grains surrounded by a solution of rim of high silica glass, which can be seen in X400 magnification is also shown in fig 4.12. The outlines of glass mullite areas corresponding to the original feldspar grains and the unresolved matrix corresponding to the original clay can be clearly distinguished. Dark spots are also

seen to be present, which may be explained as the pull out of the particles during grinding and polishing. Although mullite is the crystalline phase in both the original feldspar grains and in the clay matrix, the crystal size and development are quite different. Here the dark matrix shows the presence of mullite, though it is not visible as separate mullite needle in the lower (X100) magnifications but can be realized in the higher magnification SEM images. From the microstructures, the quartz particles are the only phase to be cared about. The particle size, shapes are also to be considered. A quartz particle and the surrounding solution rim of high silica glass are shown in the microstructures. Usually the quartz forms only the glassy phase, but for some compositions fired at high temperature, there is a transformation into cristoballite or tridymite, which starts at the outer surface of the quartz particle. The cracks were caused by the greater contraction of the quartz grains compared to that of the surrounding matrix

The microstructures fired at 1250⁰C show large number of quartz grains and also some dark spots and the rim around the quartz grain are negligible. The small area of black matrix is mullite crystal.

The microstructures fired at 1275⁰C also show almost the same features as the samples fired at 1250⁰C. The figure shows slightly increased amount of black matrix. As the sample was fired at high temperature for almost 24 hours (in the firing zone) the mullite crystals become more prominent than the samples fired at lower temperature. The glassy rim around the quartz grain has no change. The dark spots are also observed in the structure.

The microstructures fired at 1300⁰C-show undissolved quartz, a significant area of glass rim around the quartz particle and the mullite crystal increasing a bit. The only distinguished feature is the development of glassy phase around the quartz grain. Here the dark spots or pores are in large size, The reason for this is clearly explain earlier..

The microstructures fired at 1325⁰C show lower quartz content than the samples fired at lower than 1325⁰ C. The mullite increases significantly. As glassy phase increases in a

higher order. Although the percentage area of mullite crystal decreases, the amount of mullite microstructures increases than before.

The microstructure fired at 1350^oC is quite similar to that of the sample fired at 1325^oC. The significant feature is the size of the quartz grain, which seems to be smaller and smaller. The rim area increases significantly as well as the mullite crystal zone. The microstructure at 1350^oC shows large number of very small quartz grains with mullite crystals in the highest amount. This signifies that there would be a considerable number of large size quartz grains. But as the temperature increases the quartz dissolves and becomes smaller or fully converted to the glassy phase. That's why large number of small-undissolved quartz particle was found.

The microstructure at 1375^oC shows few number of quartz grain, which still not dissolved yet. The microstructure in higher magnification (X400) shows larger area of glassy phase and mullite crystal growing in length.

The microstructures at 1400^oC show fewer numbers of quartz grain and glassy phase in the matrix of unresolved clay matrix. The mullite crystal is also present and considerable amount of pores was also present. The temperature is so high that there is a chance of burn out of particles, which makes pores inside the body.

4.8 SEM Image Analysis

Fig 4.13 to fig 4.18 shows the SEM images of porcelain ceramic insulator. Due to inconveniency of working at high voltage in the Scanning Electron Microscope of BUET the test was carried out to only one type of samples. The sample, which is fired at 1325^oC, was examined in SEM. All the structure contains undissolved quartz particle, mullite needle, a rim of glass around undissolved quartz particle and a background of unresolved matrix corresponding to the original feldspar. Cracks are also seen in the clay matrix nearly where the mullite percentage is less or where the undissolved quartz

particle sits on the glassy phase. The important features of SEM images are described below.

The quartz particles are observed in the SEM images. At the boundary of quartz small rim of glassy phase is observed which is due to the partial melting of quartz. The particles observed are in the size of 1 micron to 5 micron or even 10-micron quartz particles can be seen. Undissolved quartz particle is not coherent with the unresolved clay matrix.

SEM images of the porcelain show mullite needles and EDAX analysis on that needles support the exact chemical composition of the mullite. Images indicate mullite's preferential orientation on the surface of clay or kaolinite matrix. Probably the mullite in the clay matrix is the seed for the crystallization of the mullite needles. Those mullite needles observed in the clay matrix is generally termed as primary mullite. The morphology of the mullite needle is like acicular crystal. The mullite needles seem to be interlocked, which actually act as the strength increaser. When mullite crystal forms from the clay matrix it increases the volume by 10%. The increase in volume heals up any cavity or porosity or any cracks formed due to shrinkage and other thermal expansion. The SEM image clearly describes this nature. Where there is a low mullite content or no mullite the cracks become more prominent.

The matrix surrounding the quartz particle and beneath the mullite needles is supposed to be the unresolved clay matrix. The glass rim around the quartz particle is shown as the partial dissolution of quartz.

The glass rim is observed surrounding the quartz particle. These because the temperature causes the quartz particle fused and the result is the glass. There are some important features of glassy phase, which can be described. At first the glassy phase helps the property by filling the pore around the quartz particle. It helps both mechanical and electrical strength to increase. So at lower temperature (below 1350°C), the strength decreasing effect was not so observed. But after 1350°C it only increases the volume and then it decreases the strength and other properties.

Cracks are observed in the images. The cracks are observed mainly near the quartz particle and those regions where the crystalline phase or mullite phase is less or absent. The cracks are peripheral around the quartz grain. At the crack tip some expansion cracks are also to be observed. Cracks are elongated to the clay matrix. Almost all the cracks are interrelated. The reasons for crack development are described below.

Cracks can be occurred for various reasons. Cooling through the quartz inversion (573°C) results in a quartz particle volume decrease of 2% which can produce sufficient strain to cause cracking of the glassy matrix and even in a rare case quartz itself. The cracking severity largely depends on cooling rate. Slow cooling rate through the transformation zone will produce small strain.

The nature of cracks in porcelain body is dependent on the expansion coefficient of the matrix and the particle. If the particles contract more than the matrix resulting in circumferential cracking around the particles. This is true for quartz particle in the feldspathic glass of the porcelain body matrix. The stress generation and associated cracking due to the presence of quartz particles tend to be severe because of rapid displacive phase transformation of quartz during cooling. Again if the matrix contracts more than the particle resulting in the residual cracks emanating from the particles. In figure 4.15 the large quartz particle exhibits continuous peripheral fracture at or near the grain boundaries and interconnected matrix fracture. An effect that can lead to artifacts in microstructural evolution is the release of induced stresses during specimen preparation like grinding and polishing of samples might lead to some observed cracks on the surface because of stress release. Crack size can be seen in the SEM images which is shown in 4.14, the crack width is very small seems to be 0.1 micron or less which is not visible in the optical microscope. This type of micro cracks surely deteriorate the properties of ceramic insulator

Another important reason is the incoherence of undissolved quartz to the matrix. Undissolved quartz particle is not coherent with the unresolved clay matrix. That is why the cracks formed due to changes in composition, phase and thermal expansion.

Mullite is a crystalline phase. With the nucleation of mullite phase from the clay matrix the volume expands slightly as much as 10% [3]. But in area where no mullite crystal forms, the cracks are observed in the matrix due to shrinkage. As the temperature cools down from a very high sintering temperature (say around 1325^o C), there is a differential thermal contraction occurring in the matrix, which cause in cracks. The region where there is sufficient mullite crystal, the cracks were healed up by the volume increase by mullite. But in areas of no mullite or little mullite the cracks cannot be healed up. So those cracks were observed in the matrix.

4.9 Dielectric Strength Data

In general, the dielectric strength will increase with increasing temperature. Experimental studies convinced that the dielectric strength of the ceramic insulators is mainly dependent on the firing temperature. Because the amount of crystalline phases present at different temperatures are largely responsible for the improvement of the dielectric strength. The crystalline phase, mullite contributes most to the strength of the insulating materials. This phase is increased with increasing temperature thus increases the dielectric strength with increasing temperature. Mullite is a phase of Al_2O_3 and SiO_2 [$Al_6Si_2O_{13}$], which result from a peritectic reaction. The increase of temperature will increase the glassy phase. Increasing amount of glassy phase is responsible for the strength decreasing effect. First the glassy phase content fill up the pores, which helps in increased strength but after that the strength decreases with glassy phase as it only increases the volume. On the other hand, the strength can be greatly increases by undissolved quartz. If it is possible to retain the undissolved quartz with higher amount of mullite then the strength would be greatly increased. Undissolved quartz has a higher strength increasing effect than dissolved quartz. If the firing temperature is extremely high, the dielectric strength will drop because of the dissolution of quartz grains. So the

firing temperature should be selected at an optimum range, which is suitable to obtain the desired dielectric strength. For this purpose the dielectric strength of materials fired at different temperatures was studied.

From the experimental results it is observed that, the dielectric strength of the insulating materials fired at temperatures between 1250^o to 1300^oC is found to be 20-25 kV/mm and for the specimen fired at 1325^o to 1350^o varies from 24-29 kV/mm. Further increase in temperature creates a major fall in dielectric strength. The maximum dielectric strength is observed at 1350^oC. The variation is shown in fig 4.19. The reason behind this type of dielectric behavior with temperature in the light of Optical and SEM micrography is described below.

From the optical micrography it is well understood that with increasing temperature the mullite content and the glassy phase content increases and the partial dissolution of quartz to glassy phase makes lower quartz content in the structure. Again cracks and pores are also seen in SEM and optical micrography, which also has some adverse effect on dielectric strength. Dark spots and cracks if contain within the structure will contain air.

At first when the temperatures rises from 1250^oC to 1275^oC or 1300^o C glassy phase didn't increase greatly but after that sharp increase in glassy phase was observed. In this course the glassy phase's contribution is only to fill the pore and heal up the cracks. Also mullite phase increases with this temperature increase. For this the dielectric strength is observed to be increased. At still higher temperature like 1325^oC or 1350^oC, the mullite phase still has the increasing effect on dielectric strength above the decreasing effect on dielectric strength due to the decreasing amount of quartz is not much to offset the advantage. As the temperature increases the probability of cracks and porosity to retain in the specimen is quite higher and as the glassy phase content also increases, pore filling and crack heal up by glassy phase is still be possible. After that, from figure of variation of glassy phase content with temperature, the glassy phase still increases and there are very small pores to be filled out or unable to be filled out. That's the decreasing rate of dielectric strength was observed although there is increase of mullite phase. After 1350^oC

increase in mullite phase cannot alone increase the dielectric strength, but the combined effect of higher amount of glassy phase and lower amount of quartz content become the dominant factor. This is the main reason that after 1350^oC the dielectric strength drops sharply and at 1400^oC the strength is very lower and cannot be describe those fired samples in high tension ceramic insulator. There are several other reasons, which contribute to the decrease in dielectric strength, which is described below.

The properties of an insulating material become degraded and eventuality dielectric, breakdown occurs at a field below that predicted experiments on freshly formed samples if the ceramic insulator is fired at higher temperatures like 1375^oC and 1400^oC. Aging therefore determines the useful life of the insulation.

During firing the insulator samples was probably subjected to higher temperature for longer times, which can develop structural defects as microcracks, which are quite damaging to the dielectric strength, as mentioned above

Firing for longer time at higher temperature also experiences electrical aging as a result of the effects of the field on the properties of the insulation. For example, dc fields can dissociate and transport various ions in the structure and thereby slowly change the structure and properties of the, insulation.

The dielectric strength results show very scattered results. Some results are still out of range. There are various reasons for these scattered results. The reason may be any of those listed below.

1. The surface contamination by furnace conditions such as excessive moisture, deposition of pollutants, dirt, dust etc
2. The inhomogeneity of the ceramic body depends on its composition and on the forming and filling process. Improper filling of the pores will cause air to retain within the structure, which will conduct electricity and decrease the strength.

3. The formation of closed pores depends on the firing temperature. At higher temperature spherical pores are observed which if not filled by the glassy phase will deteriorate the strength.
4. The inhomogeneity of the dielectric causes retention of airgaps in the porcelain structure.
5. Sometimes the oxide particles, non-metallic inclusion or other form of impurities are present on the surface of the specimen as the temperature increases. So the applied voltage find a conductive path on the surface and passed through the surface instead of through the entire insulator.
6. The relative humidity influences the dielectric strength to the extent that moisture absorbed by, or on the surface of, the material under test affects the dielectric and surface conductivity.
7. The surrounding medium (the transformer oil) can effect the results of dielectric strength. Because it affects the heat transfer rate, external discharges, the field uniformity, thereby greatly influencing the test results.

4.10 Phase Analysis by X-ray diffraction

X-ray diffraction technique (Henawalt method) was carried out on the samples prepared for this study. The XRD technique was also applied to the samples of fired body fired at different firing condition. The phase observed and their corresponding planes and arbitrary intensities were recorded. The data thus obtained were presented graphically from fig 4.20 to fig 4.26. The data recorded are also shown in table 4.4 to 4.10.

The XRD pattern clearly identifies mullite in all the samples fired at different temperatures. The intensities of mullite peak increases with temperature indicate that with

increasing temperature the amount of mullite phase increases. The maximum intensity of mullite among the samples tested was found in the samples fired at 1400°C indicates that mullite's percentage can still be increased if the firing temperature exceeds 1400°C. XRD pattern for lower temperature samples show quartz particle and clay matrix. But with increasing temperature glassy phase arises, which also increases with increasing temperature.

With increasing temperature the intensity of quartz peak become weaker and some peaks even diminishes notifies the decreasing of quartz particle from the structure of higher temperature. The clay matrix is eventually same in all the patterns. Although the intensity become slightly weaker, indicating the formation of more primary mullite crystal from clay particle, the strength of those clay peaks do not change much. The analysis of XRD result supports the results already achieved by optical micrography, bending strength test and dielectric strength test.

4.11 EDAX Analysis

The EDAX spot analysis results are shown in fig. 4.27 to fig 4.30. The spots were chosen in four different regions in SEM micrographs. The fig 4.27 was chosen on the needle shape are. The analysis shows aluminium content almost three times of silicon. Mullite is crystalline phase the chemical formula of which is $3\text{Al}_2\text{O}_3 \cdot 2\text{SiO}_2$. From this formula, it can be shown that the weight of aluminium is exactly 2.89 times greater than the silicon in a molecular form of mullite. The figure also shows the same behavior, which determines that those needles are mullite.

Fig 4.28 shows very high amount of silicon and a very low amount of aluminium and considerable amount of Na and K. This is clearly indicated to the glassy phase. This spot is chosen in the area surrounding the large particle. Clearly this is the glassy phase gone.

Fig 4.29 shows high silicon and almost half of it is aluminium and Na, K, Fe and Ti is also detected. Oxygen content is also very high and it seems to be a mixture of all oxides.

This notifies the presence of clay. The spot was taken in the matrix zone and the result came as clay. So from this analysis it can be stated that the matrix is a clay matrix.

Fig 4.30 is a spot analysis result in the region of large particle. The results show very high amount of silicon and minor amounts of Al, K and Fe with considerable amount of oxygen. It is the quartz particle, which is composed of SiO_2 .

The spot analysis thus clearly describes the presence of mullite, glassy phase, clay matrix and quartz.

CONCLUSION

In this project we tried to correlate the structure with the properties. First the structure was identified and then the properties were measured for different types of sample. Among the results the following features can be gathered.

1. The density is highest at 1350°C indicates that sintering and pore filling by glassy phase is the best among the samples fired at different temperatures.
2. The glassy phase increases with increasing temperature. The reason behind this is the dissolution of quartz particle into glass.
3. The bending strength is highest for samples fired at 1350°C . As the quartz particle and mullite contributes much for the mechanical strength of porcelain and as quartz particle decreases with increasing temperature, bending strength decreases after 1350°C .
4. Dielectric strength increases with increasing temperature, reaches maximum at 1350°C then drops again with further increase in temperature. As glassy phase has a decreasing effect on dielectric strength and as the glassy phase content increases with increasing temperature, the dielectric strength drops after 1350°C .

From these findings, it can be concluded to the fact that, 1350°C is the optimum temperature where maximum dielectric strength of porcelain body can be achieved.

SUGGESTED FUTURE WORKS

The project had a target to reach the dielectric strength of 30kV/mm. Although the target could not be reached but gone very close to it and the project was able to specify a temperature (1350°C) in which maximum dielectric strength can be achieved than other temperature if other variables are closely controlled. Another important point is that microstructural features are clearly identified.

At the end of this project it is suggested to the researcher of coming age who will work in this field is to augment the strength contributing phase that is crystalline phase. If it can be done then the dielectric strength will be further improved.

The impurities mainly come from ball clay. Now if this ball clay is replaced by bentonite clay then a significant change will occur due to elimination of impurities as far the project suggests. It is also likely to use the bejoypur clay after treating it and lowering its impurity content. If that huge amount of bejoypur clay is used then large amount of foreign exchange can be saved

97401

BIBLIOGRAPHY

1. Buchanan, R.C., "Ceramic Materials for Electronics – Processing Properties and Application" Marcel Dekker Inc., 2nd Edition, pp. 1-69, 1991.
2. McPhee, J.A., Macgregor, S. J. & Tidmarsh, J R, Annual Report "Conference On Electrical Insulation and Dielectric Phenomena", IEEE Dielectrics and Insulation Society Vol. II, 2000.
3. Espe W, Materials of High Vacuum Technology, Vol. 2: Silicates, Pergamon Press, Oxford, Chaps. 10-12, 1968.
4. Insul./Circuits(Directory/Encyclopedia), 19(7), 194-208, 1973.
5. Schuller, K.H., Journal of Materials Education, 4, 529-526, 1982.
6. Chaudhury, S.P., J. Br. Ceram. Soc., 73(2), 37-41, 1974.
7. Stevels, J.M., Progress in the Theory of Physical Properties of Glass, Elsevier, London, 1964.
8. Watchman, J.B., Jr., et al., eds., Japanese Structural research and developments, Science applications International Corp., Mclean, Va., July 1989.
9. Aksay, I.A and Pask, J.A., Journal of American Ceramic Society, Vol. 58, No 11-12, 1975, pp. 507-512.
10. Carty, W. M. & Senapati, U., Journal of American Ceramic Society, Vol. 81 No.1, pp. 3-20, 1998.
11. Bleininger, A. V. and Riddle, F. H , J. Amer., Ceram. Soc . 2, 564, 1919.
12. Zerfoss, S. and Utter, B. A. J Amer. Ceram Soc , 29, 205, 1946.
13. Klever, E., Glastechn Ber., 7, 85, 1929/30.
14. Gregg, S J and Stephens, M. J , J. Chem. Soc., 3951, Dec 1953.
15. Eitel, W and Neumann, B Neues, Jb. Min Geol Palaont. 53 1925.
16. Nandi, D.N., Journal of Sci. Industr. Res., Vol. V, No 9B, 1950, pp.179-184.
17. Bowen, N. L. and Greig, J. W., J. Amer. Ceram. Soc., 7, 238 ,1924.
18. Mellor, J W and Holdcroft, A. D., Trans Brit. Ceram. Soc., 10, 94, 1910/11.
19. Weiss, E. J. and Rowland, R A., , Amer. Min, 41, 117-126, 1956
20. Hyslop, J. F. and Rooksby, H. P., Trans. Brit Ceram. Soc., 27, 93, 1927/28
21. Hyslop, J. F. Trans Brit. Ceram. Soc. 43, 49, 1944.

22. Biltz, W. and Lemke, A., *Z. Anorg. Chem.* 186, 373, 1930.
23. Agafonov, V. and Vernadsky, W., *C.R. Akad. Sci U.R.S.S.*, 178, 1082, 1241
24. Iskull, W., *Trans. Ceram. Res. Inst., Uningrad*, 2, 1925.
25. Jurganov, W. W. and Sussmanowitsch, M. W., *Trans. Ceram. Moscow*, 21, (1929).
26. Kingery, W.D., Bowen, H.K., Uhlmann, D.R., *Introduction to Ceramics*, 2nd Edition, John Wiley and Sons, New York, 534-545, 1975.
27. Carty, W. M. & Senapati, U., *Journal of American Ceramic Society*, Vol. 81 No.1, 3-20, 1998.
28. Vesterberg, K. A., *Arch. Chem. Miner. Geol., Stockh*, 9 (No. 14) 1.
29. Fuchs, H. Von, *Denkschr. Akad. Wiss. Munchen* 7, 65, 1821
30. Rinne, F., *Z. Kristallogr.* 61, 119, 1924/25.
31. Zwetsch, A., Reference 101 p. 6
32. Hansen, W. C. and Brownmiller, L. Z., *Amer. J. Sci.* 15, 225, 1928.
33. Spangenberg, K. and Rhode, J., *Keram. Rdsch.* 35, 398, 1927.
34. Eitel, W. and Kedesdy, H., *Abb. preuss. Akad. Wiss. No. 5*, 37, 1943.
35. Chatelier, H. Le, *Z. Phys. Chem.* 1, 396, 1887.
36. Colegrave, E. B. and Rigby, G. R., *Trans. Brit. Ceram. Soc.*, 51, 355, 1952.
37. Roy, R., Roy, D. M. and Francis, E. E., *J. Amer. Ceram. Soc.*, 38, 198, 1955
38. Parmelee, C. W. and Rodriguez, A., *J. Amer. Ceram. Soc.*, 25, 1942.
39. Budnicov, P.P. and Schmuckler, K. M., *Zh. prikl. khim., Leningr.* 19, 1029, 1946.
40. Rhode, J., *Keram. Rdsch.* 35, 398, 1927.
41. Navias, L., *J. Amer. Ceram. Soc.*, 8, 296, 1925.
42. Michr, W., *Ber. dtsh. keram. Ges.*, 9, 339, 1928.
43. Gould, R. E., Reference 102 p. 84.
44. Clark, F.M., *Insulating materials for design and engineering practice*, Wiley, New York, Chap. 16, 1962.
45. Harrop, P.J., *Dielectrics*, Wiley, New York, Cháps. 1-6, 1972.
46. Anderson, J.C., *Dielectrics*, Reinhold New York, Chaps. 1-8, 1964.
47. ASTM (D3755).

TABLES

Table 3.1 Grain size distribution of clay raw materials used in insulator body

Fraction μm	Yield, Wt%					
	China Clay (Imported)	China Clay (Rajmahal)	Ball Clay (white)	Bejoypur Clay Grade I	Bejoypur Clay (Washed)	Ball Clay (Black)
>63	0.8	1.2	0.2	46.6	8.4	2.6
20-63	0.0	4.0	0.0	7.5	11.9	12.7
10-20	9.9	14.8	5.0	9.1	18.3	21.4
5-10	20.8	11.9	13.5	7.5	18.3	17.5
2-5	28.8	20.7	28.9	7.5	17.4	12.7
1-2	9.9	10.9	10.0	4.3	11.0	10.7
<1	29.8	36.5	42.4	17.5	14.7	22.4

Table 3.2 Chemical Analysis (%) of the raw materials used to prepare samples.

	China Clay (Plastic)	China Clay (Body)	Ball Clay (White)	Bejoypur Clay (Local)	Bejoypur Clay (Washed)	Ball Clay (Black)	Felds par
SiO ₂	50.18	51.86	54.43	72.09	59.46	61.27	74.98
TiO ₂	.014	0.50	1.84	1.02	0.85	1.41	0.08
Al ₂ O ₃	33.34	34.72	30.97	18.69	26.64	24.85	14.37
Fe ₂ O ₃	1.88	0.57	1.37	1.01	0.86	0.17	0.83
MgO	1.05	0.07	0.34	0.14	0.24	0.26	0.08
CaO	0.94	0.07	0.17	0.10	0.25	0.65	0.68
Na ₂ O	0.81	0.041	0.17	0.11	0.23	0.25	3.54
K ₂ O	2.58	0.18	0.81	0.61	0.84	0.44	4.91

Table 3.3 Typical body Composition of Ceramic Insulator

Set Of Samples	Bejoypur Clay	Ball Clay	Feldspar	China Clay (Body)	China Clay (Plastic)	Quartz	Bejoypur Clay (Washed)	Total %
1	32	8	21	8	11	20	-	100
2	-	10	25	15	25	25	-	100
3	-	10	25	-	-	25	40	100

Table 3.4 Chemical Analysis of the final products

	Set 1	Set 2	Set 3
SiO ₂	67.50	63.4	71.4
TiO ₂	0.53	0.48	0.68
Al ₂ O ₃	20.81	30.34	22.56
Fe ₂ O ₃	0.93	0.74	1.05
MgO	0.25	0.36	0.45
CaO	0.47	0.45	0.56
Na ₂ O	1.64	1.75	1.35
K ₂ O	2.90	2.48	1.95
Total %	100	100	100

Table 3.5 Samples Prepared for Testing

Sample No	Specification
1	Normal BISF Body fired at 1250 ⁰ C (Set 1 of table 3.3)
2	Normal BISF Body fired at 12750 ⁰ C(Set 1 of table 3.3)
3	Normal BISF Body fired at 1300 ⁰ C(Set 1 of table 3.3)
4	Normal BISF Body fired at 1325 ⁰ C(Set 1 of table 3.3)
5	Normal BISF Body fired at 1350 ⁰ C(Set 1 of table 3.3)
6	Normal BISF Body fired at 1375 ⁰ C(Set 1 of table 3.3)
7	Normal BISF Body fired at 1400 ⁰ C(Set 1 of table 3.3)
8	Set 2 of table 3.3 Fired at 1360 ⁰ C
9	Set 3 of table 3.3 Fired at 1360 ⁰ C

Table 4.1 Density of the ceramic insulator materials

Sample No	Specification	Average density, gm/cc
01	Fired at 1250 ⁰ C	2.25
02	Fired at 1275 ⁰ C	2.27
03	Fired at 1300 ⁰ C	2.31
04	Fired at 1325 ⁰ C	2.30
07	Fired at 1350 ⁰ C	2.39
08	Fired at 1375 ⁰ C	2.37
09	Fired at 1400 ⁰ C	2.31

Table 4.2 Hardness profiles of the ceramic insulator materials

Sample No	Specification	Vickers Hardness kg/mm ²
01	Fired at 1250 ⁰ C	6421
02	Fired at 1275 ⁰ C	6773
03	Fired at 1300 ⁰ C	6421
04	Fired at 1325 ⁰ C	6960
05	Fired at 1350 ⁰ C	7154
06	Fired at 1375 ⁰ C	6960
07	Fired at 1400 ⁰ C	6773

Table 4.3 Bending strength Data

Sample No	Firing Temperature	Load reading (Newton)	Diameter (cm)	Bending Strength (kg/cm ²)	Mean Bending Strength Kg/cm ²
1	1250 ^o C	295	1.027	707	663.4
2		278	1.026	668	
3		285	1.032	673	
4		275	1.027	659	
5		277	1.037	610	
6	1275 ^o C	305	1.031	723	711.8
7		292	1.028	698	
8		285	1.028	681	
9		310	1.029	739	
10		302	1.03	718	
11	1300 ^o C	310	1.026	745	720.6
12		275	1.01	693	
13		285	1.024	689	
14		292	1.025	704	
15		311	1.016	770	
16	1325 ^o C	324	1.02	793	762.2
17		325	1.015	807	
18		311	1.017	768	
19		285	1.018	701	
20		302	1.019	741	
21	1350 ^o C	307	1.021	749	791.3
22		335	1.01	844	
23		321	1.024	776	
24		341	1.025	822	
25		313	1.02	766	

36	1375 ⁰ C	299	1.031	708	680.8
37		297	1.024	718	
38		265	1.025	639	
39		278	1.026	668	
40		280	1.027	671	
41	1400 ⁰ C	285	1.028	681	663.4
42		282	1.029	672	
43		265	1.021	646	
44		278	1.024	672	
45		265	1.021	646	

Table 4.4 Determination of Glassy phase

Sample No	Specification	Glassy phase content %
1	Fired at 1250 ⁰ C	7.34
2	Fired at 1275 ⁰ C	7.97
3	Fired at 1300 ⁰ C	14.45
4	Fired at 1325 ⁰ C	18.72
5	Fired at 1350 ⁰ C	27.45
6	Fired at 1375 ⁰ C	28.78
7	Fired at 1400 ⁰ C	28.89

Table 4.5 Normal BISF body Fired at 1250^o C

Diffraction Angle (2θ)	d spacing	I/I₀	Diffraction Planes, hkl	Phases present
10.2	3.99	30	200	mullite
11.6	3.51	60	210	mullite
14.5	2.81	20	001	mullite
15.5	2.63	20	220	mullite
18	2.27	15	201	mullite

Table 4.6 Normal BISF body Fired at 1275^o C

Diffraction Angle (2θ)	d spacing	I/I₀	Diffraction Planes, hkl	Phases present
10.2	3.99	30	200	Mullite
11.4	3.57	35	120	Mullite
11.8	3.09	60	210	Mullite
13.2	2.81	25	001	Mullite
14.5	2.63	20	220	Mullite
15.5	2.27	20	201	Mullite
26.5	1.55	15	211	Quartz
27.9	1.47	20	212	Quartz
29.2	1.40	20	203	Quartz

Table 4.7 Normal BISF body Fired at 1300⁰ C

Diffraction Angle (2θ)	d spacing	I/I₀	Diffraction Planes, hkl	Phases Present
11.2	3.57	35	120	Mullite
11.8	3.09	65	210	Mullite
13	3.02	30	001	Clay
13.5	2.81	25	112	Mullite
14.5	2.27	20	001	Mullite
18	1.86	20	201	Mullite
26	1.47	20	211	Quartz
27.9	1.40	20	212	Quartz
29.2	1.35	25	203	Quartz

Table 4.8 Normal BISF body Fired at 1325⁰ C

Diffraction Angle (2θ)	d spacing	I/I₀	Diffraction Planes, hkl	Phases present
10	4.07	40	111	Clay
10.9	3.88	40	021	Clay
11.8	3.45	70	210	Mullite
12.8	3.23	30	111	Clay
13	3.13	25	112	Clay
14.9	2.74	25	220	Mullite
15.8	2.58	25	111	Mullite
18.2	2.24	25	201	Mullite
26.5	1.55	20	211	Quartz
28	1.46	20	421	Mullite

Table 4.9 Normal BISF body Fired at 1350^o C

Diffraction Angle (2θ)	d spacing	I/I ₀	Diffraction Planes, hkl	Phases present
10.3	3.95	30	200	Mullite
11.8	3.45	70	210	Mullite
13.6	3.001	20	112	Clay
14.8	2.75	20	220	Mullite
17.5	2.33	20	102	Quartz
18.2	2.24	20	040	Clay
22.2	1.84	15	311	Mullite
26.3	1.56	15	211	Quartz
29	1.42	10	250	Mullite

Table 4.10 Normal BISF body Fired at 1375^o C

Diffraction Angle (2θ)	d spacing	I/I ₀	Diffraction Planes, hkl	Phases present
10.3	3.95	30	200	Mullite
11.8	3.45	70	210	Mullite
13.6	3.001	20	112	Clay
14.8	2.75	20	220	Mullite
17.5	2.33	20	102	Quartz
18.2	2.24	20	040	Clay
22.2	1.84	15	311	Mullite
26.3	1.56	15	211	Quartz
29	1.42	10	250	Mullite

Table 4.11 Normal BISF body Fired at 1400° C

Diffraction Angle (2θ)	d spacing	I/I₀	Diffraction Planes, hkl	Phases present
10.3	3.95	30	200	Mullite
11.8	3.45	80	210	Mullite
15	2.72	25	022	Clay
18.2	2.24	20	040	Clay
22.2	1.84	15	311	Mullite
26.3	1.56	10	211	Quartz
27.8	1.47	10	241	Mullite

Table 4.12 Dielectric Strength of insulating materials fired at 1250^o C

Specimen No	Applied Voltage (kV)	Specimen Thickness (mm)	Dielectric Strength (kV/mm)	Average (kV/mm)
1	42	2.89	16.26	18.31
2	51	2.42	21.07	
3	48	3.02	16.00	
4	47	2.56	18.35	
5	46	2.93	15.69	
6	39	2.46	15.85	
7	52	2.35	22.12	
8	56	2.56	21.85	
9	50	2.69	18.58	
10	45	2.65	17	
11	47	2.54	18.5	
12	46	2.69	17.1	
13	45	2.36	19.06	
14	55	2.89	19.03	

4.13 Dielectric Strength of Insulating materials fired at 1275⁰ C

Specimen No	Applied Voltage (kV)	Specimen Thickness (mm)	Dielectric Strength (kV/mm)	Average (kV/mm)
1	49	2.74	17.88	20.86
2	55	3.31	16.62	
3	75	3.28	22.87	
4	39	1.99	19.59	
5	74	2.85	26.01	
6	65	3.07	21.14	
7	57	3.06	18.63	
8	60	2.27	26.43	
9	70	3.00	23.33	
10	50	2.81	17.77	
11	65	3.38	19.23	
12	58	2.39	24.27	
13	70	3.28	21.34	
14	50	2.95	16.95	

Table4.14 Dielectric Strength of insulating materials fired at 1300^o C

Specimen No	Applied Voltage (kV)	Specimen Thickness (mm)	Dielectric Strength (kV/mm)	Average (kV/mm)
1	55	2.65	20.75	20.94
2	58	2.62	22.13	
3	59	2.54	23.22	
4	48	2.7	17.77	
5	61	2.45	24.89	
6	58	2.36	24.57	
7	55	2.89	19.03	
8	62	2.65	23.39	
9	63	2.54	24.80	
10	51	2.45	20.81	
11	45	2.65	16.98	
12	49	2.54	19.29	
13	45	2.58	17.44	
14	42	2.32	18.10	

Table 4.15 Dielectric Strength of insulating materials fired at 1325^o C

Specimen No	Applied Voltage (kV)	Specimen Thickness (mm)	Dielectric Strength (kV/mm)	Average (kV/mm)
1	49	2.84	23.99	22.75
2	57	3.01	18.97	
3	68	3.05	22.33	
4	68	2.99	22.70	
5	64	2.49	25.75	
6	57	2.88	19.77	
7	62	2.68	23.13	
8	46	1.99	23.17	
9	55	2.64	20.83	
10	65	2.98	21.85	
11	75	3.01	24.92	
12	72	3.04	23.68	
13	70	2.85	24.60	
14	63	2.76	22.83	

Table 4.16 Dielectric Strength of insulating materials fired at 1350^o C

Specimen No	Applied Voltage (kV)	Specimen Thickness (mm)	Dielectric Strength (kV/mm)	Average (kV/mm)
1	85	2.46	34.55	28.36
2	70	2.54	27.55	
3	75	2.39	31.38	
4	70	2.74	25.54	
5	75	2.86	26.22	
6	82	2.97	27.45	
7	71	2.41	29.46	
8	70	2.65	26.41	
9	65	2.49	26.1	
10	82	2.82	28.92	
11	73	2.28	32.01	
12	70	2.6	26.92	
13	75	2.94	25.51	
14	76	2.61	29.11	

Table 4.17 Dielectric Strength of insulating materials fired at 1375^o C

Specimen No	Applied Voltage (kV)	Specimen Thickness (mm)	Dielectric Strength (kV/mm)	Average (kV/mm)
1	32	2.84	17.268	19.40
2	28	1.27	22.04	
3	31	1.9	18.32	
4	22	1.97	11.168	
5	24	1.02	23.52	
6	25	1.42	17.61	
7	34	1.86	18.28	
8	35	1.5	23.33	
9	32	1.73	18.49	
10	33	1.38	23.91	
11	29	1.45	20.0	
12	33	1.36	24.36	
13	29	1.89	15.34	
14	32	1.78	17.97	

Table 4.18 Dielectric Strength of insulating materials fired at 1400^o C

Specimen No	Applied Voltage (kV)	Specimen Thickness (mm)	Dielectric Strength (kV/mm)	Average (kV/mm)
1	45	2.42	18.59	17.74
2	42	2.96	14.19	
3	53	2.78	19.06	
4	39	2.99	13.04	
5	49	2.67	18.35	
6	51	2.49	20.48	
7	41	2.53	16.20	
8	49	2.08	23.55	
9	43	2.87	14.98	
10	46	2.72	16.91	
11	43	2.14	20.09	
12	54	2.39	22.59	
13	45	2.46	18.29	
14	35	2.90	12.068	

FIGURES

Table 4.18: XRF results of various raw materials and the fired body

Samples	SiO ₂	TiO ₂	Al ₂ O ₃	Fe ₂ O ₃	MnO	MgO	CaO	Na ₂ O	K ₂ O	P ₂ O ₅	SOMME	LOI
Ball Clay	55.59	0.65	40.48	1.00	0.01	0.33	0.21	0.01	0.86	0.03	99.16	14.92
Feldspar (Imported)	65.75	0.05	18.89	0.17	0.01	0.02	0.07	2.10	12.97	0.03	100.06	0.32
Feldspar (Local)	76.29	0.09	13.86	1.00	0.03	0.12	0.72	3.38	4.89	0.02	100.41	0.75
Sylhet Clay	63.90	1.12	27.21	3.69	0.01	0.65	0.23	0.01	2.38	0.06	99.27	11.21
Local Clay (Washed)	73.92	1.52	21.95	0.88	0.01	0.24	0.09	0.01	0.92	0.05	99.59	7.92
Local Clay (Unwashed)	83.84	0.94	13.75	0.58	0.01	0.10	0.06	0.01	0.55	0.03	99.87	5.25
China clay (Body)	55.80	0.03	39.74	0.40	0.04	0.41	0.03	0.01	2.75	0.02	99.23	13.19
China Clay (Plastic)	53.17	0.22	39.67	2.99	0.01	0.74	0.75	0.01	1.75	0.01	99.32	14.08
BISF Burned Body	70.03	0.81	22.64	1.38	0.02	0.32	0.54	1.17	2.77	0.04	99.73	0.05

FIGURES

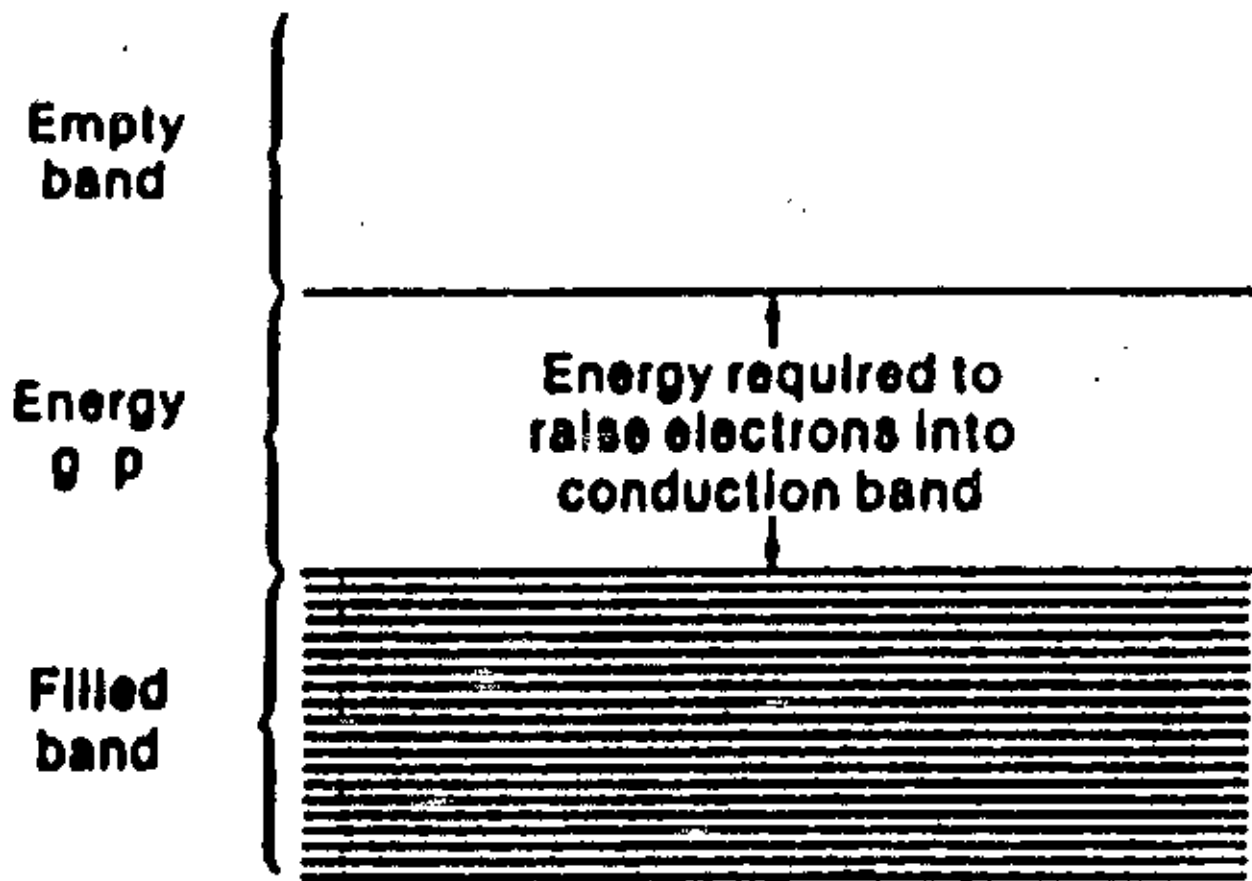


Fig 2.1: Schematic of the energy band in an insulator showing the larger energy gap between the filled band and next available empty band.

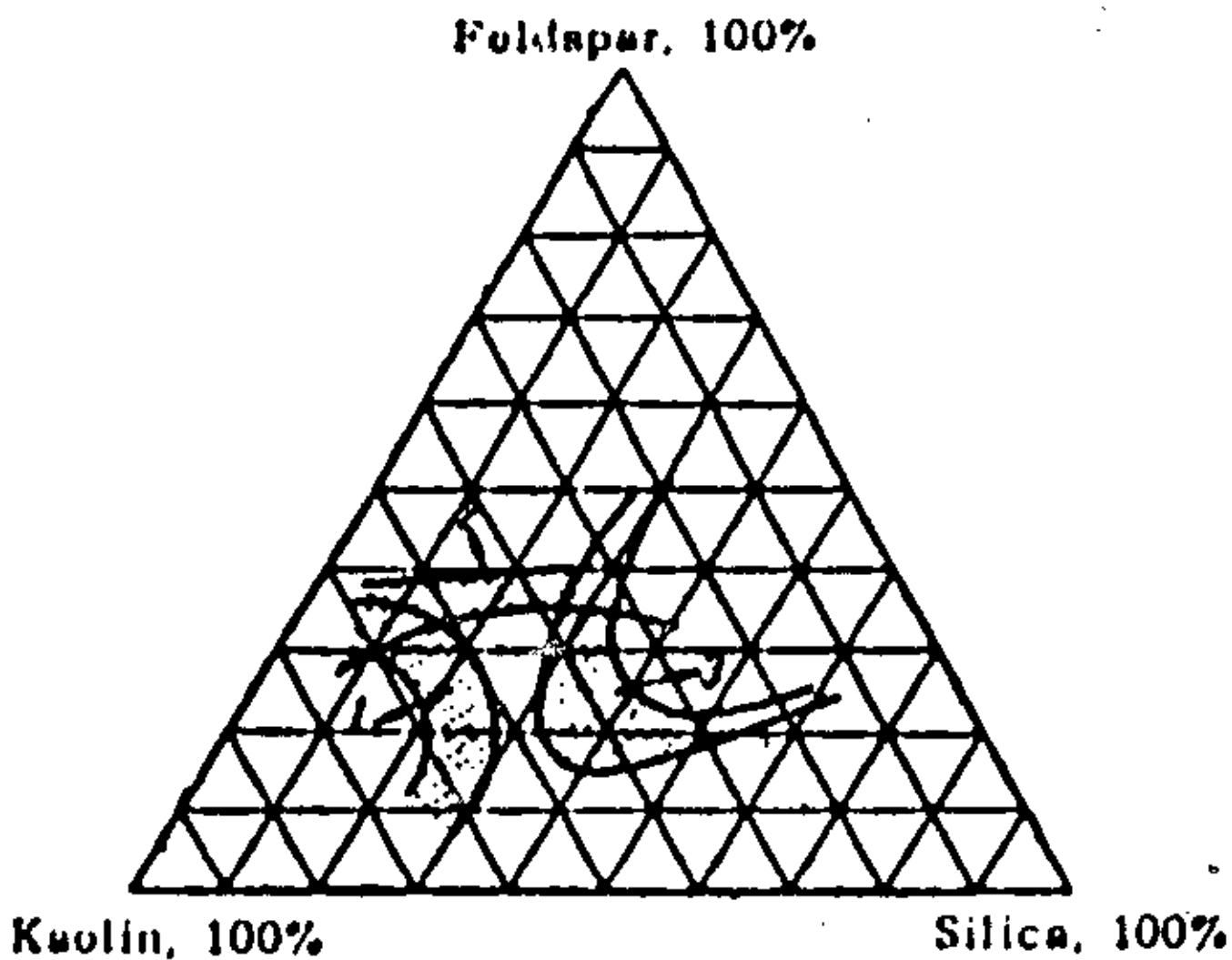


Fig 2.2: Properties of porcelain as function of a mixture composition
1-high heat resistance; 2-high electrical strength; 3-high mechanical strength

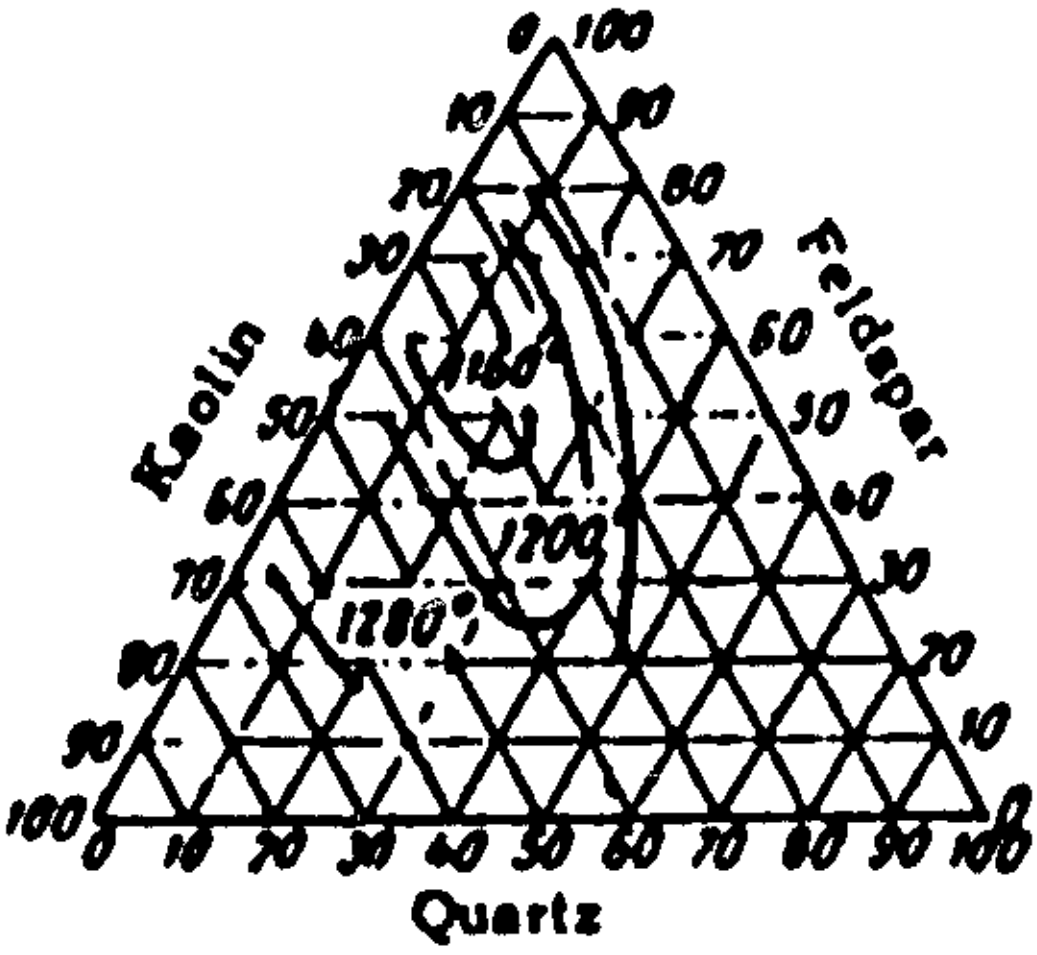


Figure 2.3: The ternary Kaolin-feldspar-quartz system

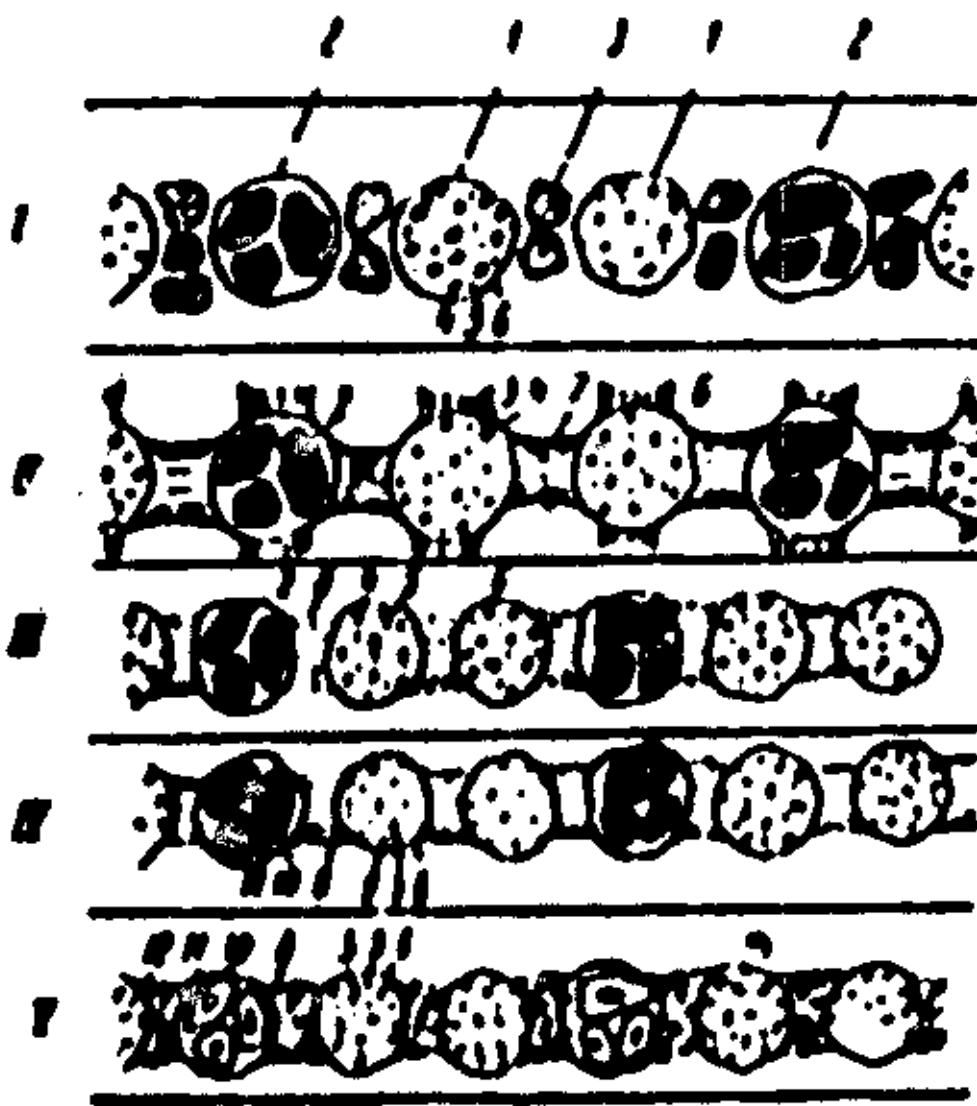


Fig 2.4: Formation of porcelain: 1 – kaolinite; 2- quartz; 3- feldspar; 4- amorphous silica; 5- primary mullite in kaolinite residue; 6- outline of kaolinite along interaction boundaries with feldspar; 7,8-feldspar melt; 9- silica and feldspar melt within kaolinite residue; 10- fused edge of quartz; 11-residue quartz; 12- mullite within feldspar melt (diffusion); I-V – phases of process.

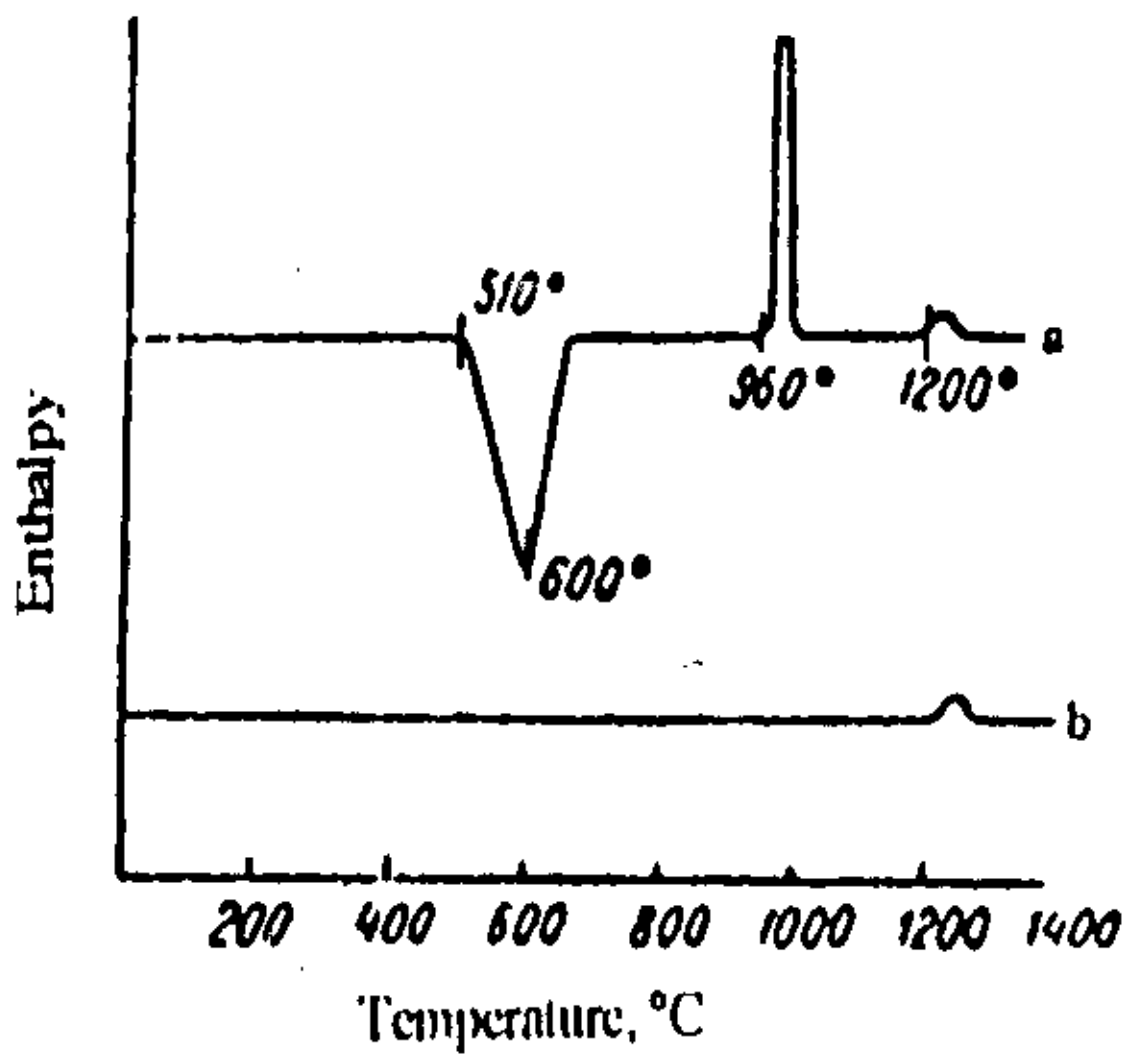


Fig 2.5: Thermogram of Kaolin: a – raw; B – calcined at 950° C.

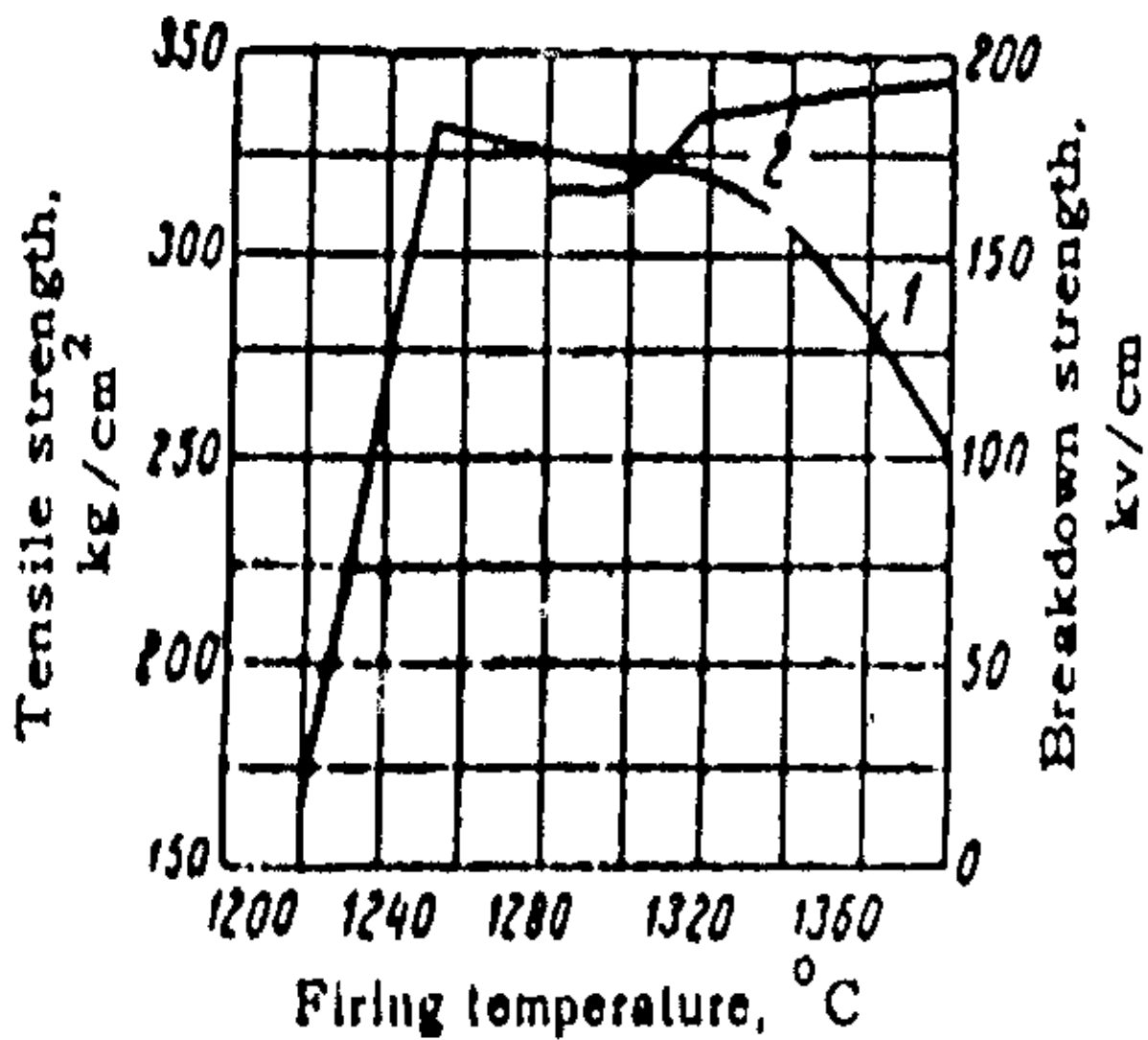


Fig 2.6: Effect of firing temperature and dielectric strength of porcelain
 Curve 1: Mechanical strength and Curve 2: Break down strength.

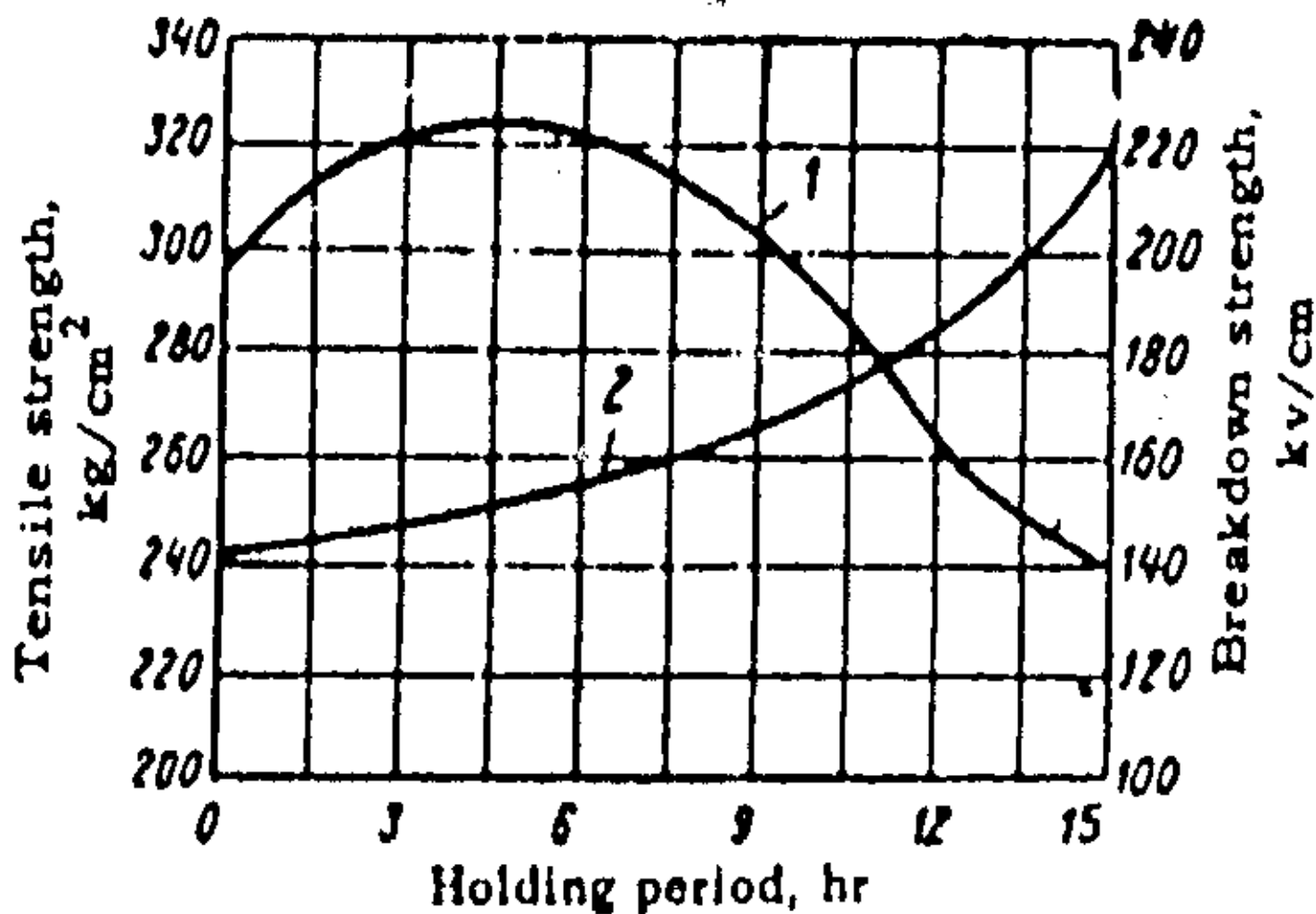
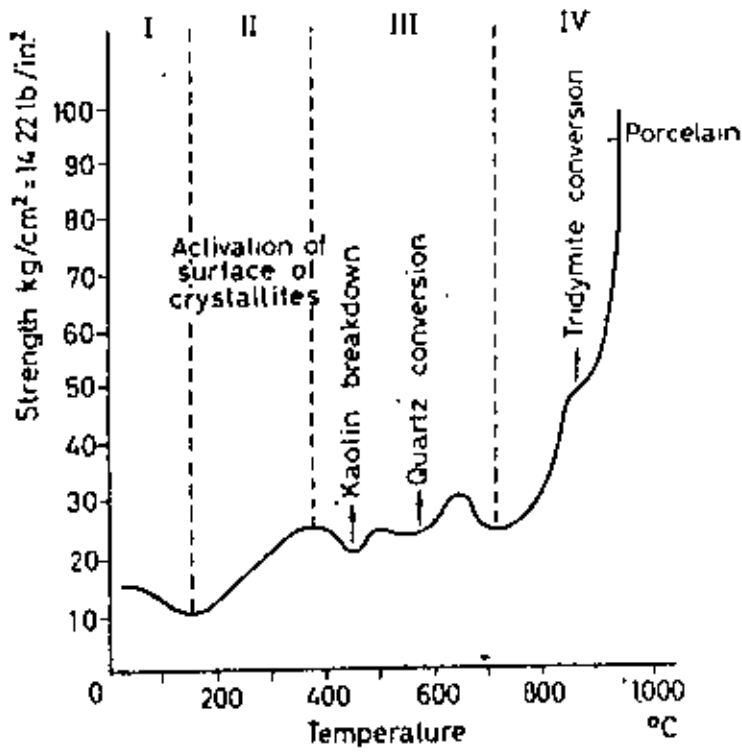


Fig 2.7: Mechanical and dielectric strength of porcelain as a function of length of period ware is held at final firing temperature.
 Curve 1: Mechanical strength, Curve 2: Dielectric strength



(a)

- I First reaction phase: evaporation of water envelopes surrounding the crystallites
- II Second reaction phase: diffusion of water vapour to exterior
- III Third reaction phase: de-activation of surface of crystallites
- IV Fourth reaction phase: interstitial diffusion

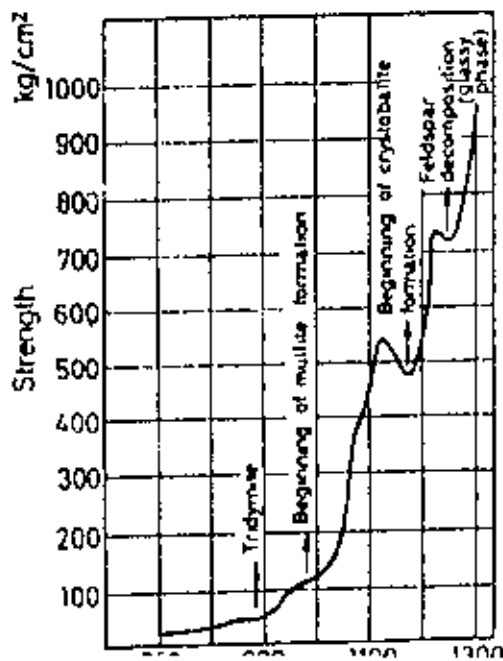


Fig 2.8a: Strength of porcelain body after firing at different temperatures.

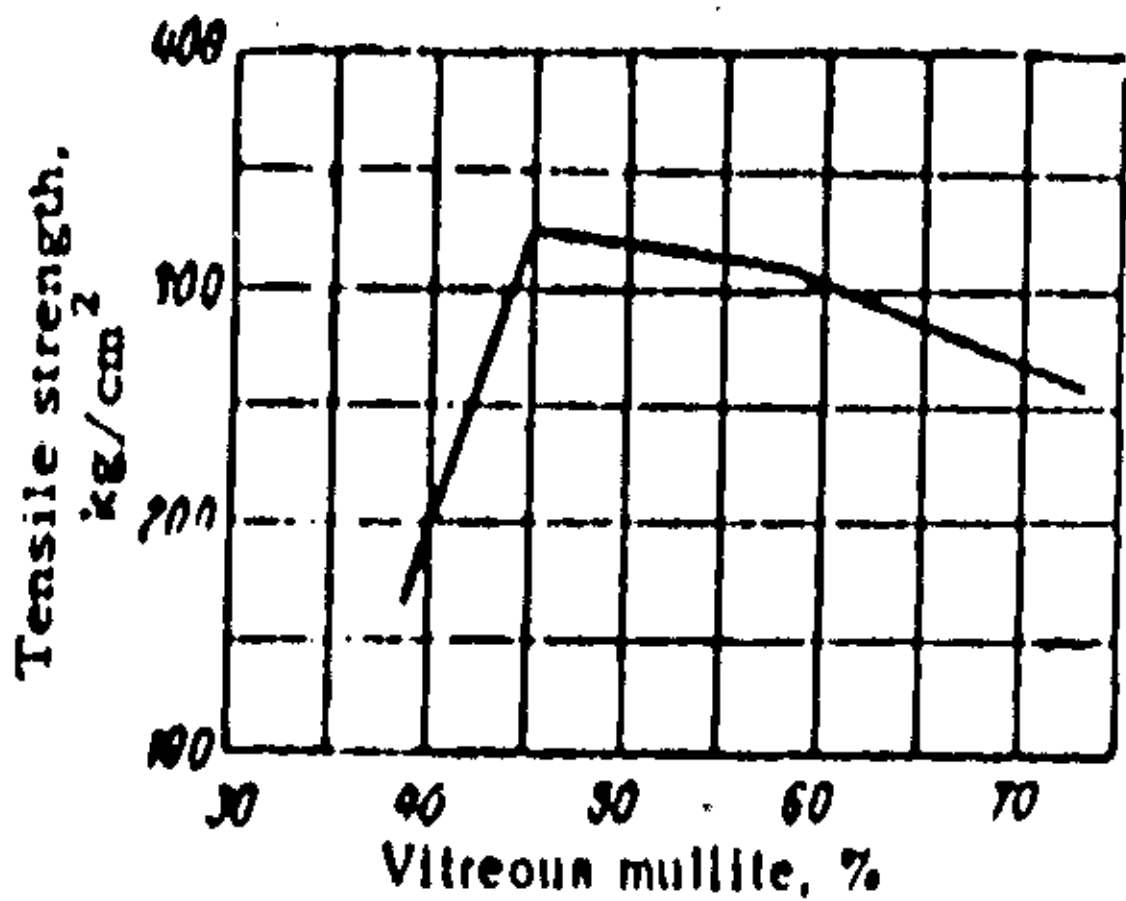


Fig 2.8b: Variation of mechanical strength with the percentage of mullite crystallization.

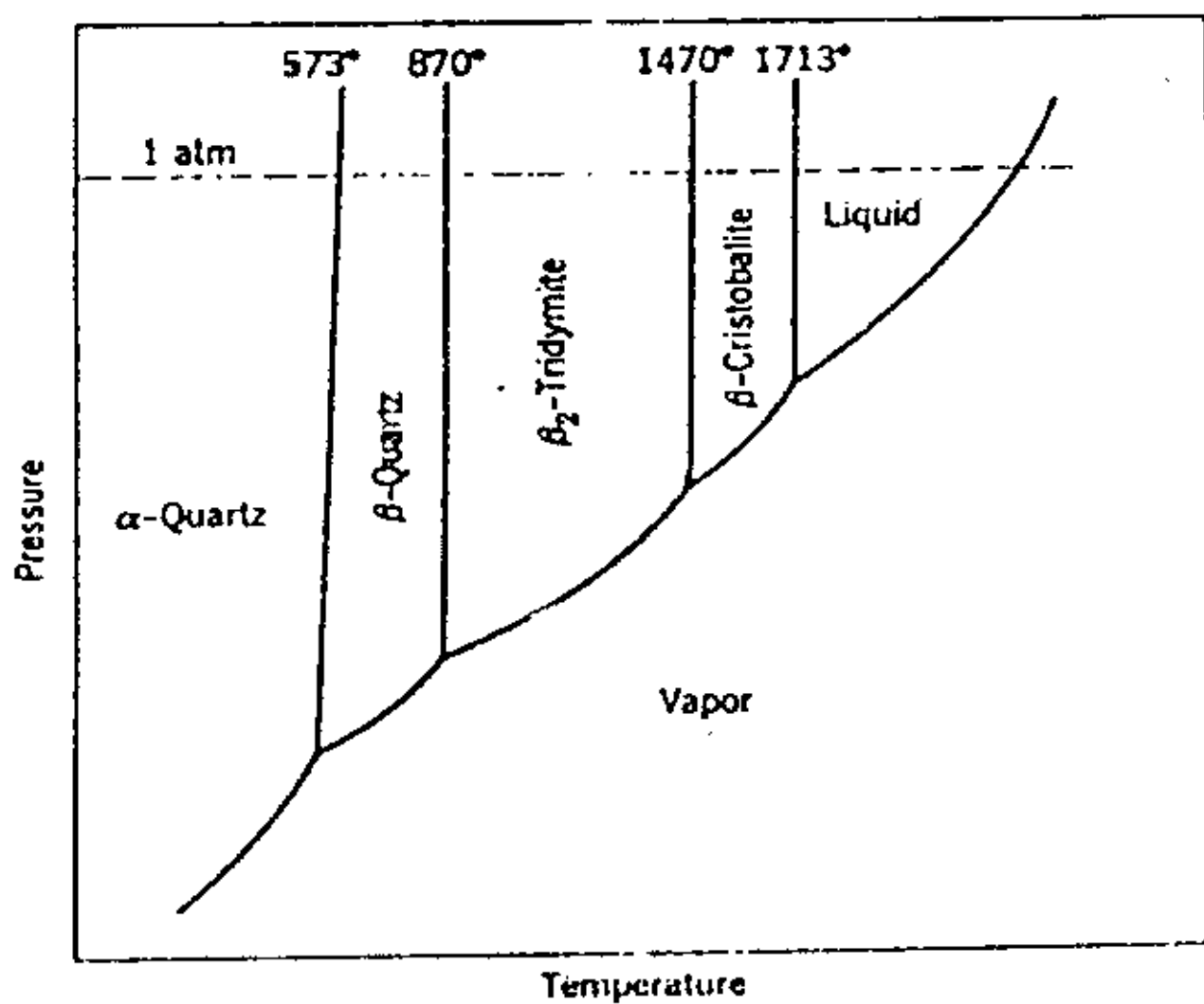


Fig 2.9: Equilibrium diagram for SiO₂

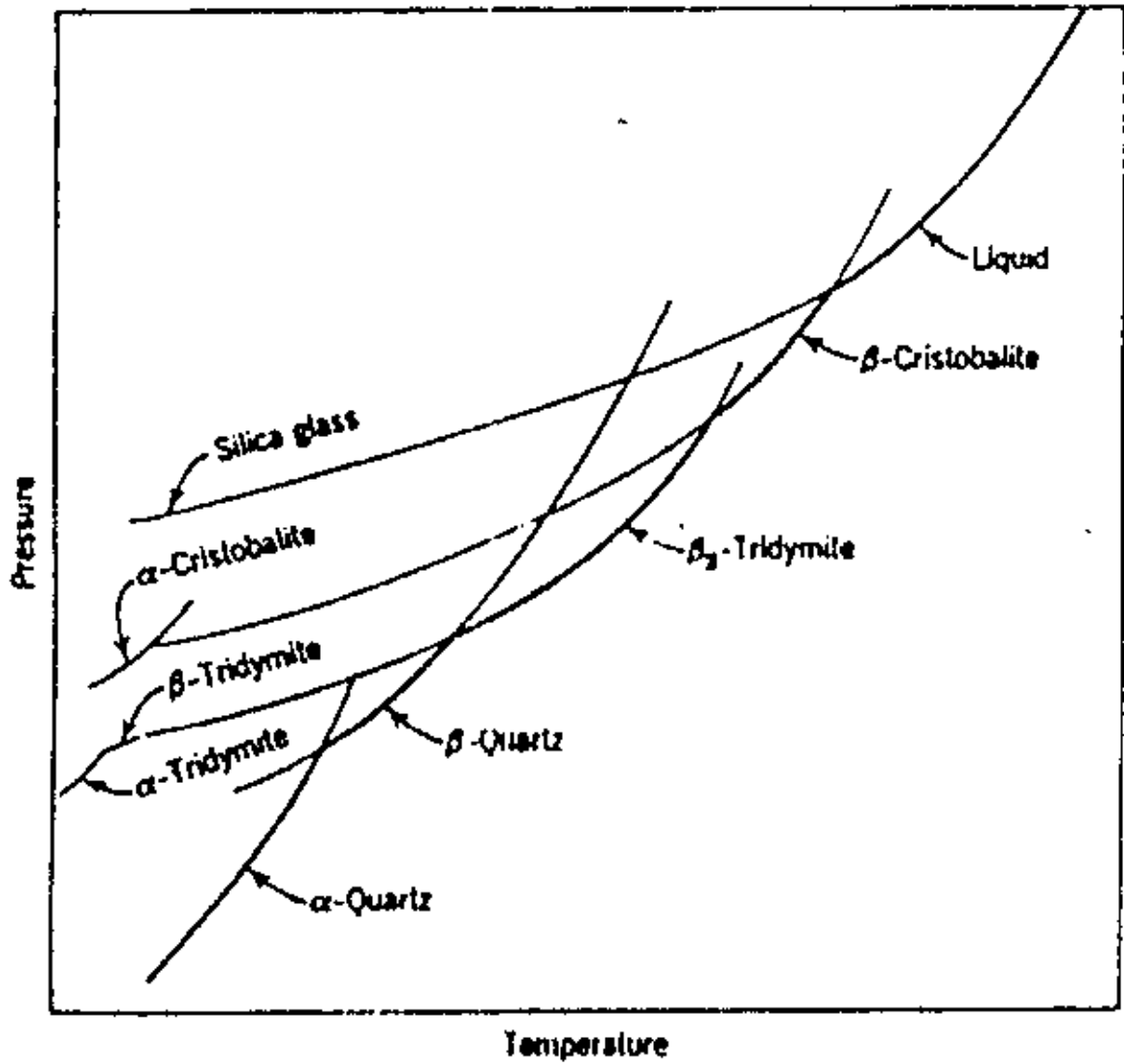


Fig 2.10: Diagram including metastable phases occurring in the system SiO₂

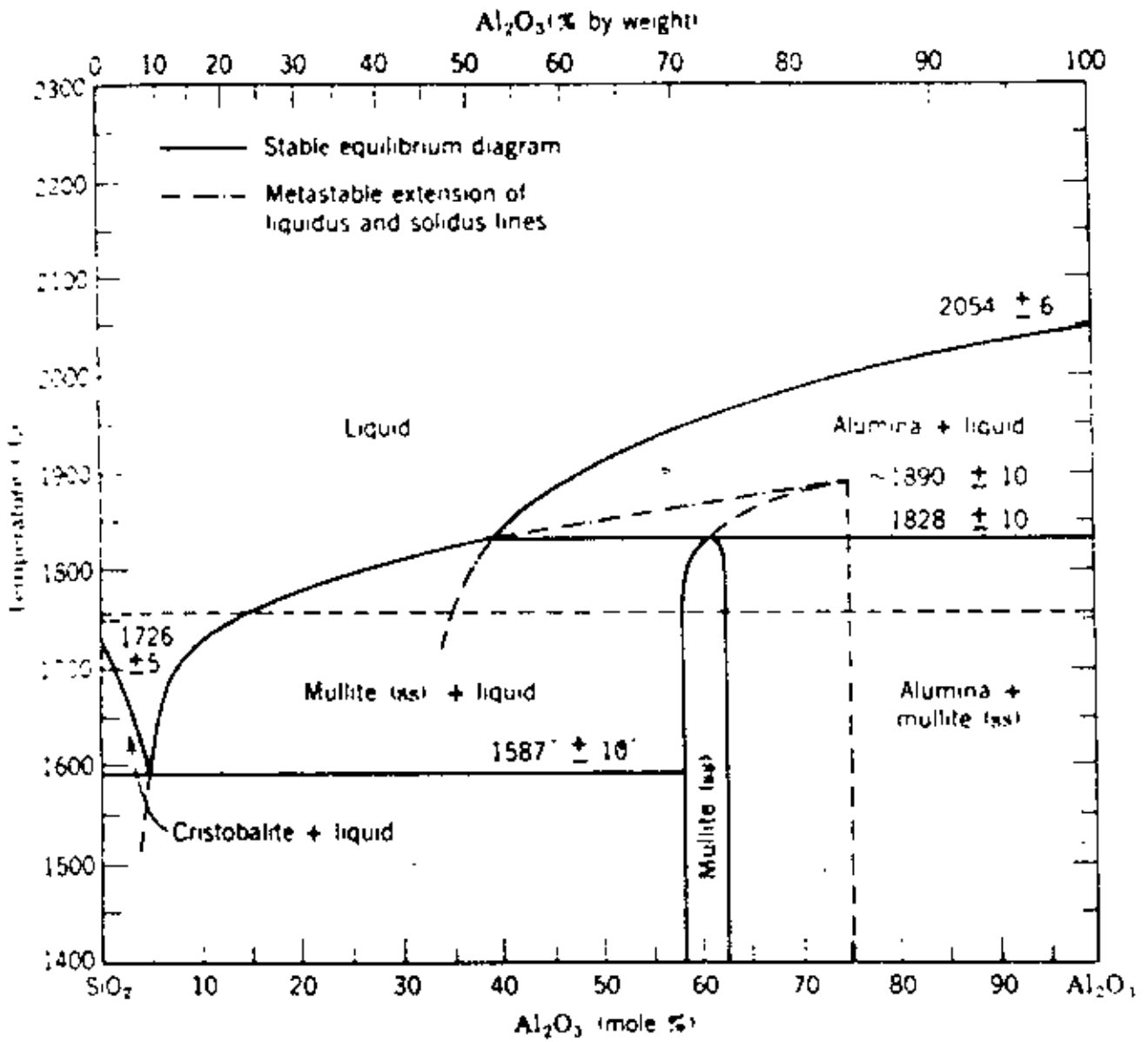


Fig 2.11: The binary Al_2O_3 - SiO_2 System

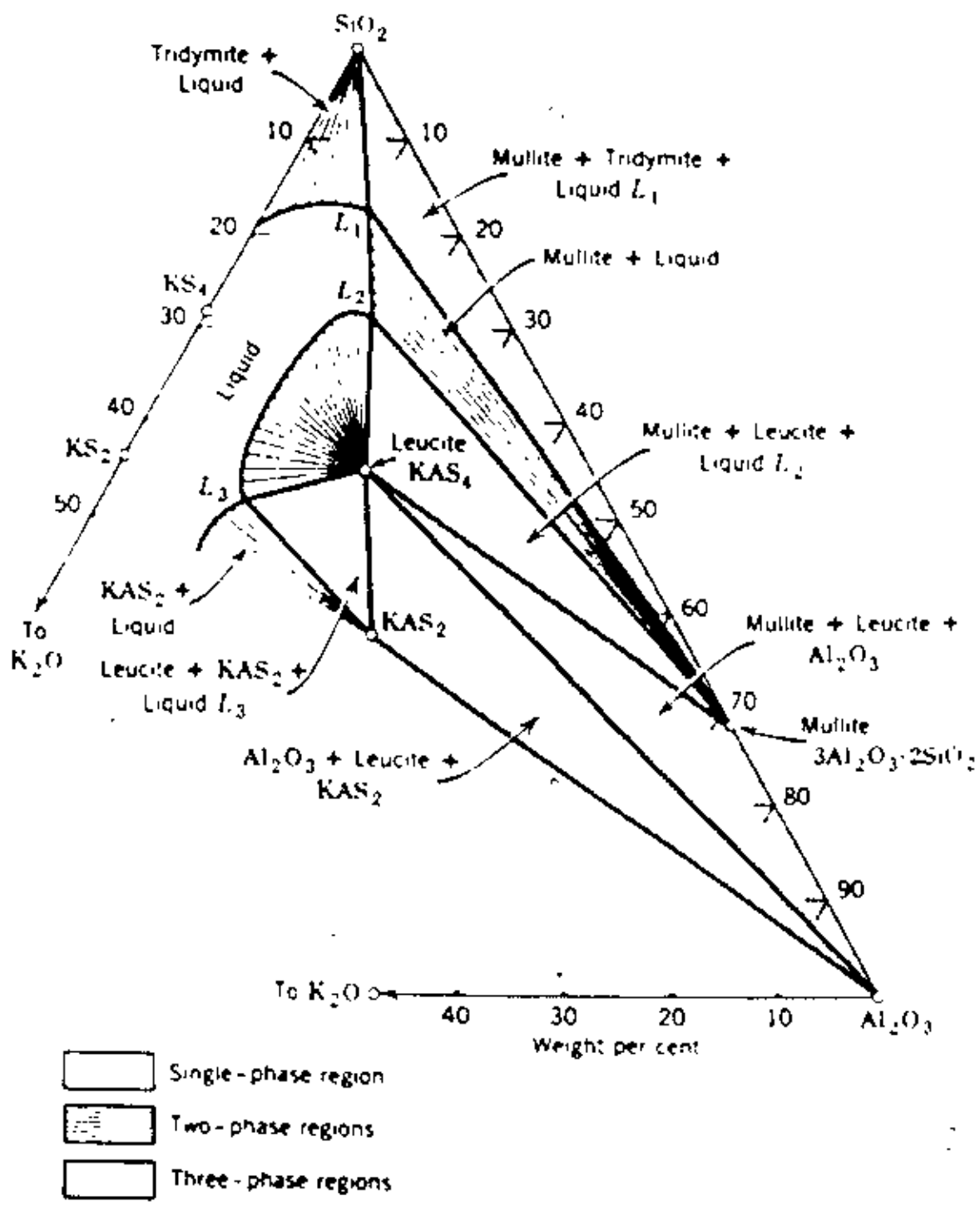


Fig 2.12: Isothermal cut in the $K_2O-Al_2O_3-SiO_2$ diagram at $1200^\circ C$

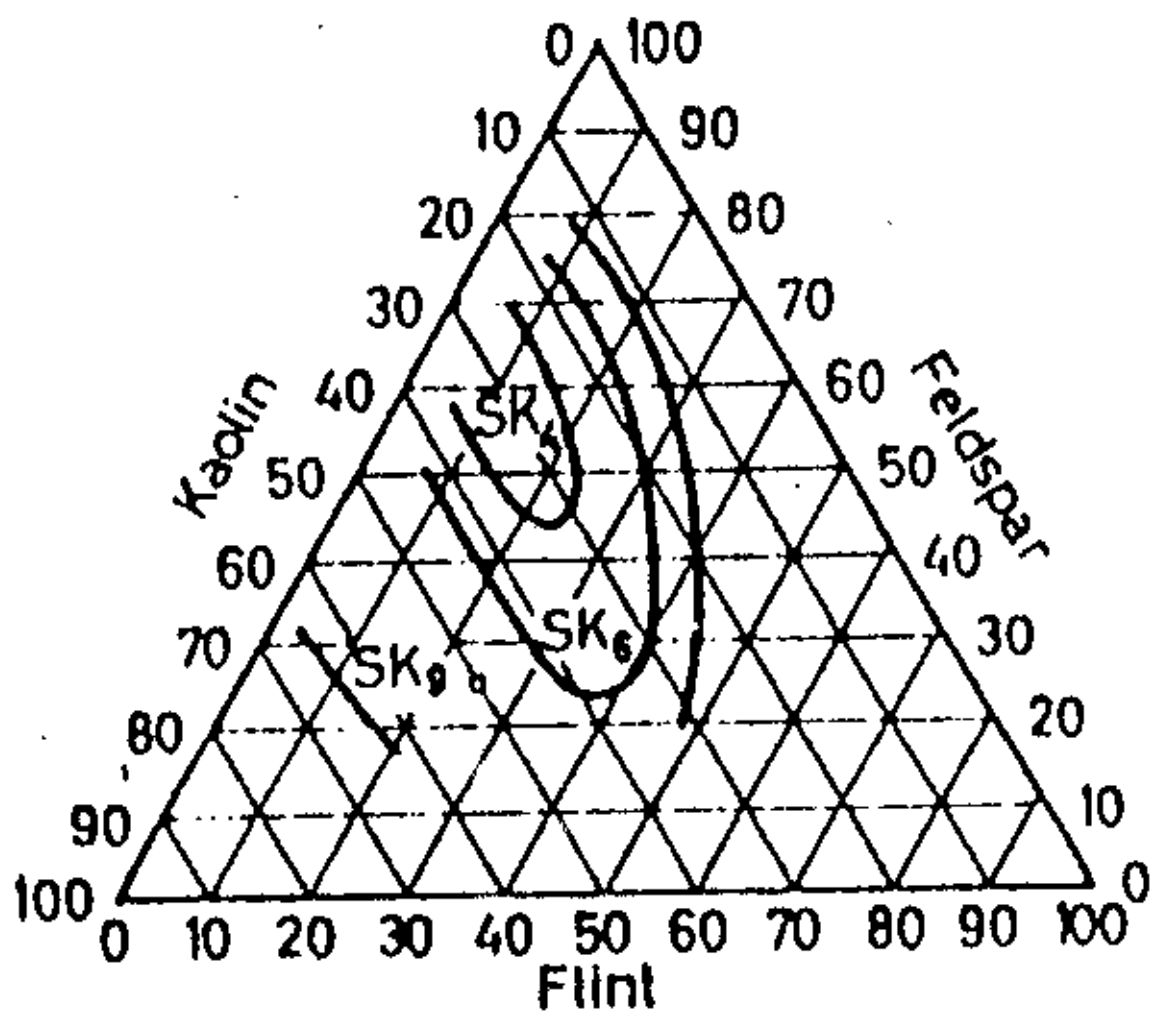


Fig 2.13: Vitrification isothermal of porcelain bodies at 990° C

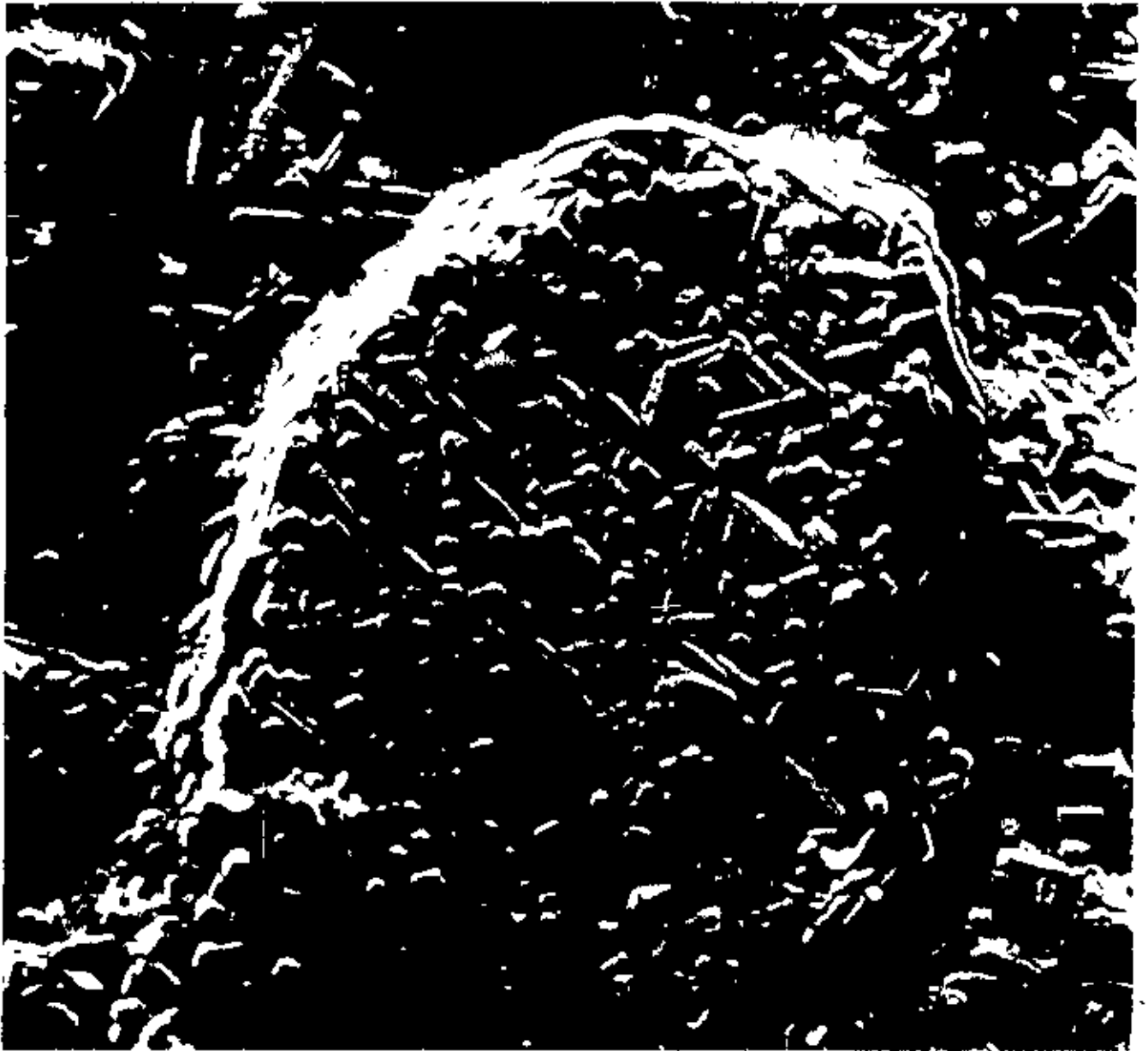


Fig 2.14: Mullite crystals in silica matrix formed by heating kaolinite

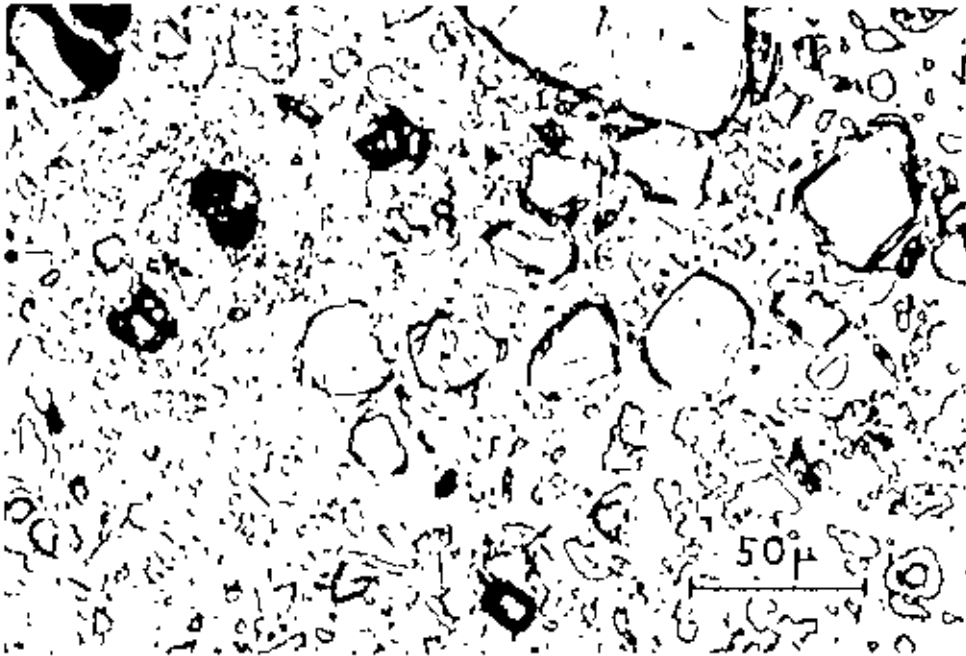


Fig 2.15: Photomicrograph of electrical insulator porcelain showing liquid quartz grain with solution rim, feldspar relicts with indistinct mullite, unresolved clay matrix and dark pores

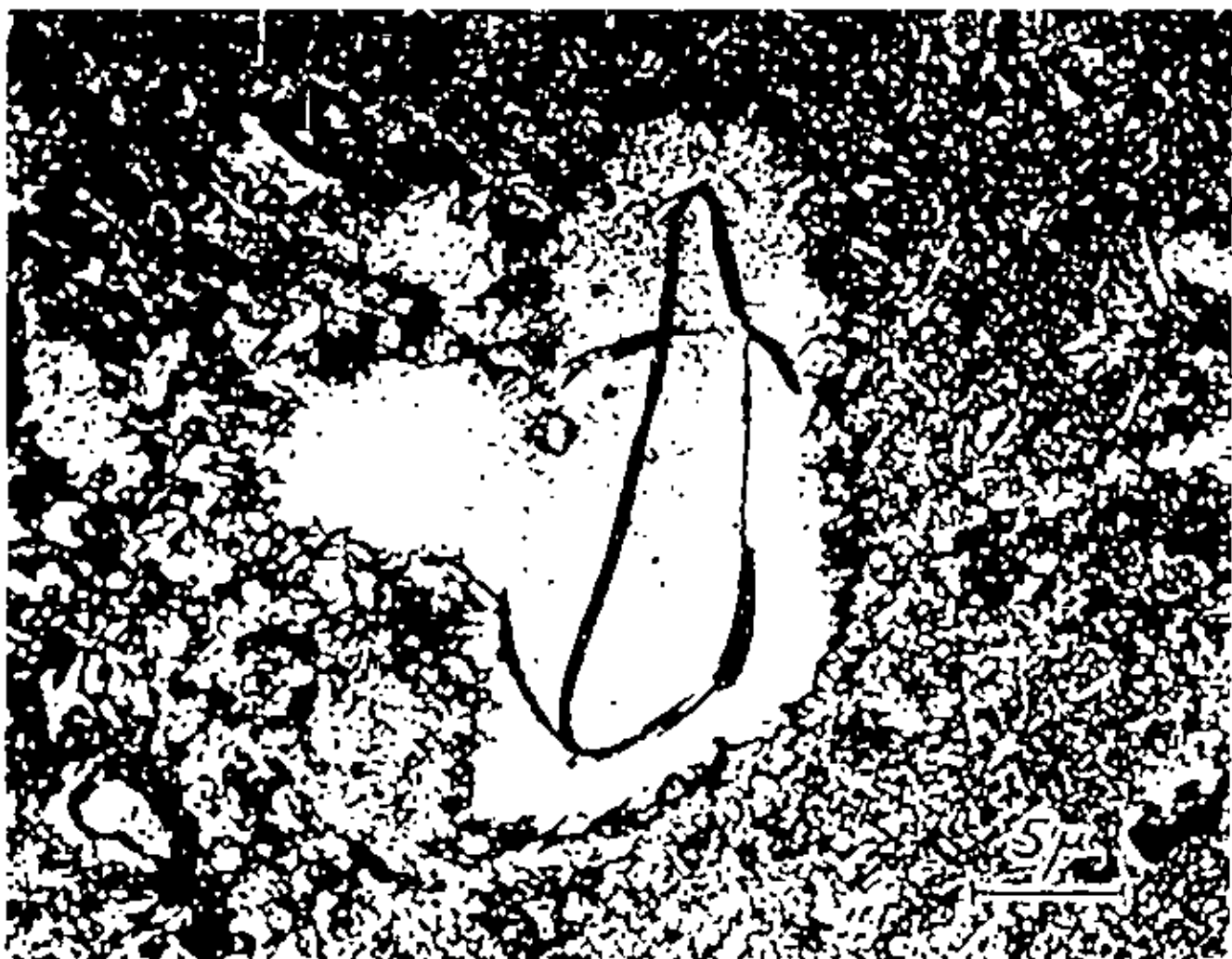


Fig 2.16: Partly dissolved quartz grain in electrical insulator porcelain.

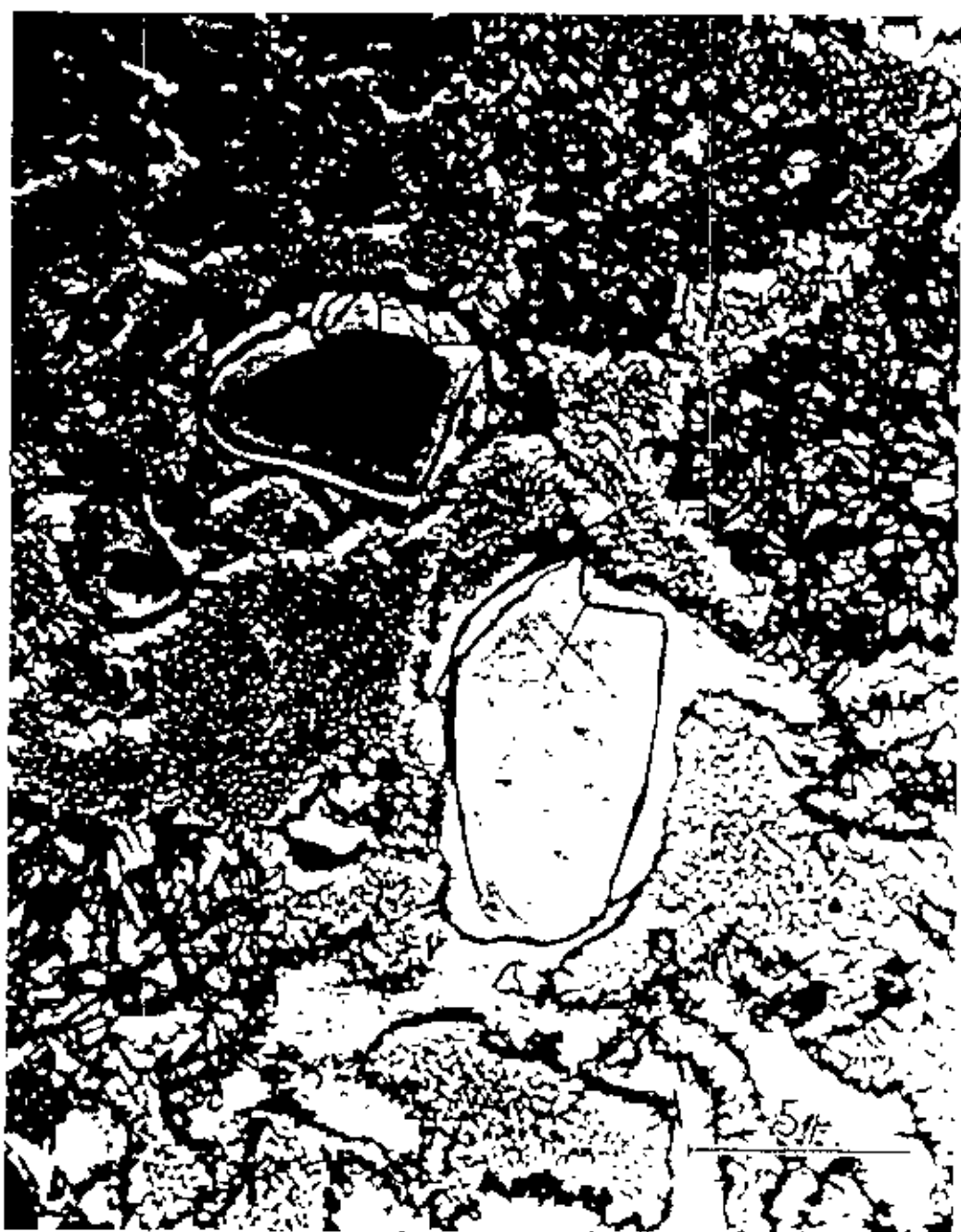


Fig 2.17: Electron micrograph of electrical insulator porcelain

RAW MATERIALS

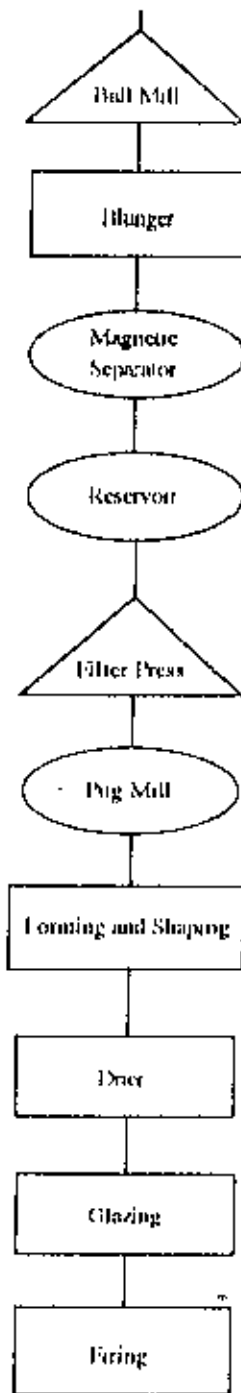


Fig 3.1: Flow chart of the insulator body processing used at the BSEF.

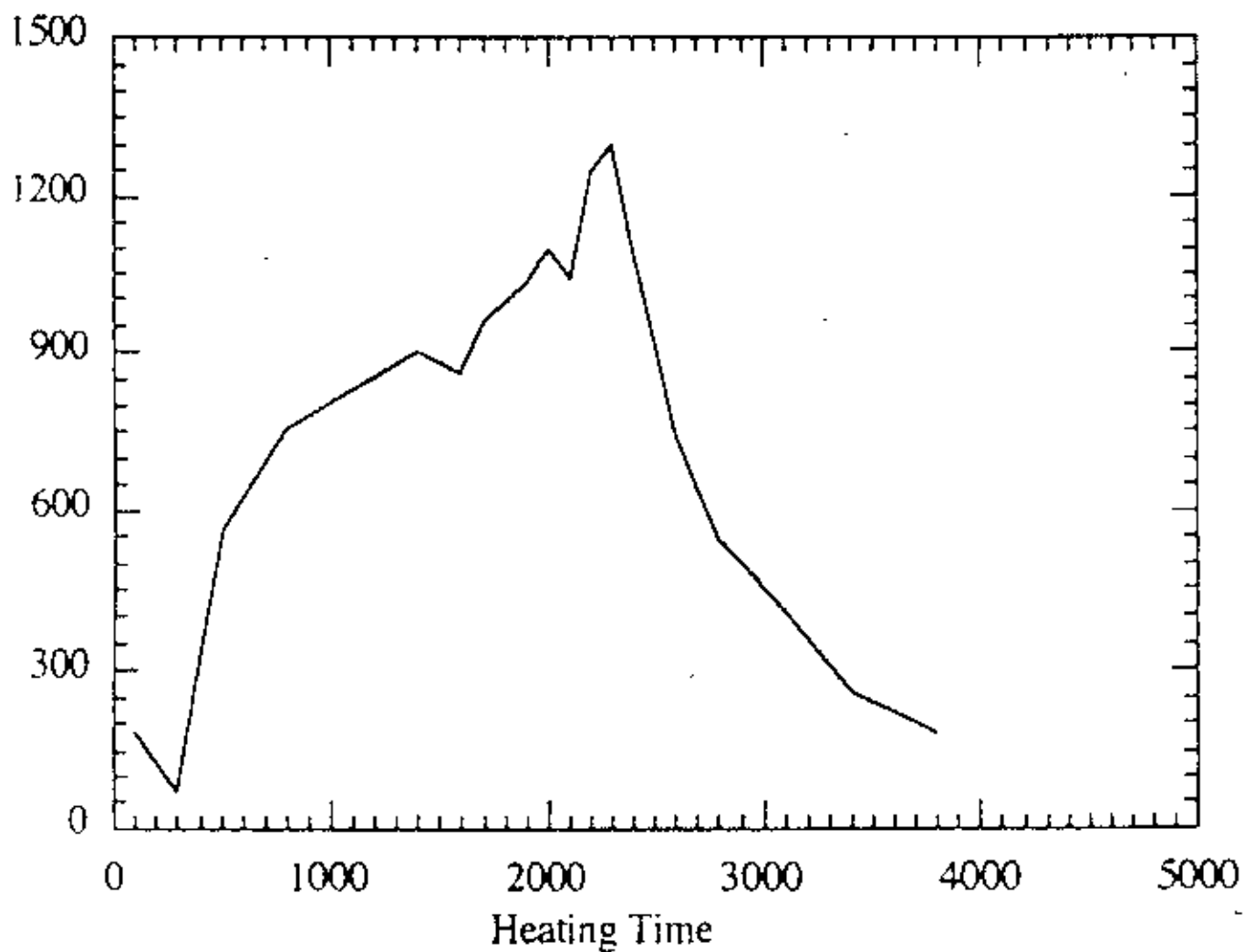


Fig3.2a: Heating cycle of the BISF Tunnel Kiln used for firing the ceramic insulator materials.

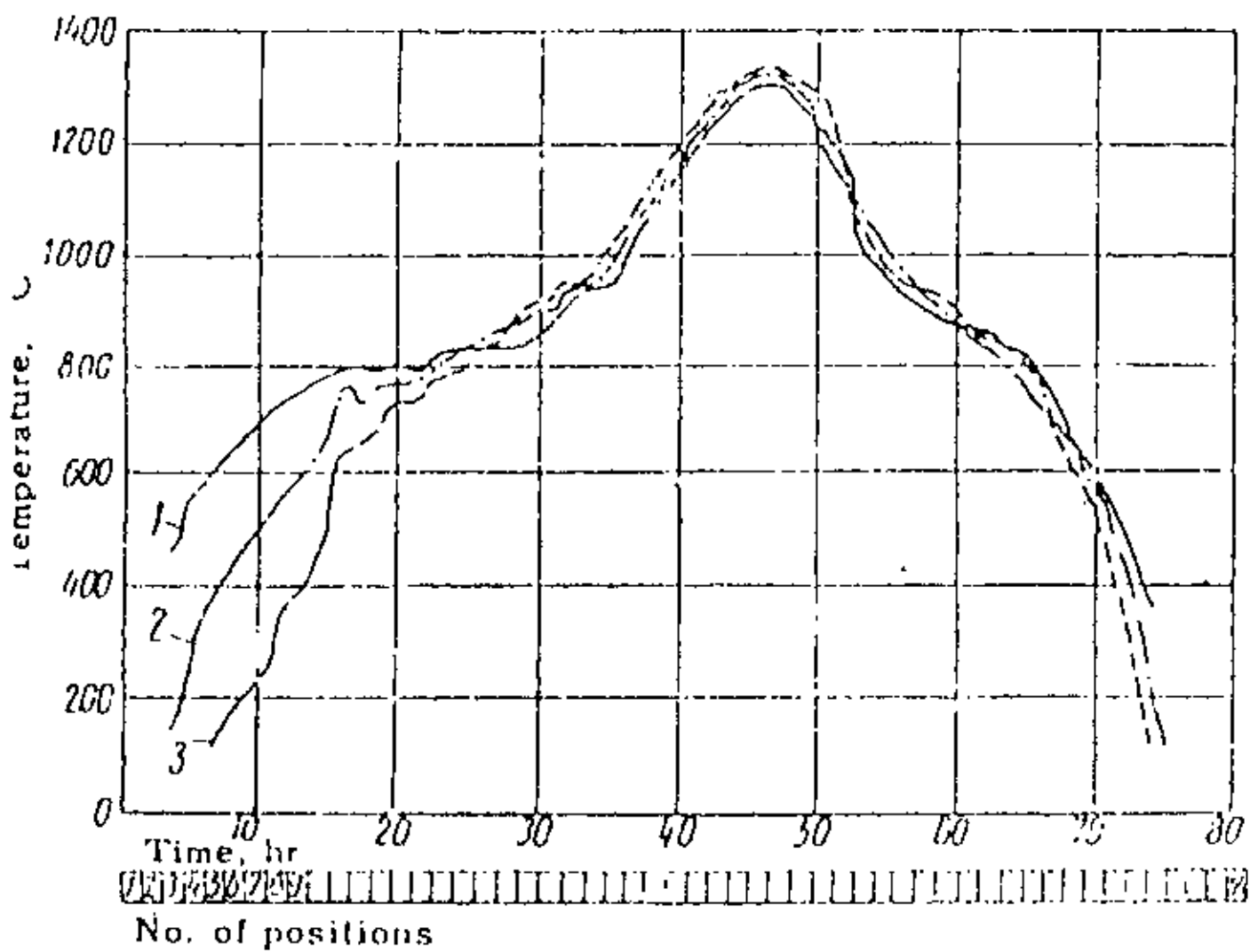
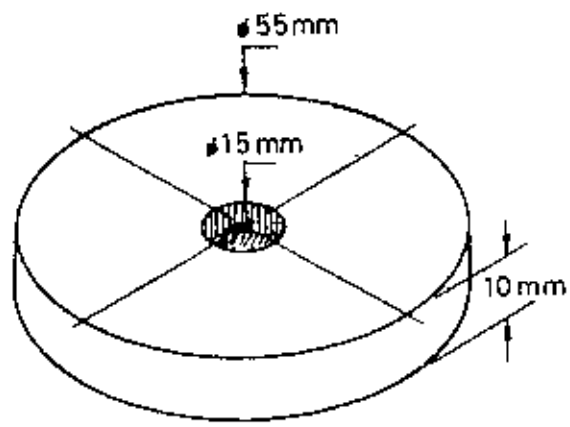
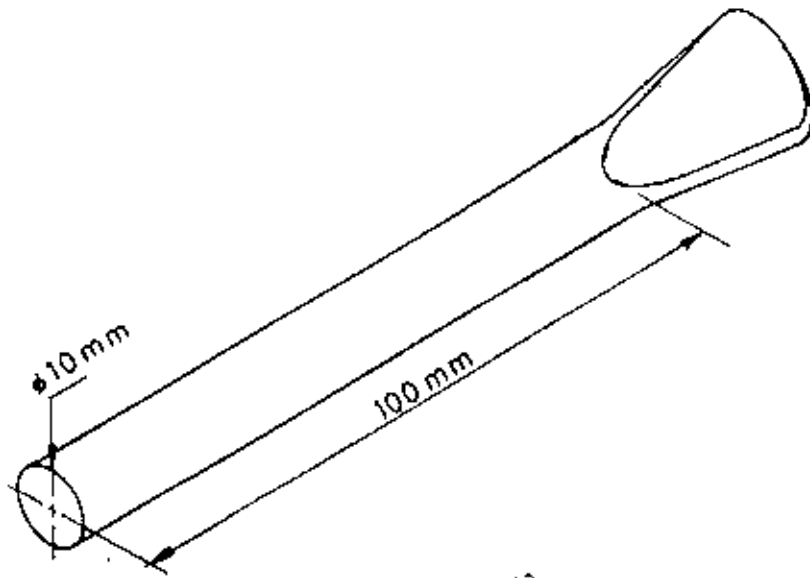


Fig 3.2 b: Standard firing curves for high voltage insulators in a tunnel kiln

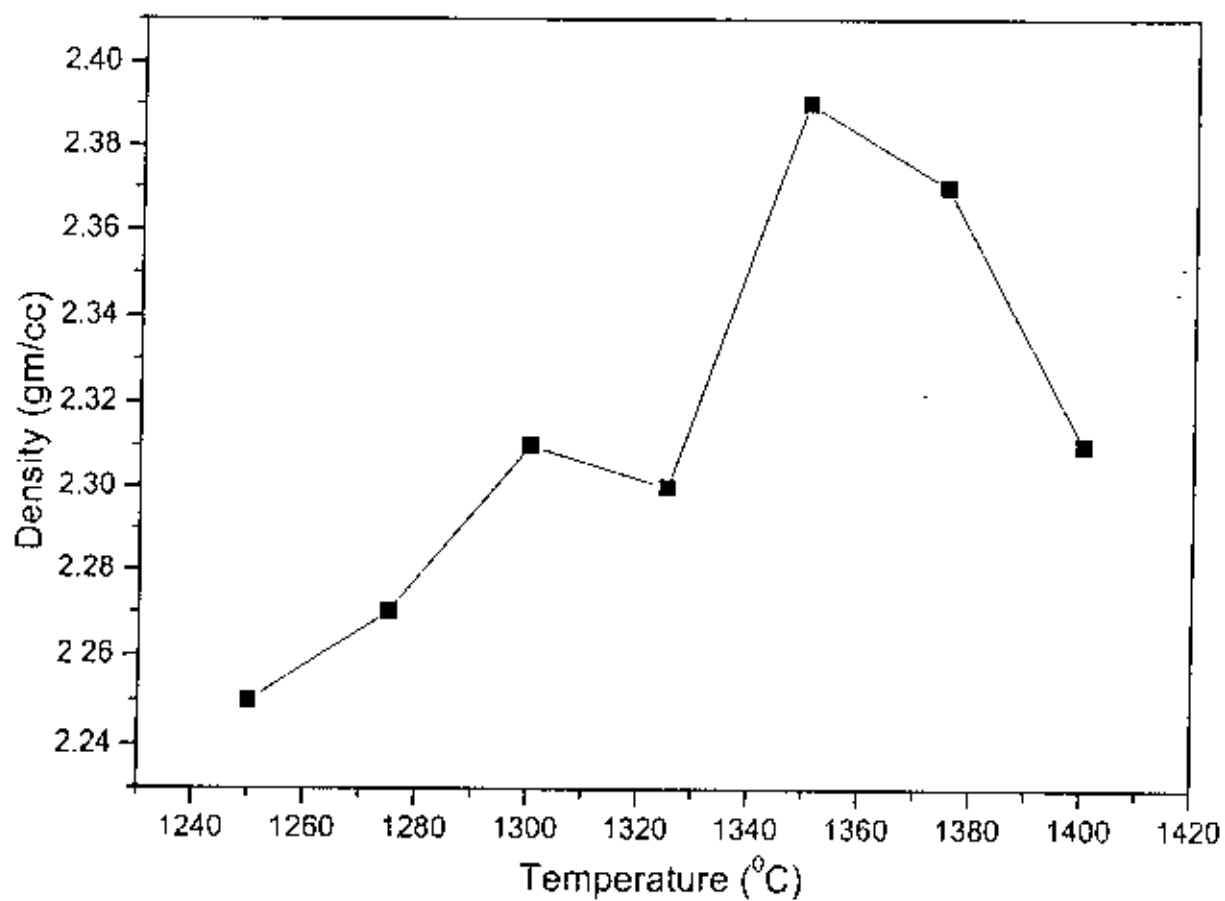


a



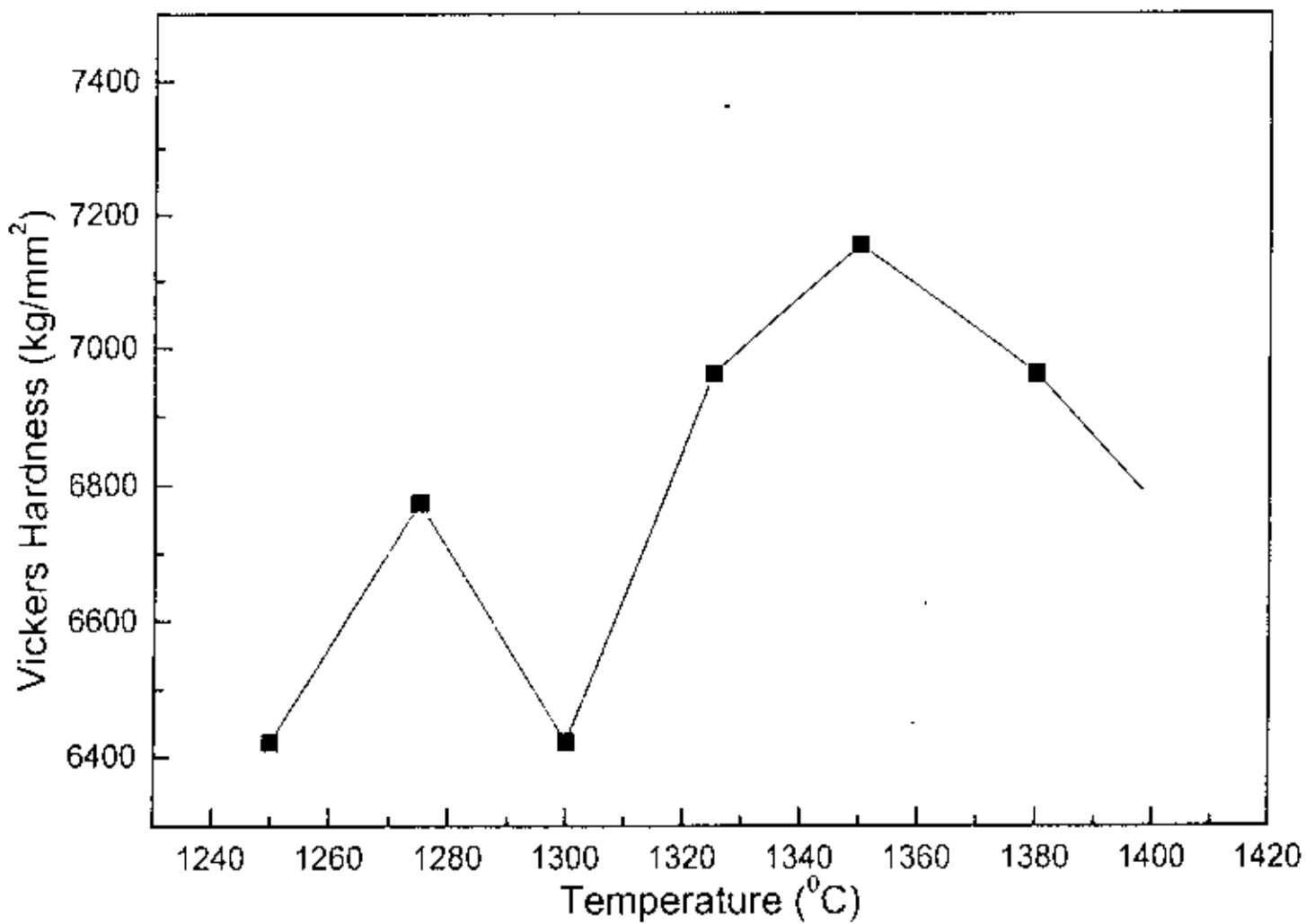
b

Fig 3.4: Test specimen for a- Dielectric strength test and b- bending strength test



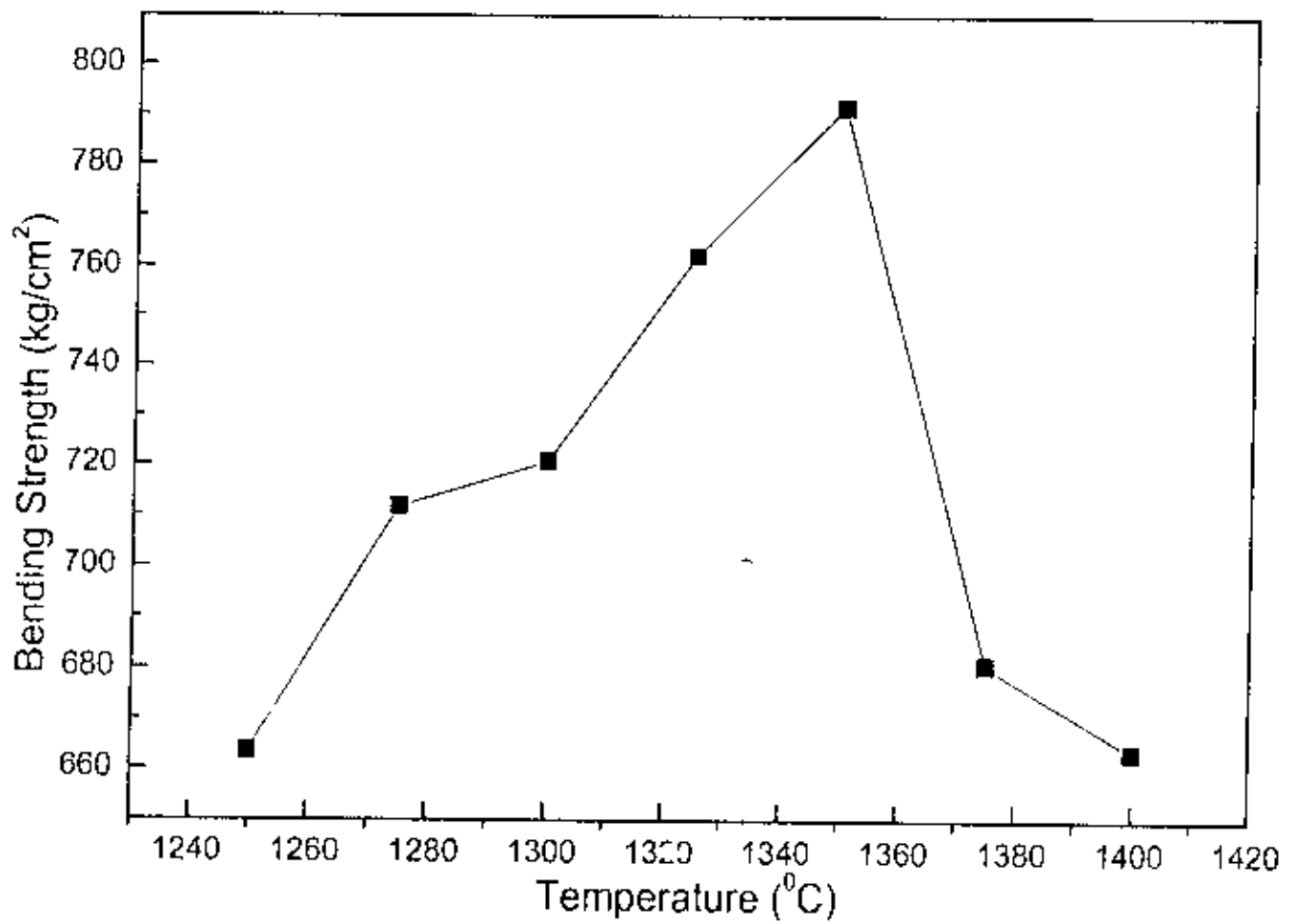
Variation of density with temperature

Fig : Variation of density with temperature



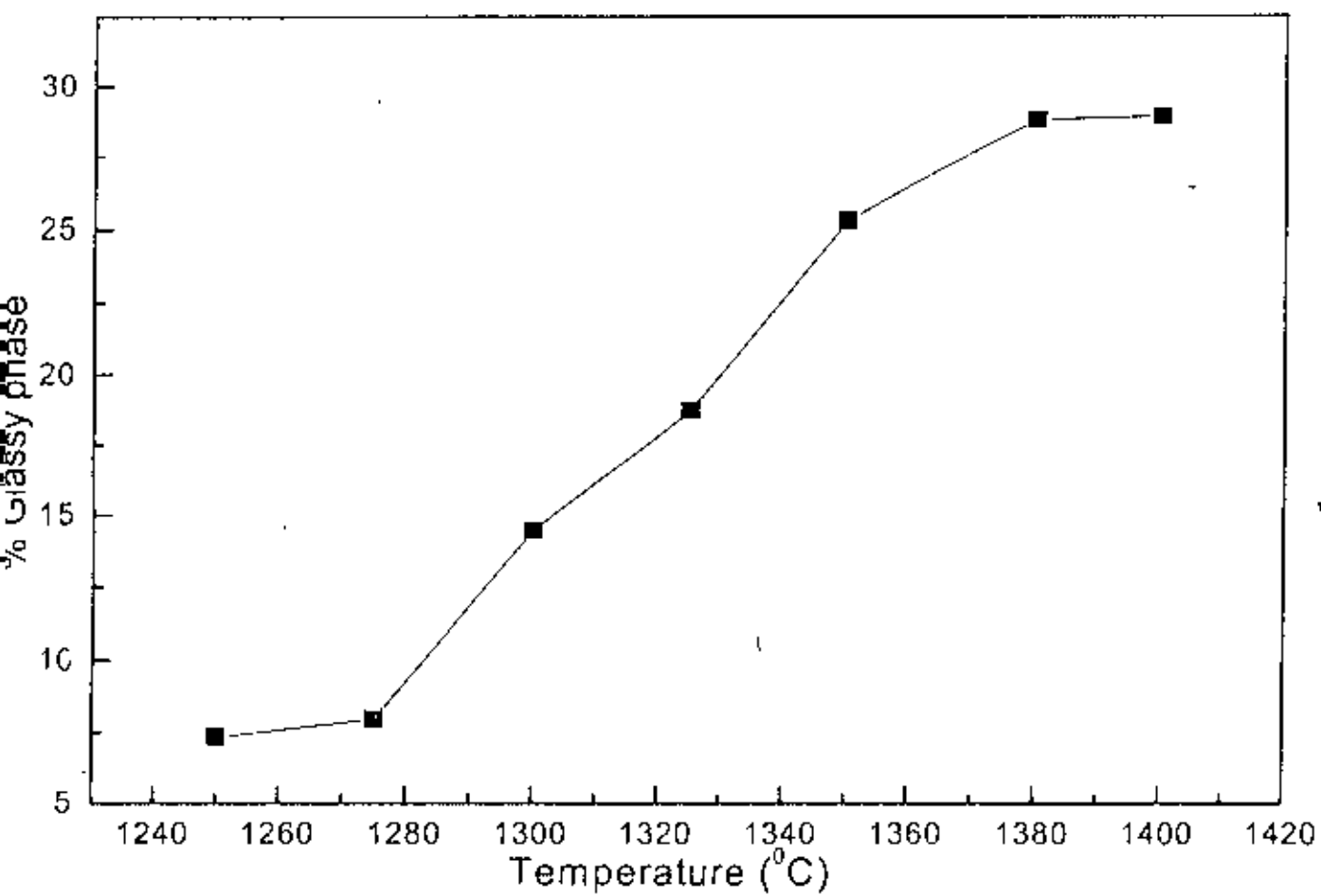
Variation of hardness at different temperatures

Fig : Variation of hardness of ceramic insulators fired at different temperatures



Variation of Bending Strength with firing Temperature

Fig : Variation of bending strength with temperature



Variation of glassy phase content with temperature

Fig : variation of Glassy phase content with temperature

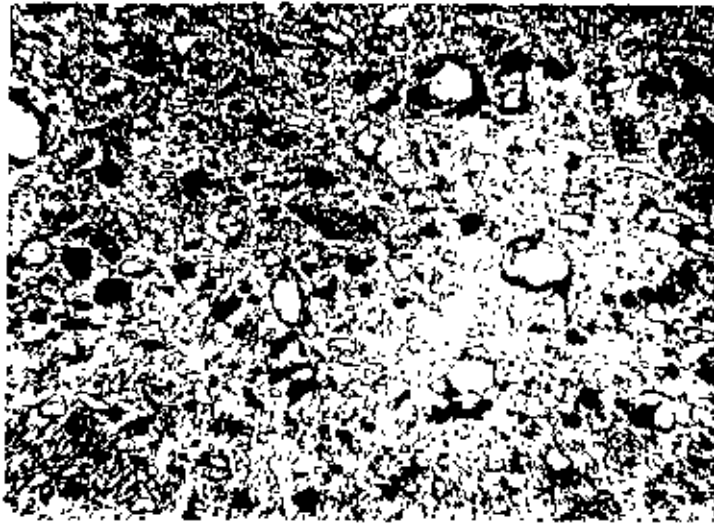


Fig 4.5: Microstructure of porcelain ceramic insulator fired at 1250°C in 100X magnification showing quartz grain (bright particle) and clay matrix (white background) and mullite crystal black areas.

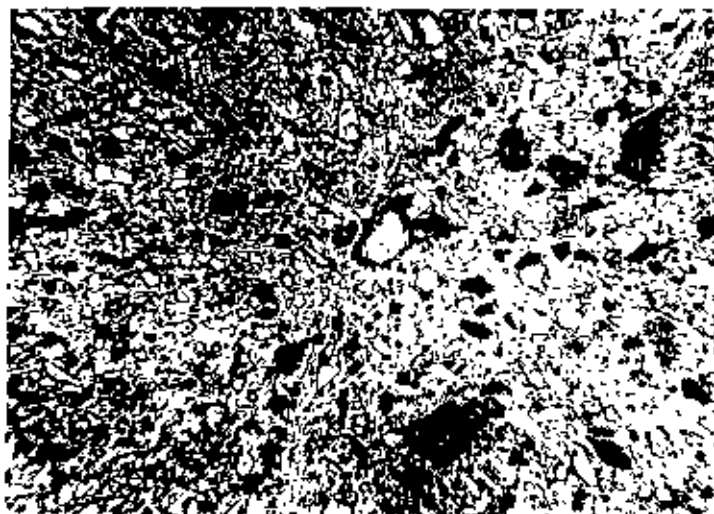


Fig 4.6: Microstructure of porcelain ceramic insulator fired at 1275°C in 100X magnification showing quartz grain (bright particle) and clay matrix (white background) and mullite crystal in black areas.

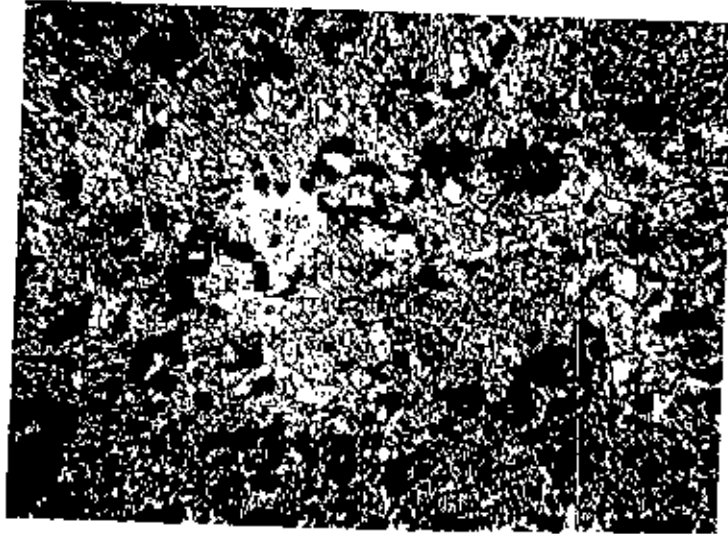


Fig 4.7: Microstructure of porcelain ceramic insulator fired at 1300°C in 100X magnification showing quartz grain (bright particle) and clay matrix (white background) and mullite crystal black areas.

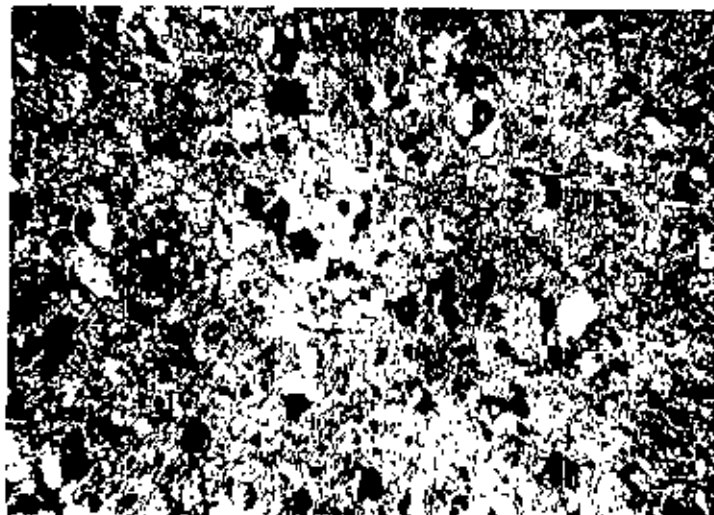


Fig 4.8: Microstructure of porcelain ceramic insulator fired at 1325°C in 100X magnification showing quartz grain (bright particle) and clay matrix (white background) and mullite crystal black areas.

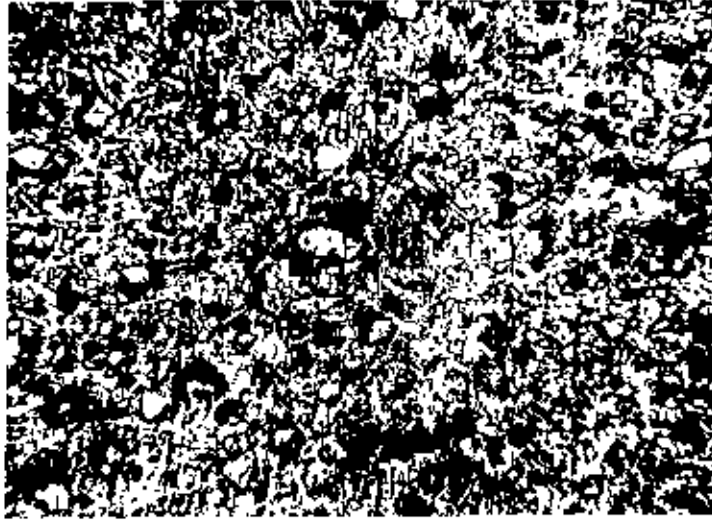


Fig 4.9: Microstructure of porcelain ceramic insulator fired at 1350°C in 100X magnification showing quartz grain (bright particle) and clay matrix (white background)

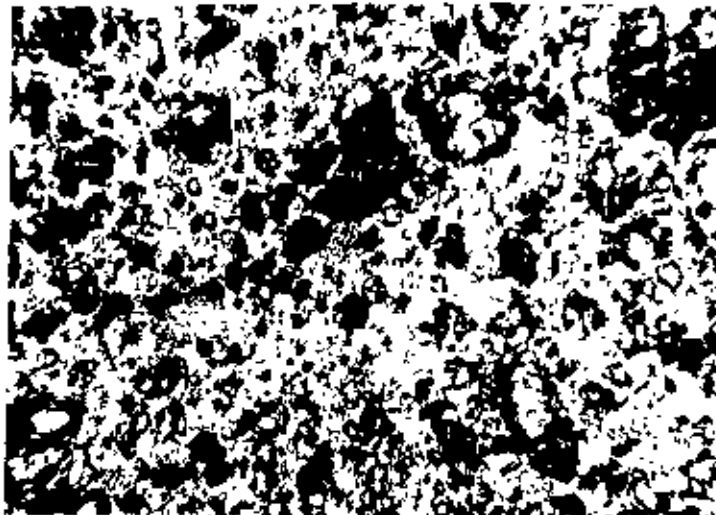


Fig 4.10: Microstructure of porcelain ceramic insulator fired at 1375°C in 100X magnification showing quartz grain (bright particle) and clay matrix (white background) and mullite crystal black areas.

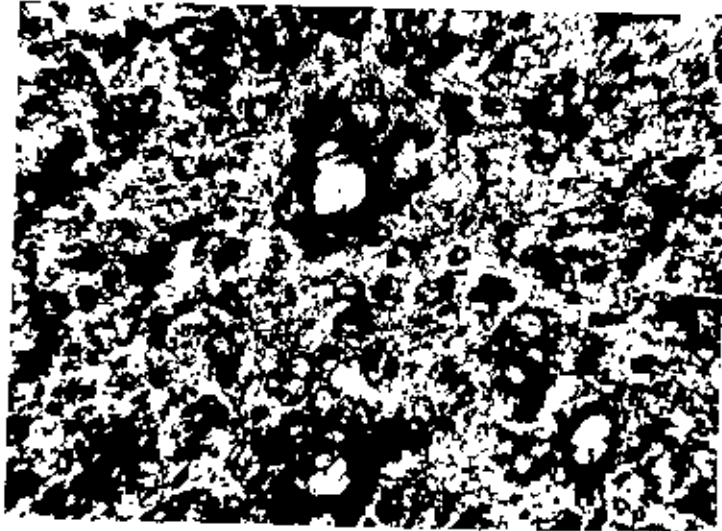


Fig 4.11: Microstructure of porcelain ceramic insulator fired at 1400°C in 100X magnification showing quartz grain (bright particle) and clay matrix (white background) and mullite crystal in black areas.



Fig 4.12: Microstructure of Porcelain Ceramic Insulator showing the glassy rim at 400X magnification glassy rim (black areas) surrounding the bright quartz particle.

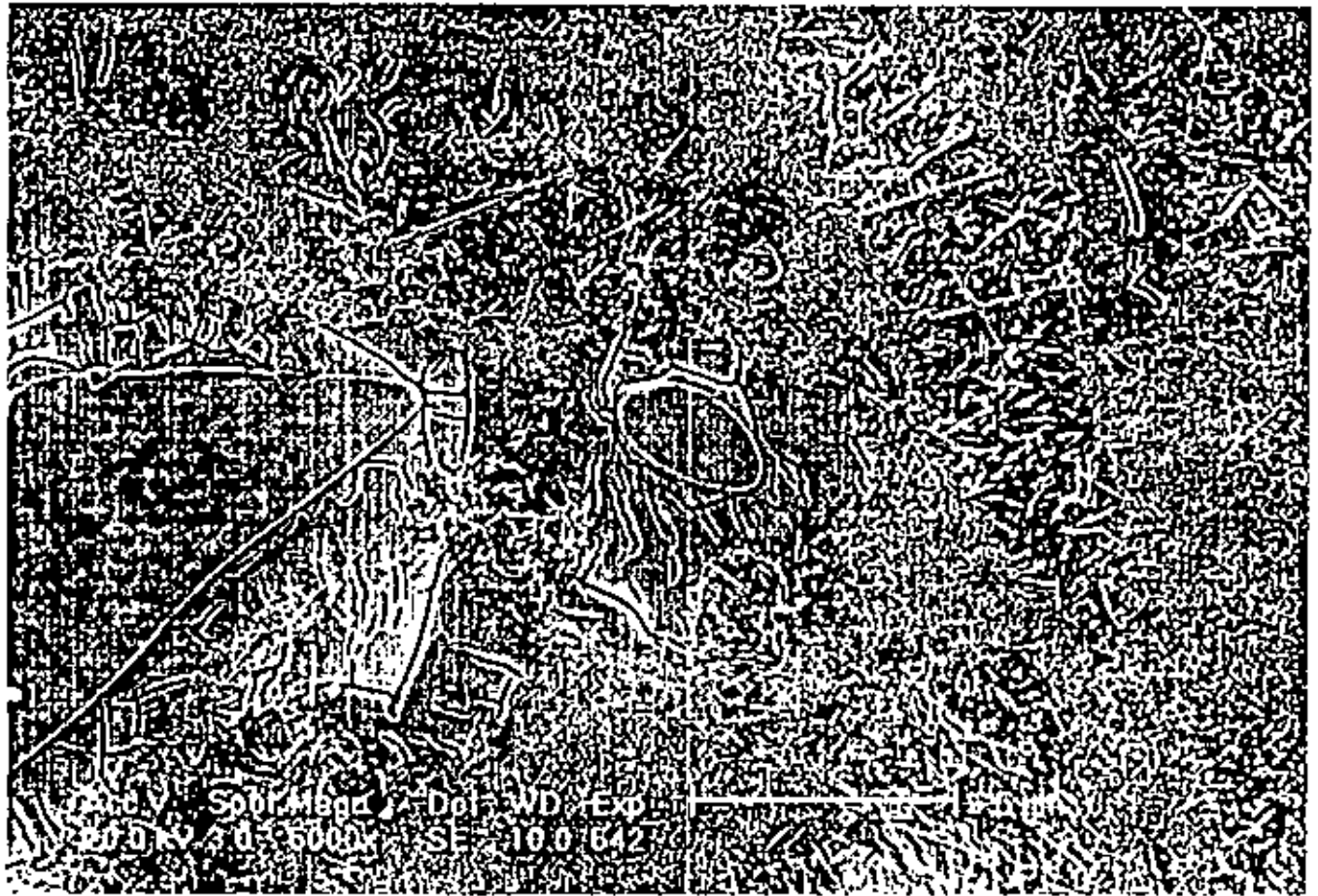


Fig 4.13: SEM image of porcelain ceramic insulator showing quartz grains, cracks, mullite needles and clay matrix (Magnification 5000X).

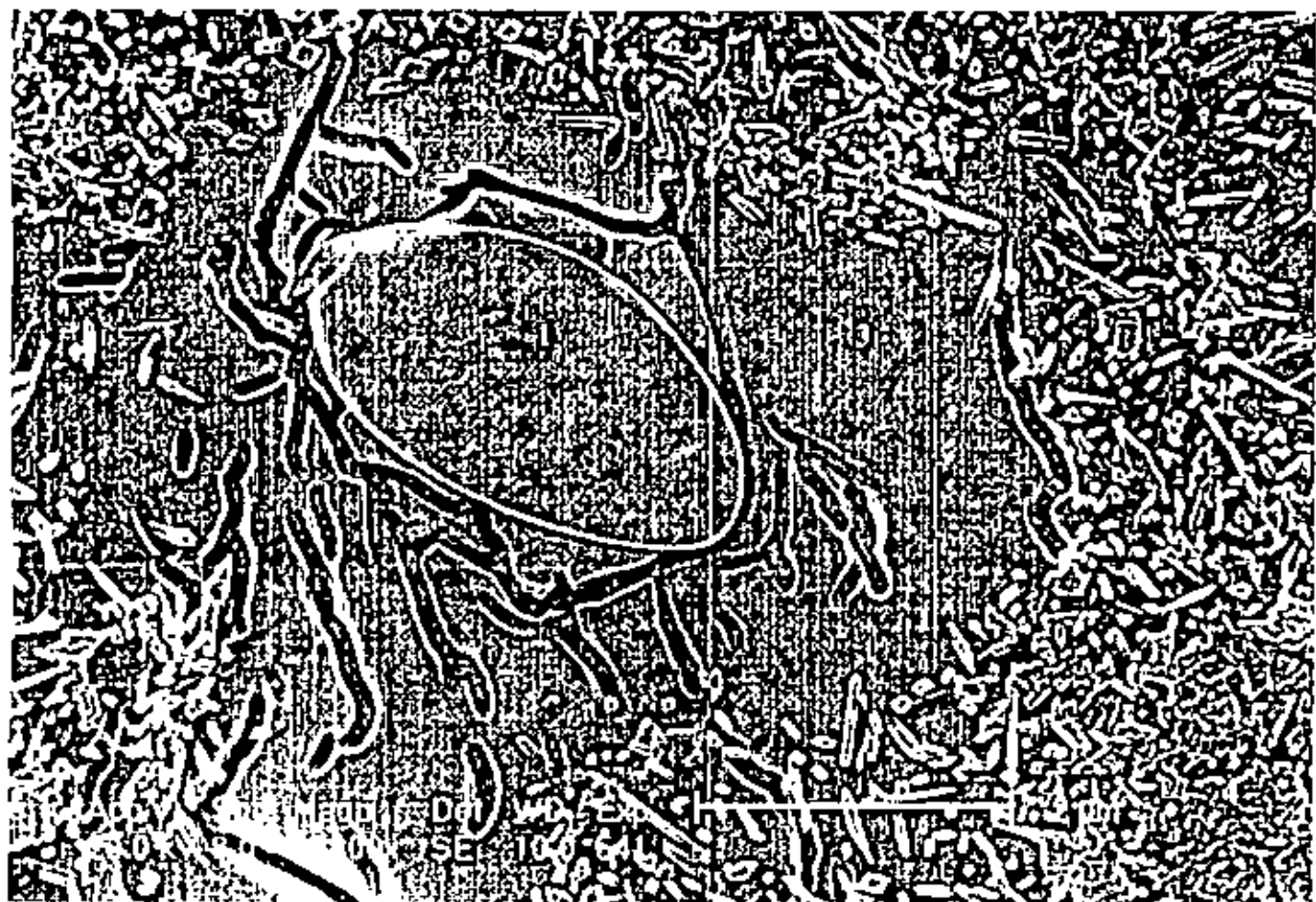


Fig 4.14: SEM image of porcelain ceramic insulator showing a quartz grain and a glassy rim surrounded by micro cracks and mullite needles in a clay matrix (Magnification 15000X).

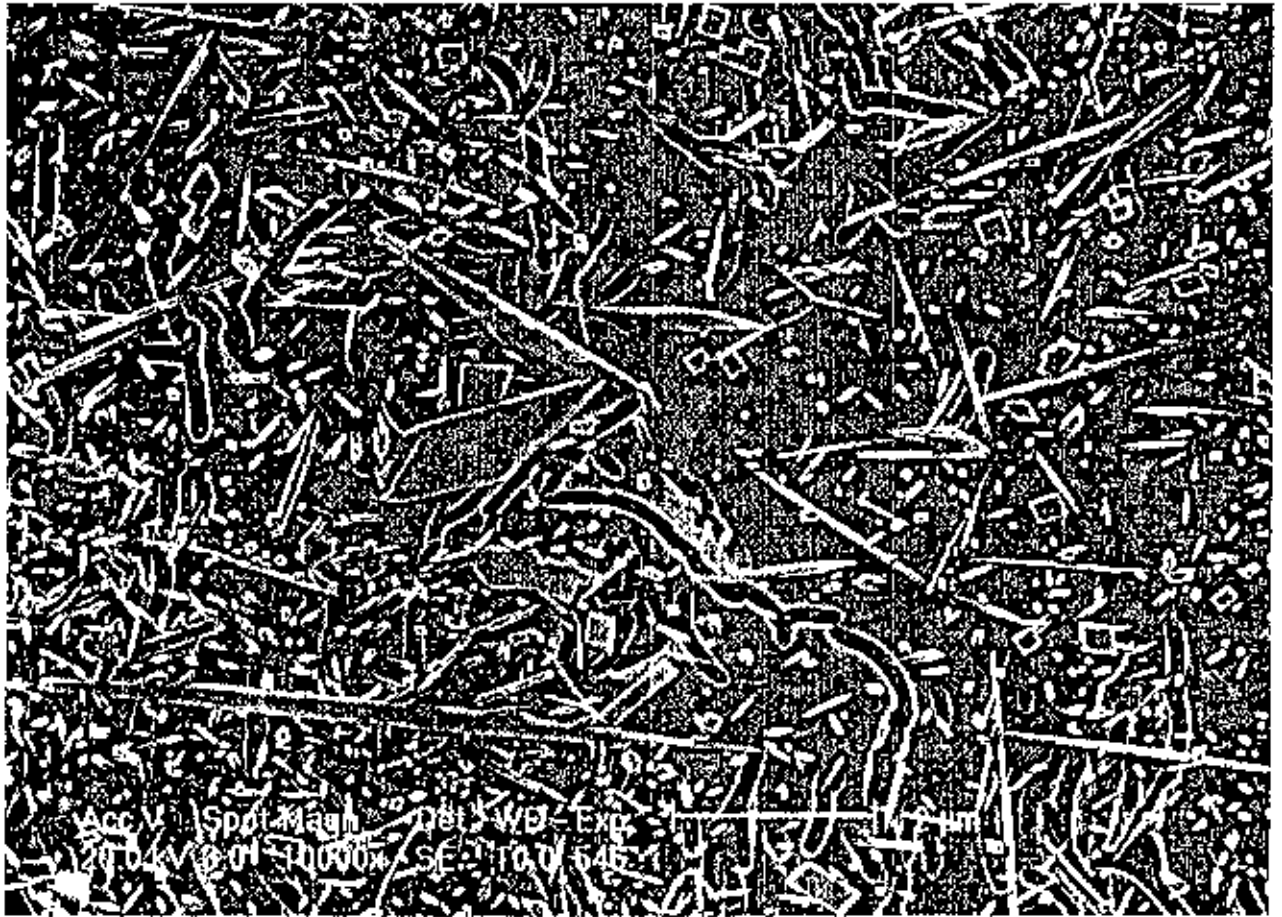


Fig 4.15: SEM image of porcelain ceramic insulator showing acicular shapes of mullite needles and some interconnected cracks in clay matrix.

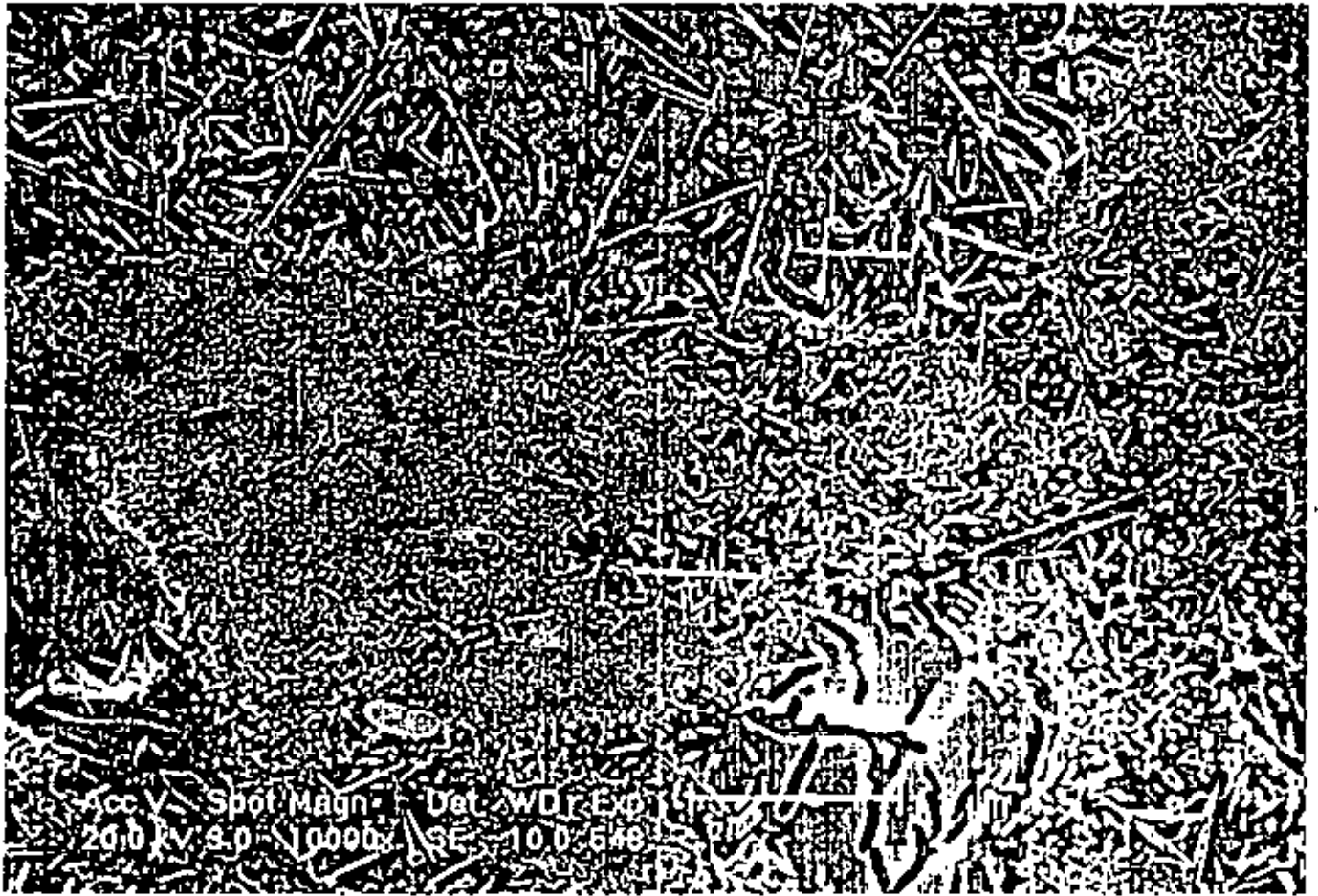


Fig 4.16: SEM image of porcelain ceramic insulator showing wide regions of mullite crystals in a matrix of clay (Magnification 10000X)

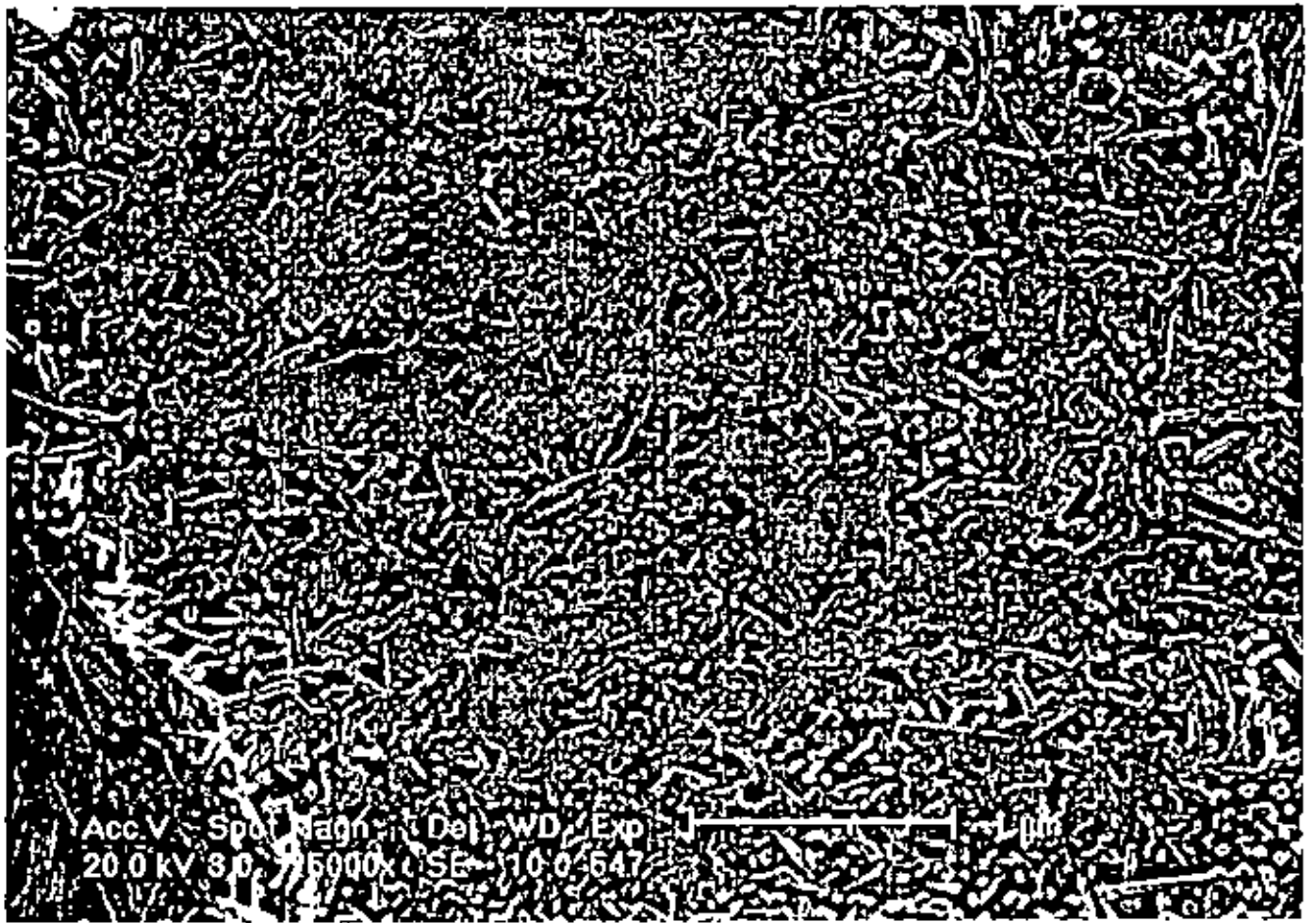


Fig 4.17: Magnified image of mullite needles (Magnification 25000X)

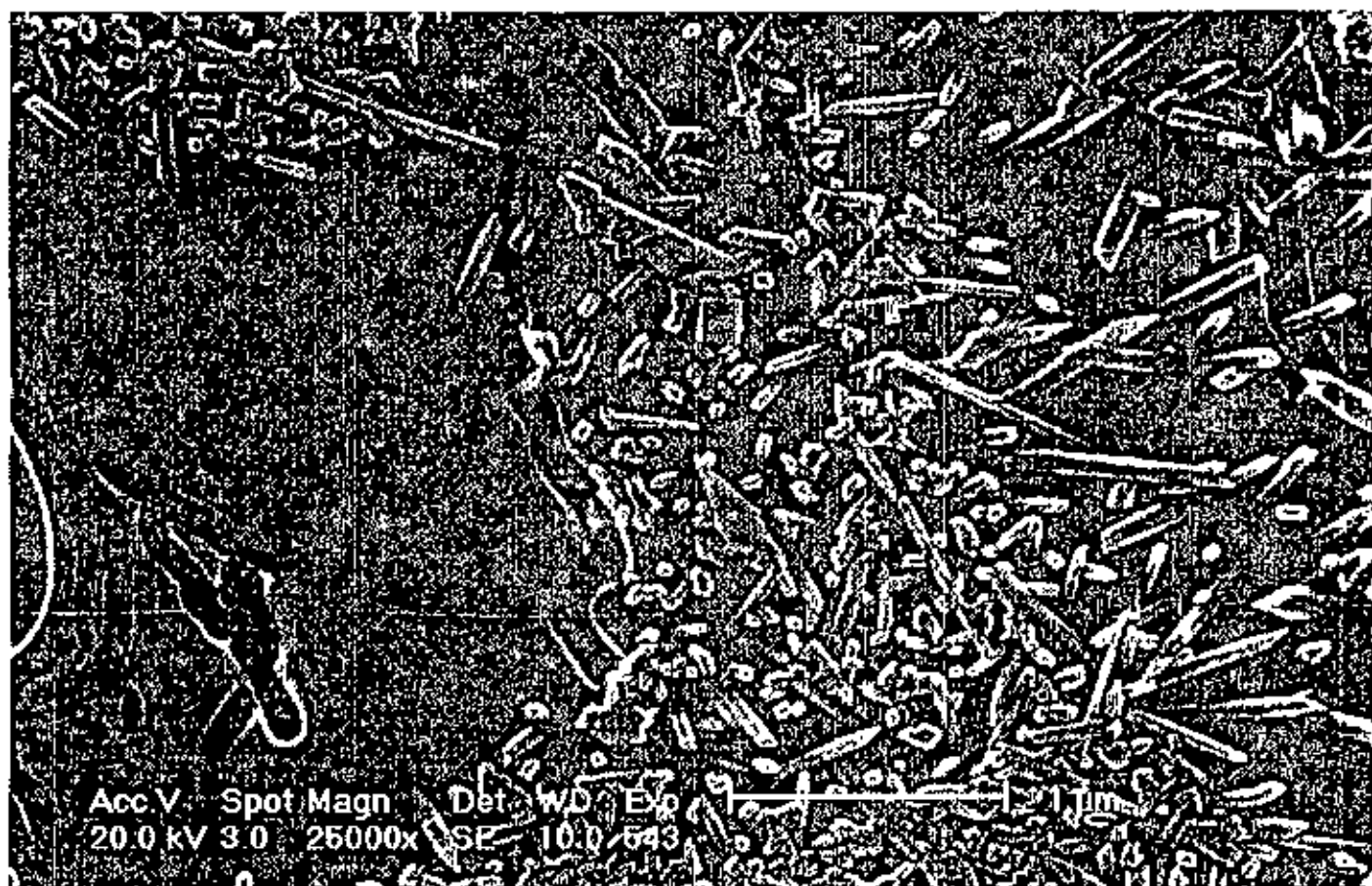
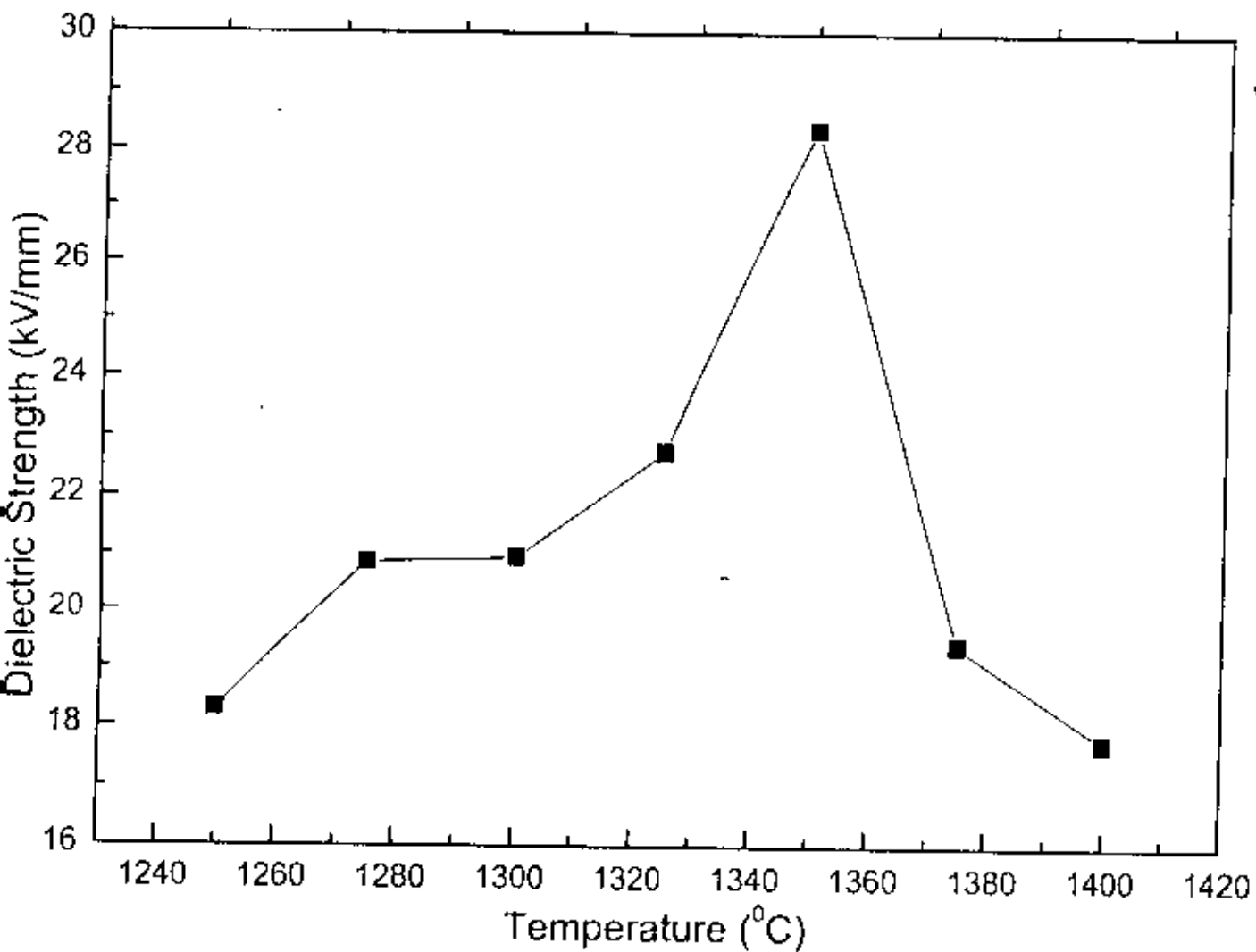
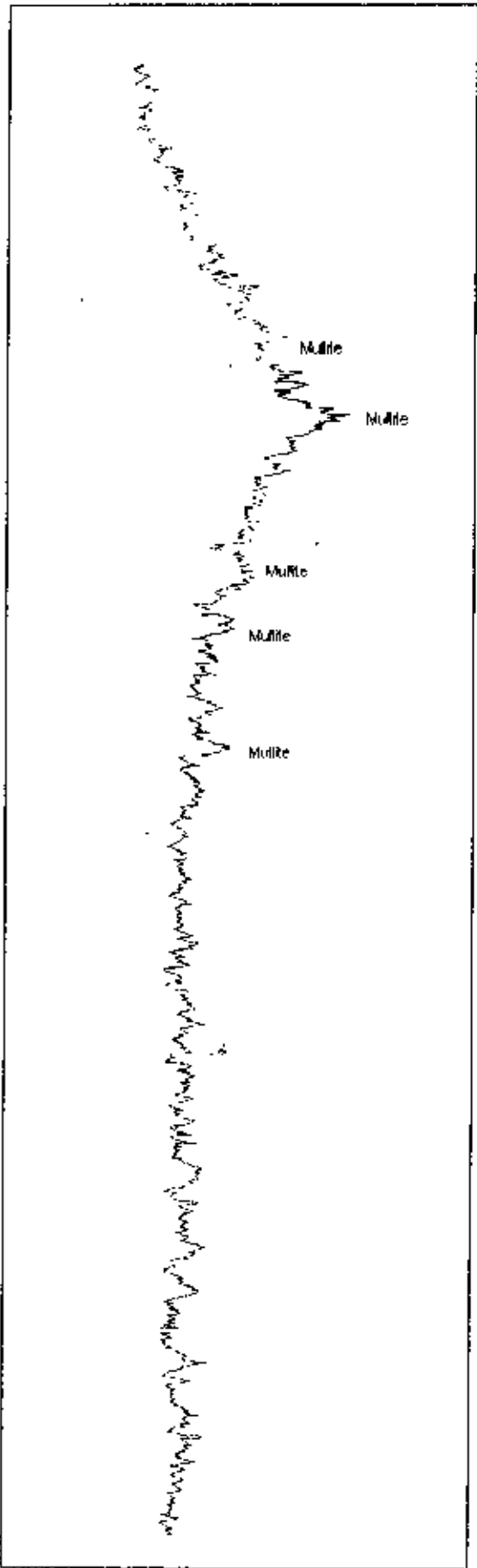


Fig 4.18: Magnified image of cracks showing their interconnected nature
(Magnification 25000X)



Variation of Dielectric strength with temperature

Fig : Variation of dielectric strength with temperature.



Diffraction angle 2θ

Fig 4.20: XRD pattern of the fired body fired at 1250°C showing Mullite, Quartz and Clay

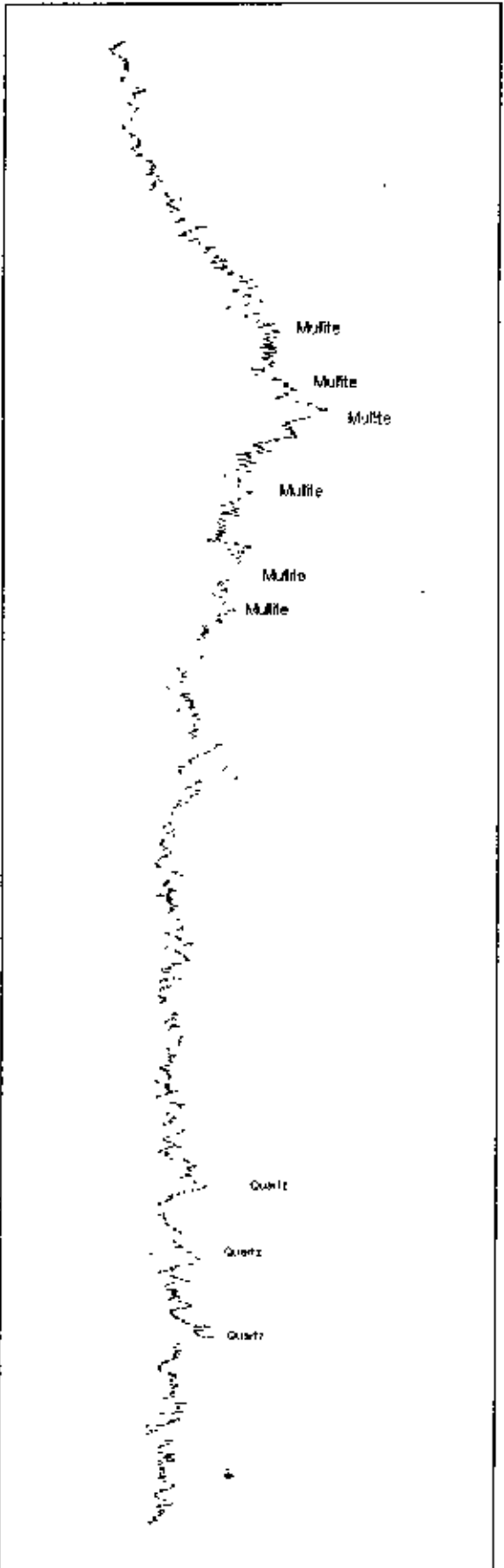


Fig 4.21: XRD pattern of the fired body fired at 1275°C showing Mullite, Quartz/Clay

Diffraction angle 2θ

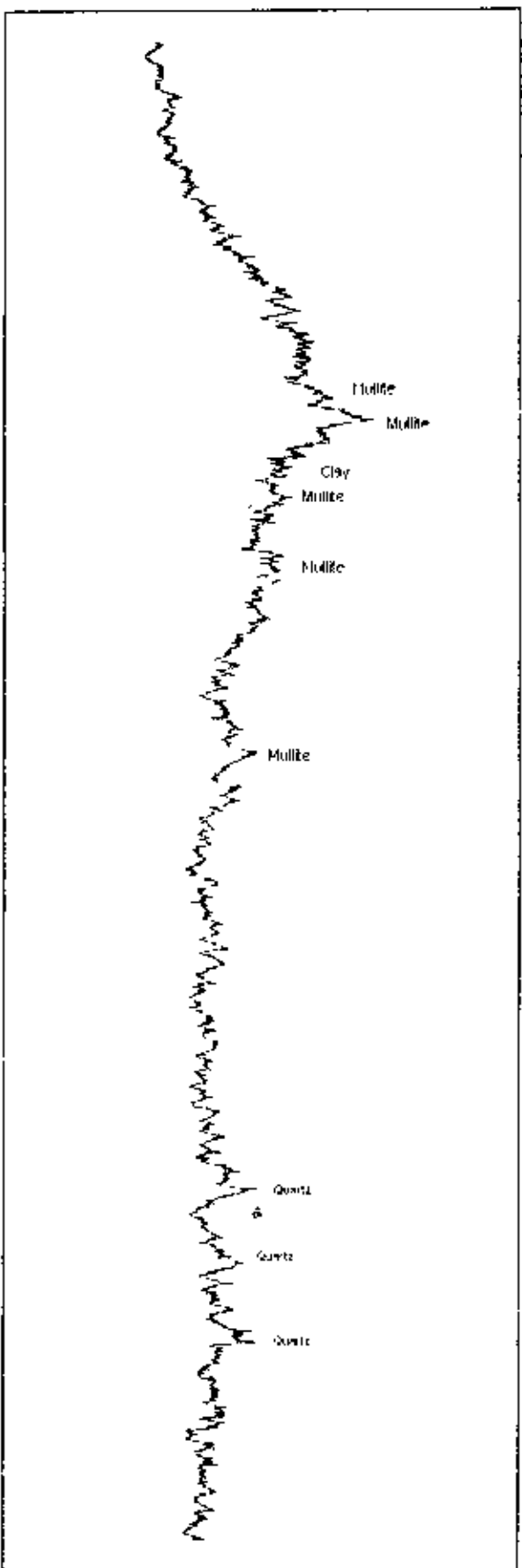


Fig 4.22: XRD pattern of the fired body fired at 1300°C showing Mullite (M), Quartz(Q), Clay(C).

Diffraction angle 2θ

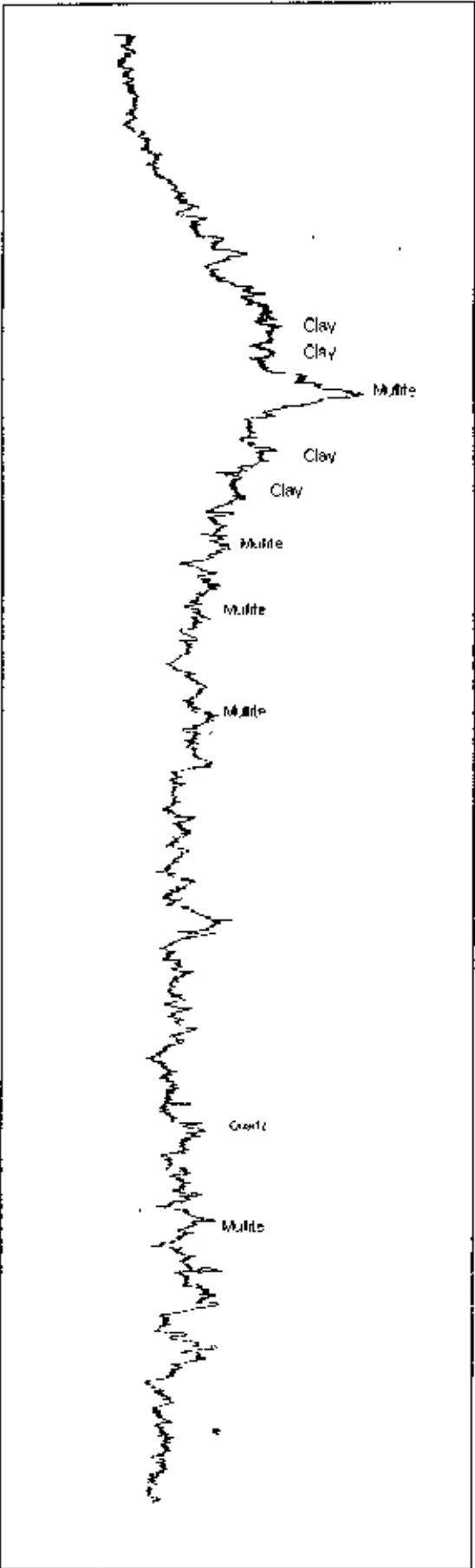


Fig 4.23: XRD pattern of the fired body fired at 1325°C showing Mullite (M), Quartz, Clay(C).

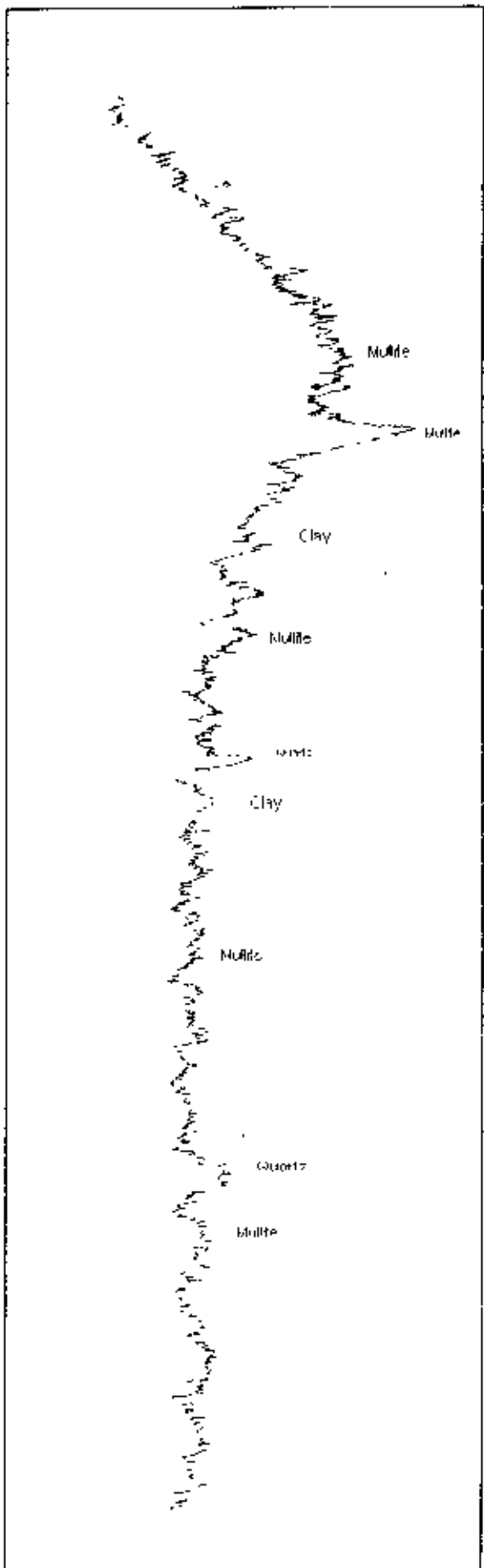
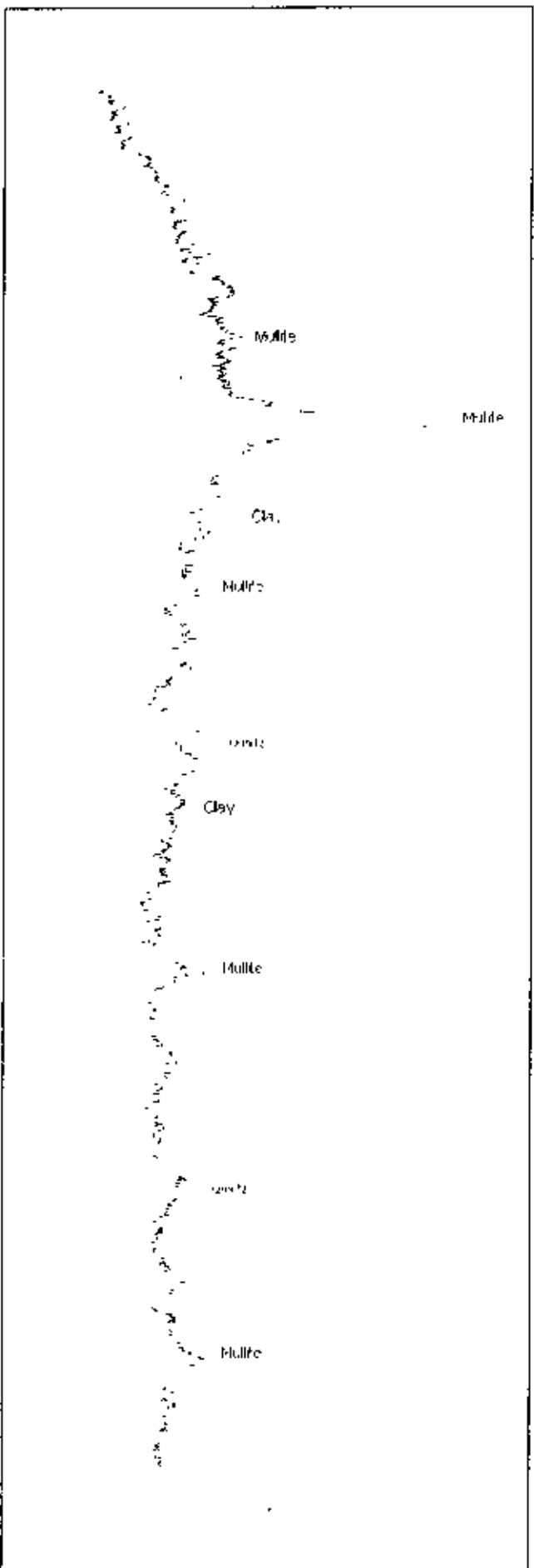


Fig 4.24: XRD pattern of the fired body fired at 1350°C showing Mullite, Quartz, Clay.



Diffraction angle 2θ

Fig 4.25: XRD pattern of the fired body fired at 1375°C showing Mullite, Quartz, Clay.

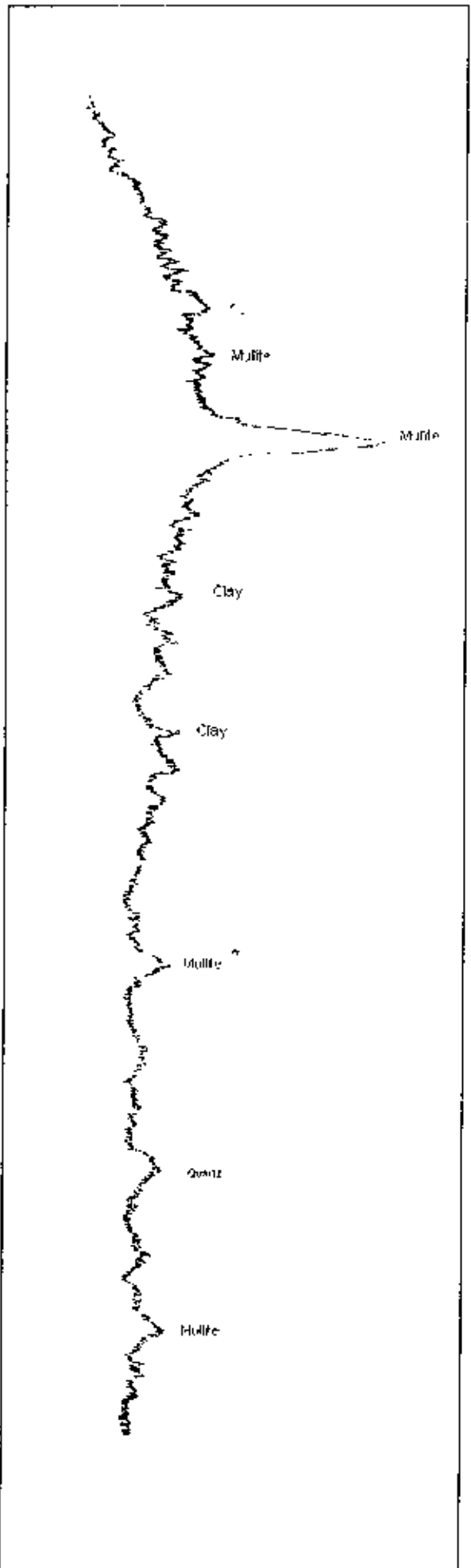


Fig. 4.26: XRD pattern of the fired body fired at 1400°C showing Mullite, Quartz, Clay

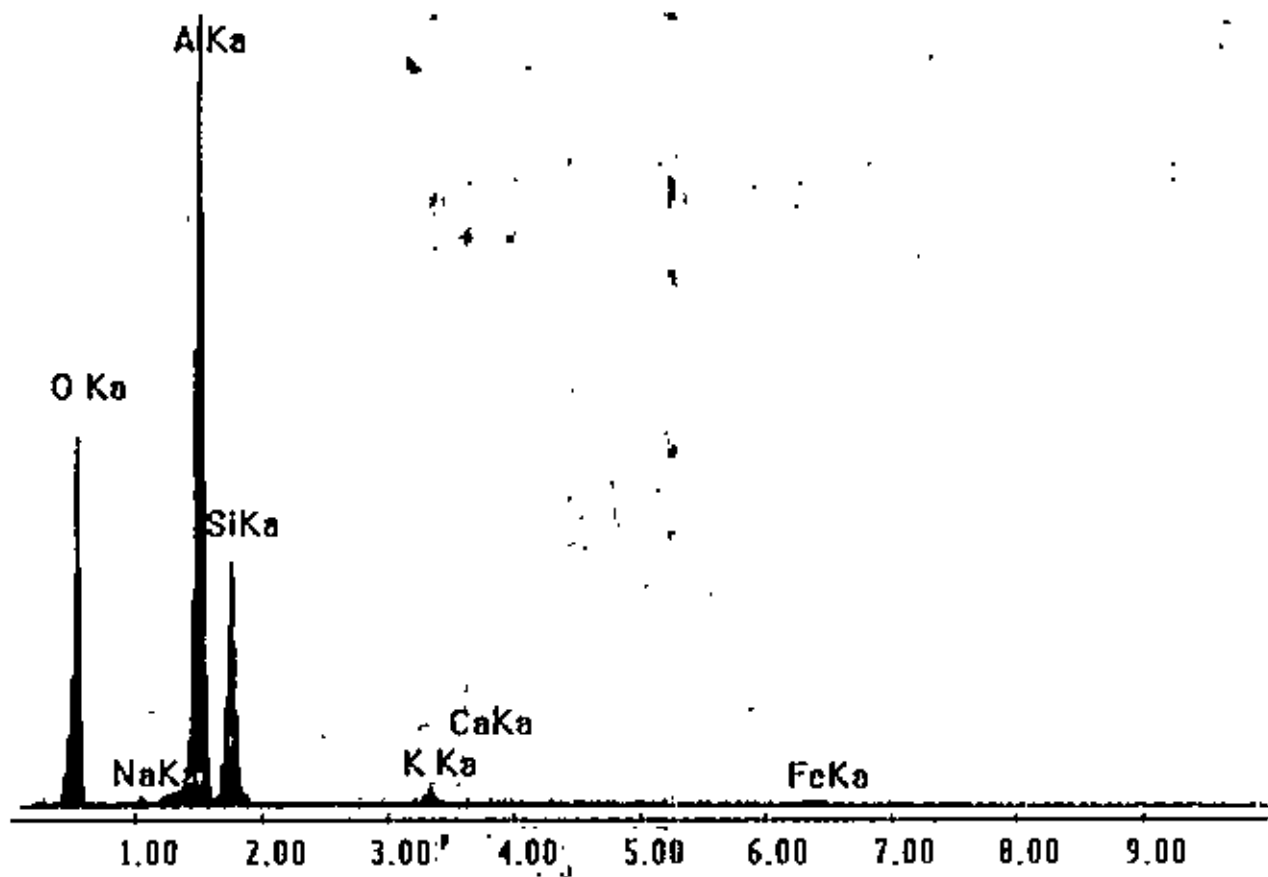


Fig 4.27: EdAX analysis of mullite needles showing stoichiometric amount of Alumina and Silica. Spot 4 was chosen in fig 4.14

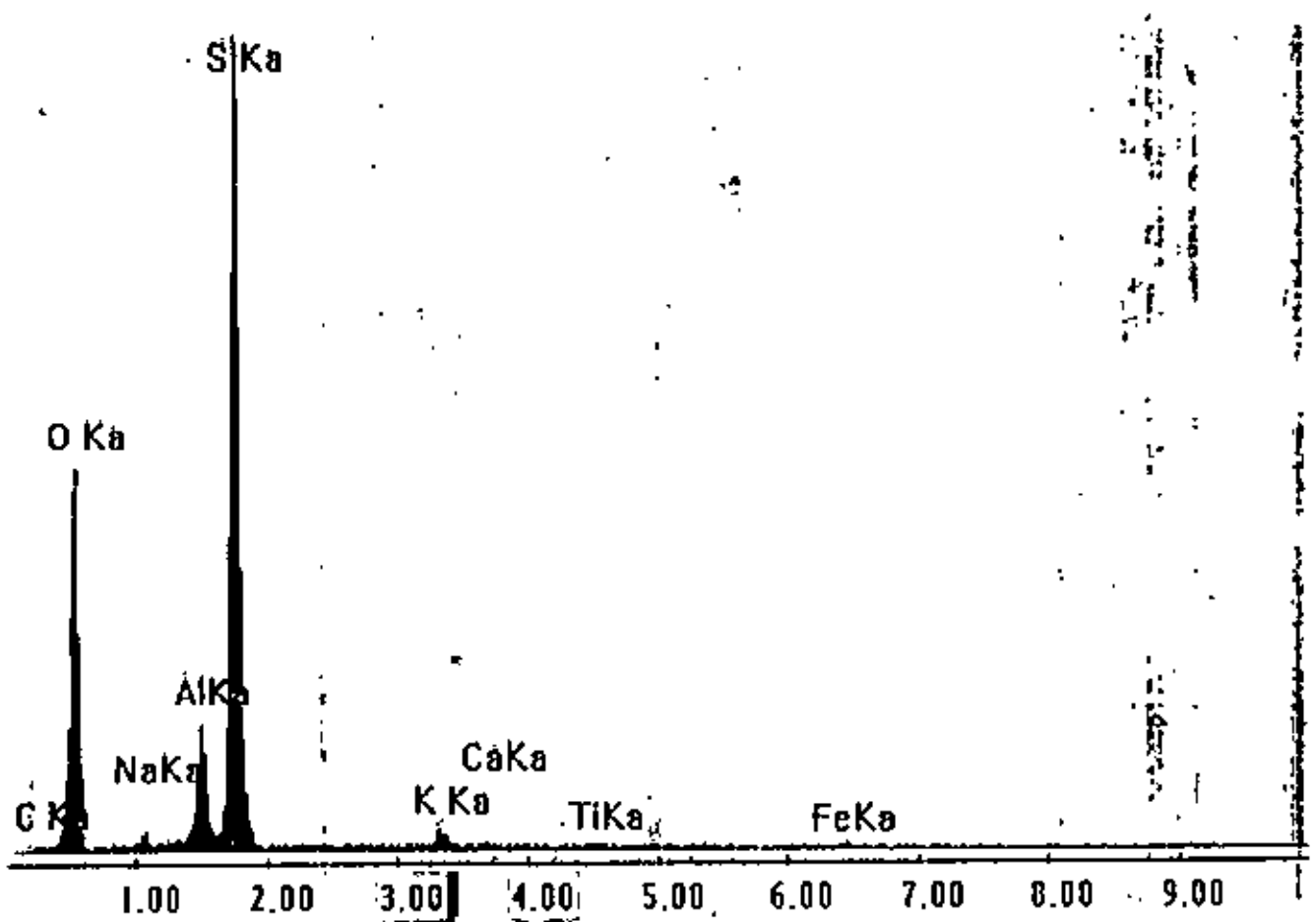


Fig 4.28: EDAX analysis of glassy phase showing high amount of silica and other oxides. Spots 2 was chosen in figure 4.14

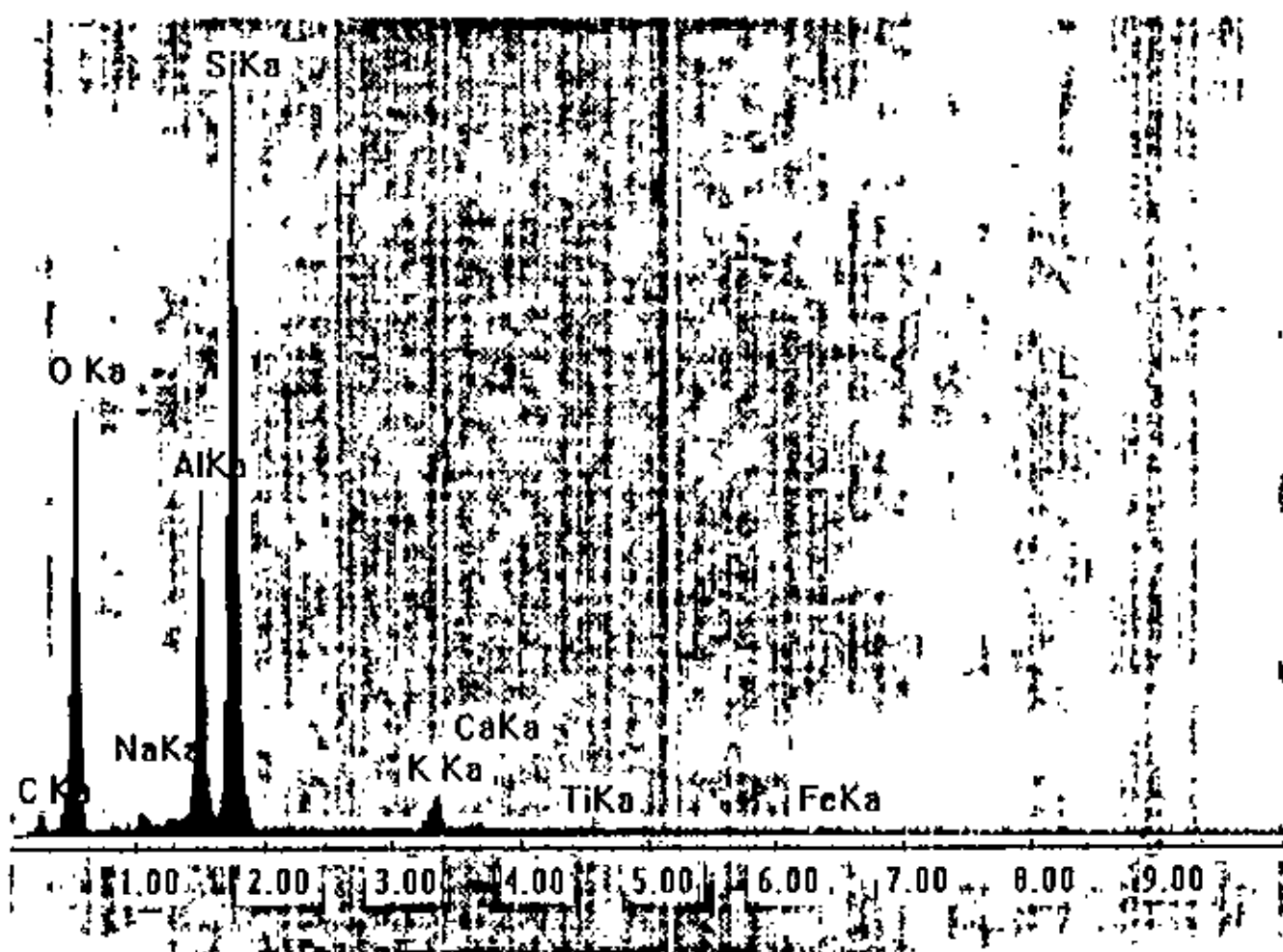


Fig 4.29: EDAX analysis of clay matrix showing the proportionate amount of silica and alumina. Spot 3 was chosen in figure 4.14.

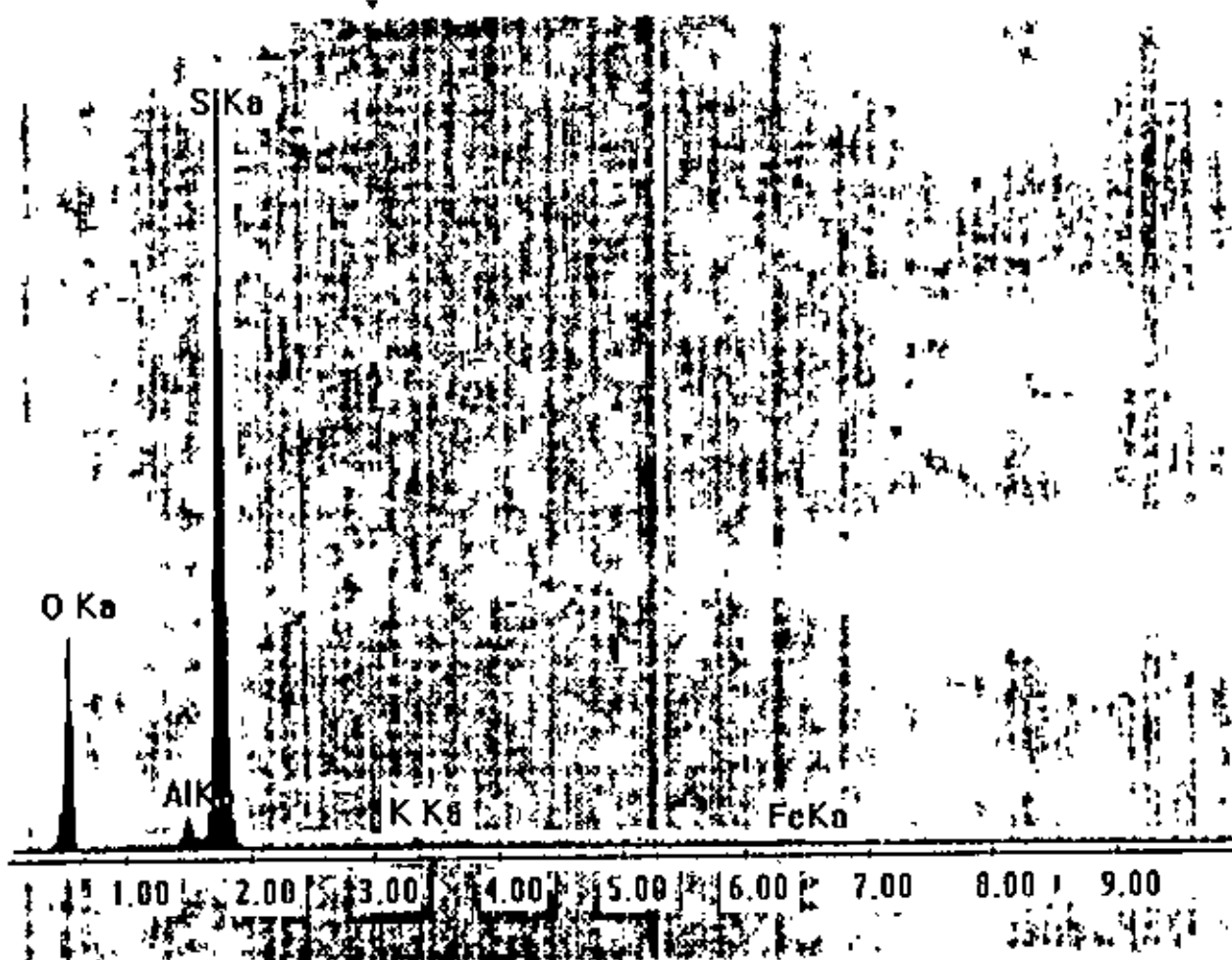


Fig 4.30: EDAX analysis of quartz showing almost all the silica. Spot 1 was chosen in fig 4.14.

